COMMISSION OF THE EUROPEAN COMMUNITIES

ENTERPRISE DIRECTORATE GENERAL

Contract Number FIF 20020686

Heavy-Duty Engine Validation of

World Harmonised Duty Cycle (WHDC)

Final Report May 2004

by

Dipl.-Ing. Leif-Erik Schulte
Dipl.-Ing. Michael Motzkau
Dipl.-Ing. Heinz Steven
Dipl.-Ing. Ralf Schiebelhut

RWTÜV Fahrzeug GmbH
Institute of Vehicle Technology
Engines / Commercial Vehicles Division

P.O. Box 103261

D-45032 Essen

CONTENT **PAGE**

0 List of Abbreviations

Abbreviation	Unit	Meaning
a	[-]	y intercept of the regression line
b	[-]	slope of the regression line
CFR	[-]	Code of Federal Regulations
CO_2	[ppm]	Carbon Dioxide
conce.	[-]	Concentration
COV	[-]	Coefficient of Variation
CRT	[-]	Continuous Regenerating Trap
CVS	[-]	Constant Volume Sampling
DPF	[-]	Diesel Particulate Filter
EC	[-]	Elemental Carbon / European Commission
EPA	[-]	Environmental Protection Agency
ESC	[-]	European Steady-state Cycle
ETC	[-]	European Transient Cycle
FF	[-]	Full flow dilution
FTP	[-]	Federal Test Procedure
GRPE	[-]	Groupe de Rapporteurs de la Pollution et de la Enneigé
INSOF	[-]	Insoluble Fraction
IUPAC	[-]	International Union of Pure and Applied Chemistry
n.a.	[-]	not applicable
NDIR	[-]	non dispersive infra-red
NO_2	[ppm]	Nitrogen Dioxide
O_2	[ppm]	Oxygen
PF	[-]	Partial flow dilution
PM	[-]	Particulate Matter
PMP	[-]	Particulate Measurement Programme
ppm	[-]	parts per million
R^2	[-]	Correlation coefficient
SO_2	[ppm]	Sulphur Dioxide
SOF	[-]	Soluble Organic Fraction
std. dev.	[-]	Standard Deviation
WHSC	[-]	World Harmonised Steady-state Cycle
WHTC	[-]	World Harmonised Transient Cycle
X	[-]	x-axis / axis of abscissae
Y	[-]	y-axis / ordinate axis

1 Introduction and Scope

Within the study for the validation of the WHDC test cycle, the cycle itself was validated as well as its applicability to the required measurement and sampling methodologies and procedures. In order to have a link to future low-emission engines, the work was performed with recent Euro III diesel engines and engines equipped with particulate traps in order to meet Euro IV (or better) PM limits. The intention of the work is to gather more knowledge about the driveability of the WHDC test cycles on the one hand, and, on the other hand to compare the existing measurement procedure for gaseous components and particulates to the ISO-procedure developed by the WHDC-sub-group "ISO-Activities" ISO 16183 /1/.

Therefore, the different selected cycles were compared in view of driveability studies based on regression analysis between the reference and actual signals of speed and torque. In addition, the engine operating ranges covered by each different cycle were compared. The influence of the engine design concept and the dynamometer control was also subject to the investigations, where possible to do.

For the comparison of the CVS to the ISO 16183 exhaust gas measurement methodology, the components CO, THC, NOx and PM were monitored over each cycle. The CVS measurement was performed via modal analysis. The work was performed under steady-state and transient conditions comparing the different worldwide cycles used today with the WHTC- (transient) and the WHSC- (steady-state) cycle. Full factorial statistical design with one factor (no parameter variations), 7 levels = 7 cycles and three repeats for each engine was used.

The major aims of the study were:

- A comparison of the final WHDC / WHSC with the world-wide existing cycles for HD-engines in order to assess the new cycle(s) in view of driveability and applicability for different engine designs.
- A comparison of the CVS and ISO measurement procedures in order to assess the new methodology in view of type approval applicability, as well as to gather more knowledge of the accuracy and repeatability of both procedures related to different engine designs
- To propose modifications to the new procedures if necessary

2 Work Programme, Study Items, Topics Under Investigation, Results

The test schedule was designed in order to investigate the influences of the following parameters:

- cycles correlation / comparison
- comparison full flow (CVS) PM vs. partial flow (ISO 16183) PM
- comparison diluted gaseous components vs. raw gaseous components
- evaluation of the variance of measurement procedures (CVS vs. ISO 16183)
- cycle driveability (validation / statistics)
- cycle / measurement procedures (improvement / modifications)

2.1 Test engines and test fuel

2.1.1 Engines

The following engines were subject to testing:

- Engine 1

  Euro III engine, with/without CRT

  VH = 11.9 l, P = 290 kW
- Engine 2

  Euro III engine, with CRT

  VH = 6.7 l, P = 189 kW
- Engine 3

  Euro III engine, without after-treatment

  VH = 15.6 l, P = 426 kW
- Engine 4

  Euro III engine, without after-treatment

  VH = 2.8 l, P = 92 kW

The engine manufacturers delivered all the engines. Before starting the measurements on each engine, the general test set-up as well as all relevant engine parameters were subject to agreement with the particular manufacturer.

Exhaust gas measurement and power performance data was given to them in order to make sure that the engines were running in an appropriate manner.

2.1.2 Fuel

During the entire measurement programme a CEC RF-06-99 reference diesel fuel with a sulphur content below 10 ppm according to 1999/96/EC was used. The detailed analysis of this fuel is shown in **Table 2.1.2-1**.

Parameter	Unit	Value	Limits		Test Method
			Minimum	Maximum	
Cetane number	-	**53,7**	52	54	ISO 5165
Density at 15 °C	kg/m^3	**833,9**	833	837	ISO 3675
Distillation:					
- 50 % point	°C	**268,9**	245		ISO 3405
- 95 % point	°C	**348,2**	345	350	ISO 3405
- final boiling point	°C	**363,8**	---	370	ISO 3405
Flash point	°C	**83**	55	---	ASTM D 93
CFPP	°C	**-18**	---	-5	EN 116
Viscosity at 40 °C	mm²/s	**2,701**	2,5	3,5	ASTM D 445
Polycyclic aromatic hydrocarbons	% m/m	**4,6**	3,0	6,0	IP 391
Sulphur content	mg/kg	**6**	---	10	EN ISO 14596
Conradson carbon residue (10 % DR)	% m/m	**0,02**	---	0,2	ASTM D 189
Ash content	% m/m	**< 0,005**	---	0,01	ASTM D 482
Water content	% m/m	**0,004**	---	0,05	ASTM D 95/D 1744
Neutralisation Numb.	KOH/g	**0,00**	---	0,02	ASTM D 974
Oxidation stability	mg/ml	**0,003**	---	0,025	ASTM D 2274

Table 2.1.2-1: Fuel Quality (CEC RF-06-99)

2.2 Test cycles

Measurements were carried on following steady-state and transient cycles::

- Steady-state cycles
  - ESC,
  - WHSC,
  - Japanese 13-mode test,
- Transient cycles
  - ETC,
  - WHTC,
  - US-FTP

2.2.1 The WHSC and WHTC cycle

For the establishment of a general test protocol to be used for the complete test programme the final versions of the WHSC / WHTC cycles were first tested on one engine equipped with a CRT-System in order to set-up the layout of the measurement systems and dynamometer settings. Since the start of the WHDC development work some major changes have become necessary in the definition of the speeds used for cycle denormalisation as well as in the cycle itself /2/.

For that reason the final cycles using the final definition of n preferred (n_{pref}) were used. These cycles are named WHTC and WHSC without any pre- or postfix in the following.

The normalised final WHSC Cycle used for the denormalisation is shown in **Fig. 2.2.1-2**. The percentage load distribution of the WHTC is indicated through different / shaded coloured areas. The relationship between the reference / normalised cycle (**Fig. 2.2.1-2**) and a de-normalised cycle for *engine 1* in particular (**Fig. 2.2.1-1**) can be easily seen by comparing both figures.

A comparison between the different speed definitions and cycles is given in chapter 2.2.2. **Fig. 2.2.1-1** shows the latest (final) status of the World Harmonised Steady-state Cycle (WHDC) in absolute / denormalised cycle data for *engine 1*.

The corresponding denormalised final World Harmonised Transient Cycle (WHTC) is shown in **Fig. 2.2.1-3**. The steady-state points of the denormalised WHSC are indicated over the WHTC transient cycle map.

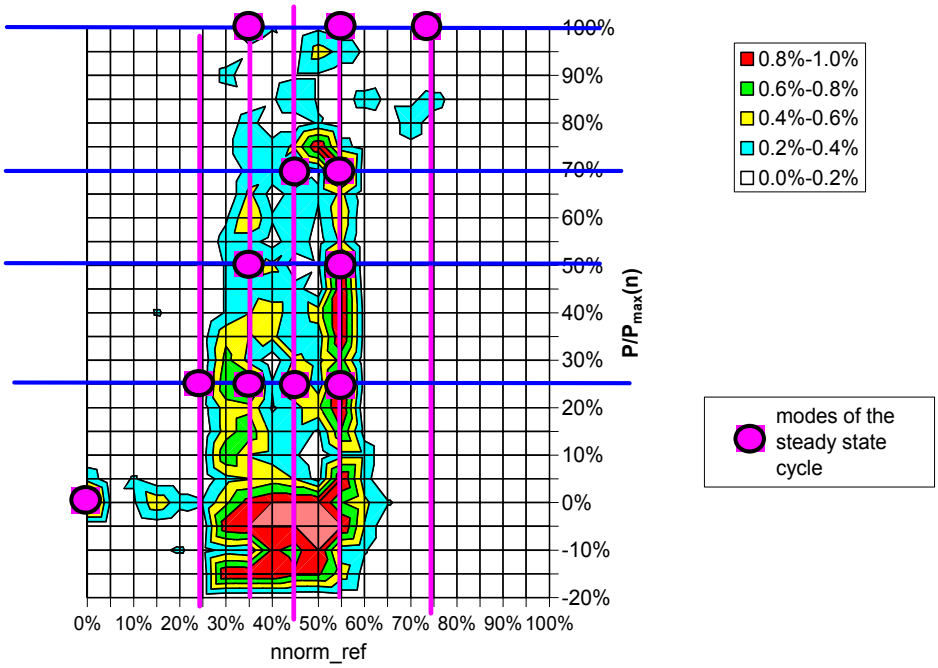

Fig 2.2.1-1.; Final WHSC / Normalized data

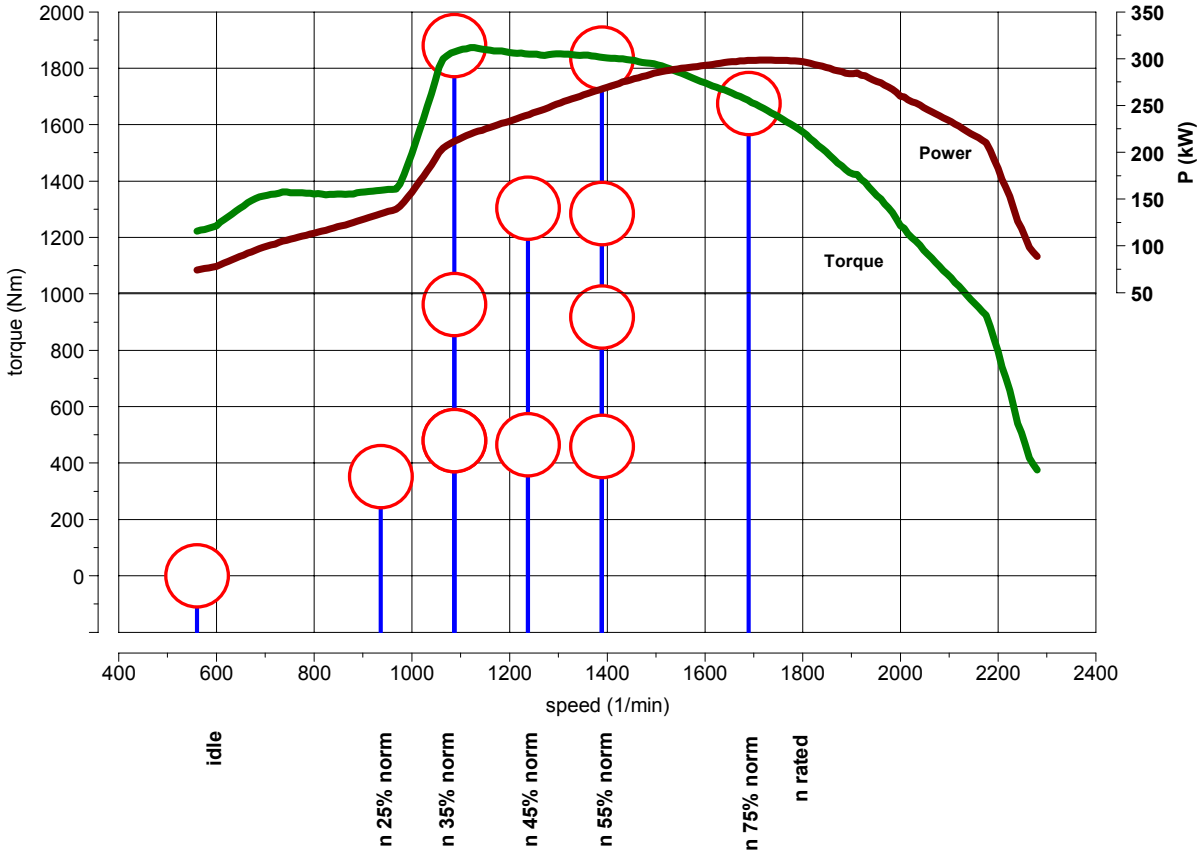

Fig 2.2.1-2.: Final WHSC in absolute / denormalised cycle data for engine 1

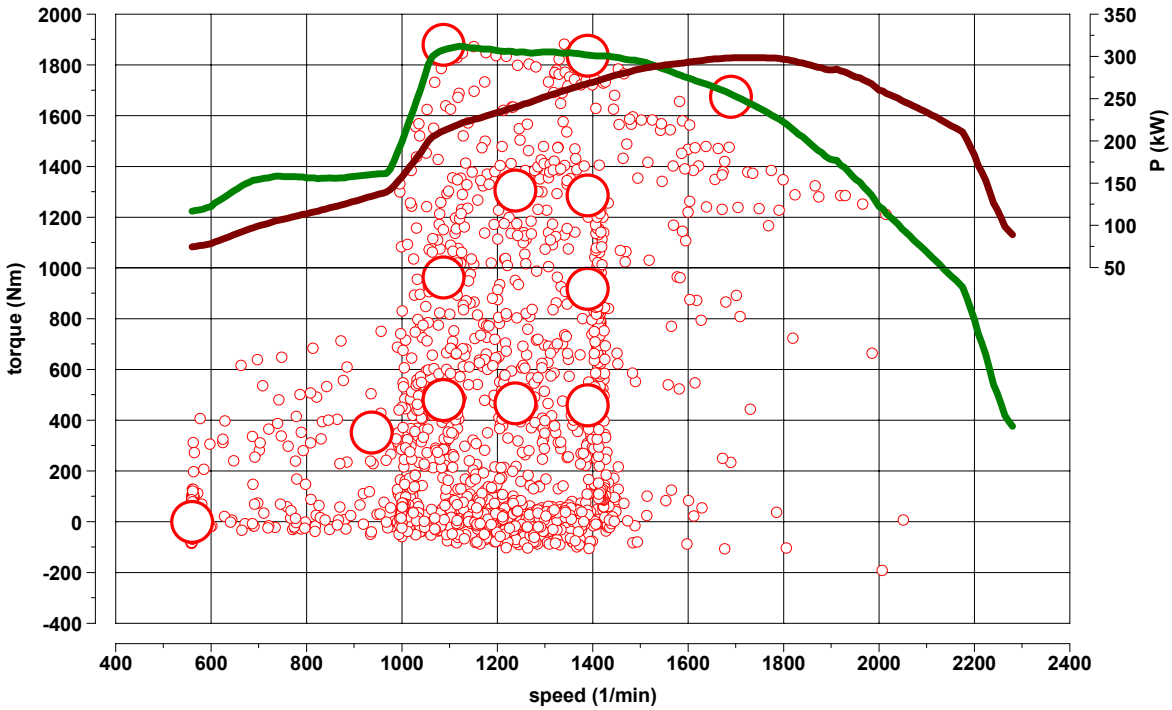

Fig. 2.2.1-3: Final WHTC (WHSC) in absolute / denormalised cycle data for engine 1

As already mentioned the latest denormalisation formulas /2/ were used for the absolute cycle speed generation. These formulas are:

$$actual\ speed = n_{norm\ ref.} \times (0{,}45 \times n_{low} + 0{,}45 \times n_{pref} + 0{,}1 \times n_{high} - n_{idle}) / 0{,}5363 + n_{idle} \quad \textbf{(1)}$$

$$n_{low} = lowest\ speed\ where\ engine\ supplies\ 55\%\ of\ full\ load\ rated\ power \quad \textbf{(2)}$$

$$n_{high} = highest\ speed\ where\ engine\ \text{supplies}\ 70\%\ of\ full\ load\ rated\ power \quad \textbf{(3)}$$

$$n_{pref} = speed\ where\ the\ integral\ of\ the\ torque\ curve\ from\ idling\ speed\ is\ 51\%\ of\ the\ whole\ integral\ from\ idling\ speed\ to\ n_{95\ high} \quad \textbf{(4)}$$

$$n_{95\ high} = highest\ speed\ where\ engine\ gives\ 95\%\ of\ its\ full\ load\ rated\ power \quad \textbf{(5)}$$

2.2.2 Definition of preferred speed and denormalisation formula

One key factor for the WHDC denormalisation procedure is the preferred speed n_{pref}, which is intended to represent the most frequently used engine speed range during in use operation. Therefore, different definitions of the preferred speed n_{pref} and the denormalisation formula for the actual speed were used and published during the WHDC cycle development /2/. For the test programme described within this report the final versions (see chapter 2.2) were used as well as the first version on *engine 1* for comparison. /3/.

The chronological development of n_{pref} is shown below:

$n_{pref\,A}$ = *the minimum engine speed where the engine torque is maximum* **(6)**

$n_{pref\,0}$ = *the centre of the speed range between the minimum speed, where the engine torque is 90% of maximum torque, and the maximum speed of 90% torque* **(7)**

$n_{pref\,1}$ = *engine speed where the integral of the power curve from idling speed is 33.33% of the whole integral from idling speed to* n_{high} **(8)**

$n_{pref\,2}$ = *engine speed where the integral of the torque curve from idling speed is 48% of the whole integral from idling speed to* n_{high} **(9)**

$n_{pref\,3}$ = *engine speed where the integral of the torque curve from idling speed is 51% of the whole integral from idling speed to the median speed between rated speed and* n_{high} **(10)**

$n_{pref\,4}$ = *engine speed where the integral of the torque curve from idling speed is 51% of the whole integral from idling speed to* $n_{95\,high}$. **(11)**

with following algorithms for the calculation of the actual speed:

actual speed (A) =

$$n_{norm\,ref.} \times (0{,}6 \times n_{low} + 0{,}2 \times n_{pref} + 0{,}2 \times n_{high} - n_{idle}) \times 1{,}8646 + n_{idle} \qquad \textbf{(12)}$$

actual speed $(0, 1, 2, 3, 4)$ =

$$n_{norm\,ref.} \cdot (0{,}45 \cdot n_{low} + 0{,}45 \cdot n_{pref} + 0{,}1 \cdot n_{high} - n_{idle}) / 0{,}5363 + n_{idle} \qquad \textbf{(13)}$$

The final n_{pref} used was $n_{pref\,4}$ which equals n_{pref} as referred to in formula ***(4)***.

2.2.3 Test programme

The measurements were performed using a statistical approach for running the tests. The schedule was designed in such a way that at least three tests of each cycle were performed; one base test and two repeats. Actually, a larger number of repeats were performed on most of the engines. Consequently a higher statistical relevance is given to the results.

All engines were measured in the same way and in a continuous programme except for *engine 1*. This engine was measured at the very beginning of the programme for the comparison of the WHTC and WHSC cycles in final version and in version 1. After that the engine was given to another laboratory for performing an UN-ECE GRPE-PMP related measurement programme due to the fact that the time frame for this programme was much tighter /4/. For that reason some delay was caused to the programme described in this report.

2.3 Comparison of partial flow / full flow PM results

2.3.1 Measurement system description

Following systems were used for the comparison programme between partial flow PM measurement and full flow CVS based measurements:

Partial-Flow-System

- manufacturer: AVL
- type: Smart Sampler SPC 472
- method: partial flow dilution with micro-tunnel
- remark: transient cycle performance via a “look ahead”operation on a pre-sampled exhaust mass flow (G_{exh}) profile
- Gexh: addition intake air mass flow ($G_{air,w}$) measured with hot wire-sensor and fuel flow (G_{fuel}) measured with a gear cell flow meter

Full-Flow-System

- manufacturer: RWTÜV
- method: full flow CFV-CVS with double stage dilution
- primary tunnel: inner diameter: 355,6 mm, total length: 6500 mm

  length of the mixing section: 3600 mm

- secondary tunnel

  inner diameter: 80 mm

  length: 460 mm

- CVS, max. flow: 3.15 m^3/s
- sampler: VEREWA MKS-4
- specification: electronic flow compensation for compensating temperature deviations in the primary tunnel

Fig. 2.3.1-1 gives an overview over the general measurement system set-up of the full flow and partial flow dilution system used during the programme.

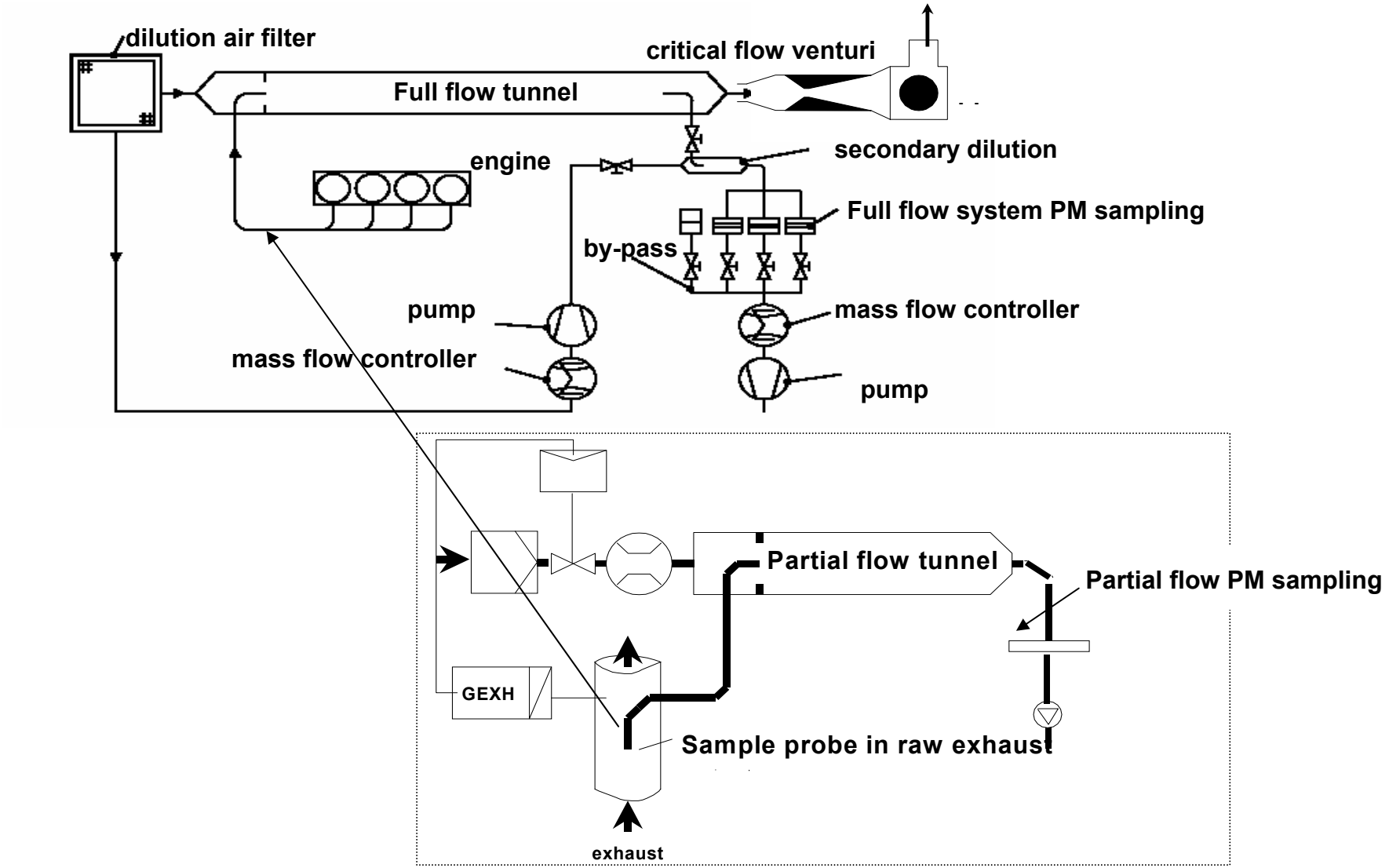

Fig. 2.3.1-1: Partial-flow / Full–flow dilution system

The comparison itself was performed by using following measurement results and parameters as indicator of the performance of each system (full flow and partial flow):

- PM FF mean value (g/kWh)
- PM PF mean value (g/kWh)
- FF stand. deviation
- PF stand. deviation
- FF COV
- PF COV
- percentage-deviation with FF as basis

The mean value was calculated by:

$$arithmetic\ mean\ value = \left(a_1 + a_2 + \ldots + a_n\right) / n \qquad \textbf{(14)}$$

and the standard deviation by using following formula:

$$std.deviation = \sqrt{\frac{n\sum x^2 - \left(\sum x\right)^2}{n^2}} \qquad \textbf{(15)}$$

The coefficient of variance (COV) was calculated by dividing formula ***(14)*** by ***(15)***:

$$COV = \frac{std.deviation\ X(n)}{meanvalue\ X(n)} * 100\% \qquad \textbf{(16)}$$

The coefficient of variance is the degree to which a set of measurement data varies. It is often called the relative standard deviation, since it takes into account the mean values. When the coefficient of variance is calculated for a number of given tests, it can be used to assess the precision. Precision is the measure of how close repeated trials are to one another.

The larger the COV is, the greater the variability. The COV is typically displayed as a percentage. As a criterion for reliable measurement results, a COV of less than 10% is generally accepted with today's engine technology.

For engines equipped with CRT-Systems and with low to very low measured emission levels it can be expected that COV's greater than 10% will occure. If such a COV is applied as an acceptance criterion it will result in falls assessment of the measurement system.

It should be considered that when (condensate / nucleation mode) particles generated by the after-treatment system exist and are taken into account, the measurement repeatability could be affected. Consequently, higher COV's could be more prevalent in the future as a result of engines after-treatment systems, rather than by the measurement system itself.

2.3.2 Particulate matter measurement results

The results indicated in the following chapter show the gravimetric mean PM results achieved with the two systems described in chapter 2.3.1. The full-flow results are given with the indices FF, the partial-flow results with a PF.

It can be seen that both systems are capable of monitoring the same PM emission map although there are slight differences in the results. Nonetheless, it has to be considered that the absolute emission level of the engines (*engine 1* and 2) equipped with a CRT-system is very low.

2.3.2.1 Engine 1

For all cycles on *engine 1* except for the Japanese 13-mode the partial flow system measured a higher particulate mass than the full flow system (**Fig. 2.3.2.1-1**).

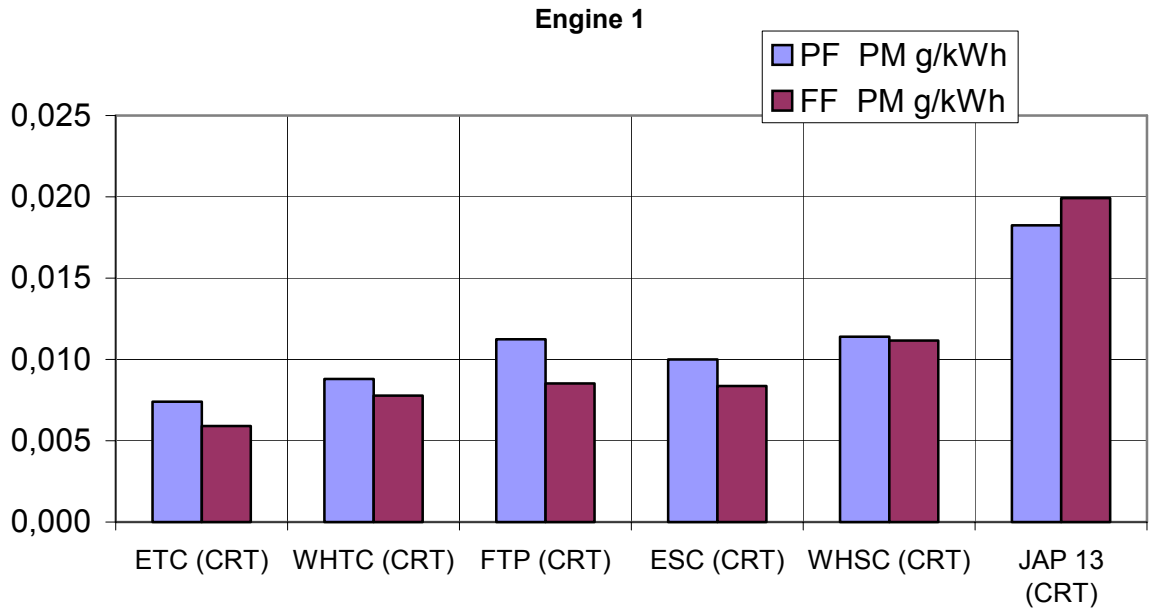

Fig. 2.3.2.1-1: PM results Engine 1 with CRT-System

Overall, the Japanese 13-mode test yields the highest PM emissions of all the cycles. By comparing the COV's on *engine 1* for all cycles (**Fig. 2.3.2.1-2)** the variability of the partial flow system is in the same range as the variability of the full flow system. . The high partial flow COV for the WHTC cycles seems to be not comparable to the other values and was for that reason considered as an outlier.

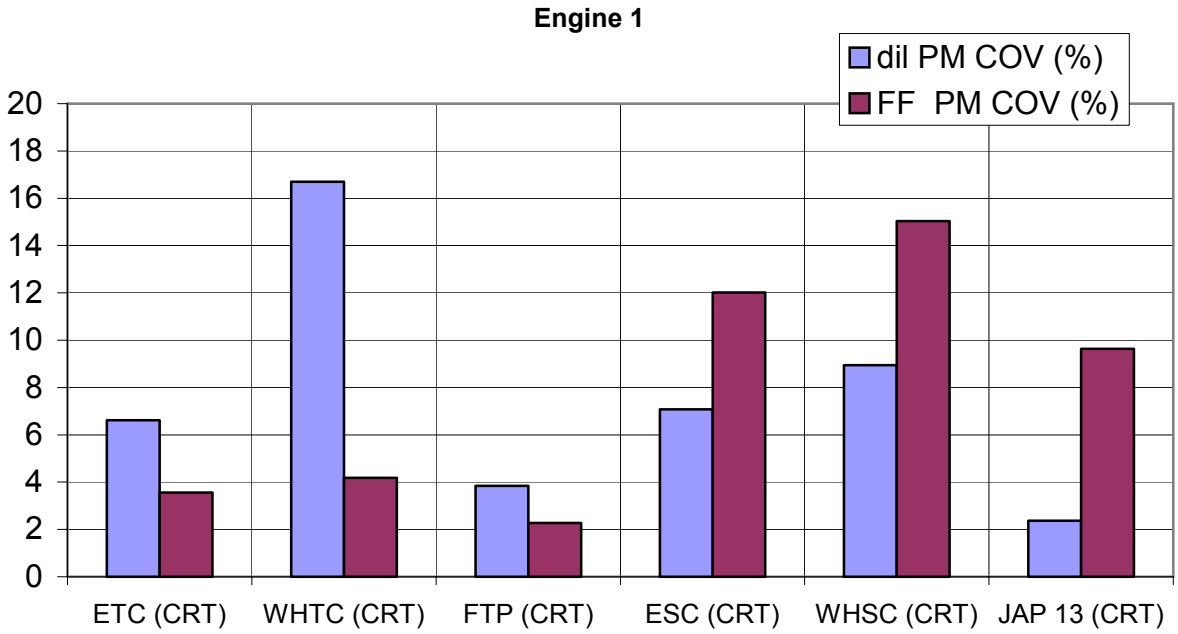

Fig. 2.3.2.1-2: PM-COV results Engine 1 with CRT-System

Table 2.3.2.1-1 gives a summary of the mean values of the transient cycle results of *engine 1* and **Table 2.3.2.1-2** of the steady-state cycles both including the standard deviation and the percentage deviation of the mean values and the coefficient of variation (standard deviation / mean value) for each system.

PM results	ETC	WHTC	U.S.-FTP
PM FF mean value (g/kWh)	0.0059	0.0078	0.0085
PM PF mean value (g/kWh)	0.0074	0.0088	0.0113
FF stand. Deviation	0.0002	0.0003	0.0002
PF stand. Deviation	0.0005	0.0015	0.0004
FF COV	3.55	4.18	2.27
PF COV	6.62	16.70	3.85
percentage-deviation (FF basis)	-25.42	-13.30	-32.04

Table 2.3.2.1-1: Summary of Transient Cycle PM results / Engine 1 with CRT

PM results	ESC	WHSC	JAP 13 mode
PM FF mean value (g/kWh)	0.0084	0.0112	0.0199
PM PF mean value (g/kWh)	0.0100	0.0114	0.0183
FF stand. Deviation	0.0010	0.0017	0.0004
PF stand. Deviation	0.0007	0.0010	0.0019
FF COV	12.01	15.03	9.63
PF COV	7.07	8.94	2.37
percentage-deviation (FF basis)	-19.04	-2.15	8.41

Table 2.3.2.1-2: Summariy of Steady-state Cycle PM results / Engine 1 with CRT

2.3.2.2 Engine 2

The same conclusion could be drawn for *engine 2*, which was also operated with CRT-System during the measurement programme. Once again the highest absolute emissions could be measured in the Japanese 13-mode cycle. The comparison shows again that both, the partial flow and the full system are able to monitor the same emission behaviour of an engine (**Fig. 2.3.2.2-1**).

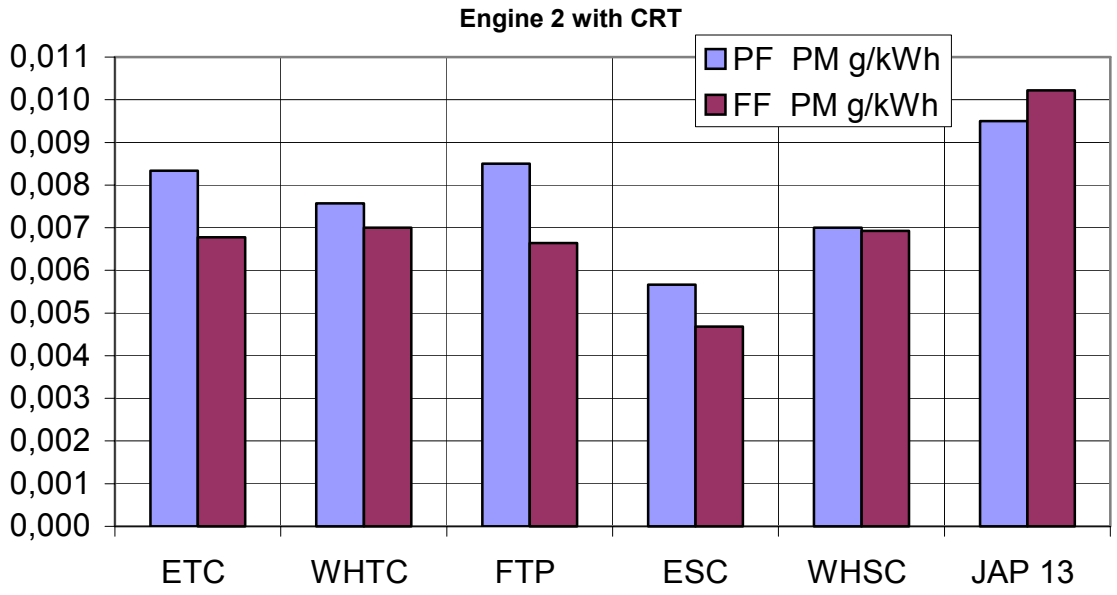

Fig 2.3.2.2-1: PM results Engine 2 with CRT-System

Looking at the variability (COV), the values are also higher than 10% (**Fig. 2.3.2.2-2**). But it has to be considered again that the very low absolute number of the results is of some importance here. The mean results of the PM measurements on *engine 2* are listed **Table 2.3.2.2-1** and **2.3.2.2-2.**

The high COV numbers for the measurements on the engine(s) with CRT-Systems are not favourable, especially not for type approval due to inter-laboratory comparison etc. Since this high variability was, however, observed for both systems (full flow and partial flow), this gives evidence that partial flow dilution systems perform as well as full flow dilution systems and could therefore be used for type approval measurements under transient conditions. In this respect, it has to be noted that the partial flow system COV were in the most cases (slightly) better than for the full flow system. It should also be noted that an absolute standard deviation between 0.001 and 0.002 g/kWh, as mostly achieved during this programme, is a relatively low variability.

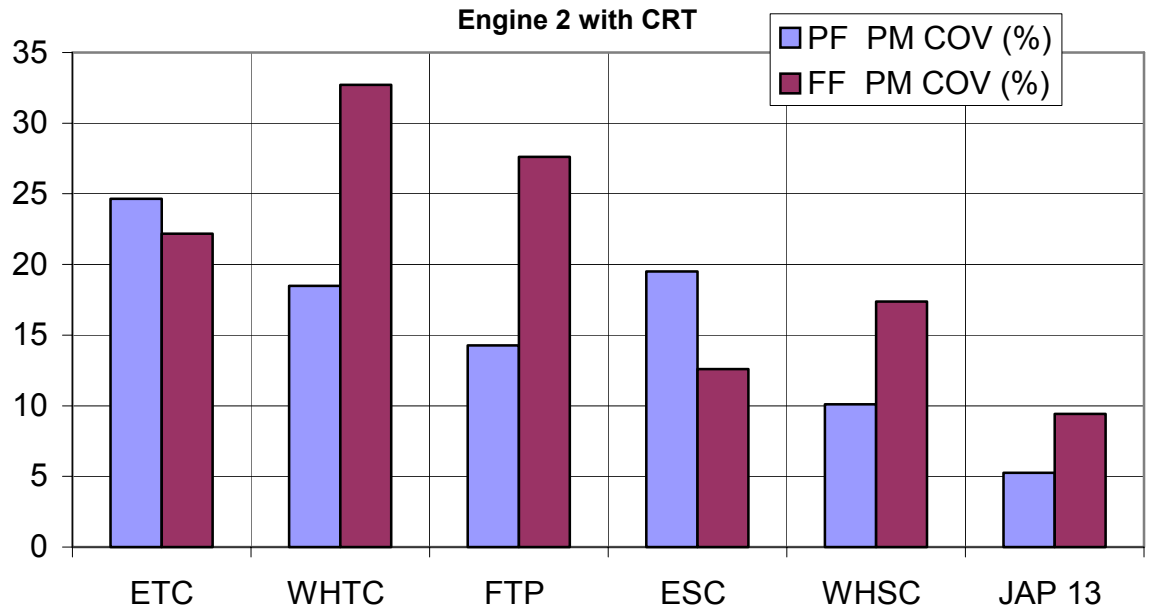

Fig. 2.3.2.2-2: PM-COV results Engine 2 with CRT-System

PM results	ETC	WHTC	U.S.-FTP
PM FF mean value (g/kWh)	0.0068	0.0070	0.0066
PM PF mean value (g/kWh)	0.0083	0.0076	0.0085
FF stand. Deviation	0.0015	0.0023	0.0018
PF stand. Deviation	0.0021	0.0014	0.0012
FF COV	22.18	32.72	27.60
PF COV	24.66	18.49	14.27
percentage-deviation (FF basis)	-22.05	-8.57	-28.78

Table 2.3.2.2-1: Summary of Transient Cycle PM results / Engine 2 with CRT

PM results	ESC	WHSC	JAP 13 mode
PM FF mean value (g/kWh)	0.0047	0.0069	0.0102
PM PF mean value (g/kWh)	0.0057	0.0070	0.0095
FF stand. Deviation	0.0006	0.0012	0.0010
PF stand. Deviation	0.0011	0.0007	0.0005
FF COV	12.60	17.37	9.41
PF COV	19.51	10.10	5.26
percentage-deviation (FF basis)	-21.27	-1.50	6.86

Table 2.3.2.2-2: Summary of Steady-state Cycle PM results / Engine 2 with CRT

2.3.2.3 Engine 3

The following figures show the transient test PM results of *engine 3*. This engine was operated without any advanced after-treatment system and therefore shows higher absolute values and COV values, which are typically well below 10%.

Both particulate matter measurement systems show very comparable data (**Fig. 2.3.2.3-1**). As for *engine 1* and *2* the highest deviations between the full flow and the partial flow system could be seen for the U.S.-FTP cycle (13,6%). For all other cycles the deviation (taking the full flow system as basis) is below 10%. For the COV all data shows very low numbers below 5%, except for the ESC (below 6%) (**Fig. 2.3.2.3-2**).

The detailed PM measurement data for *engine 3* is again listed in the tables below (**Tables 2.3.2.3-1** and **2.3.2.3-2)**.

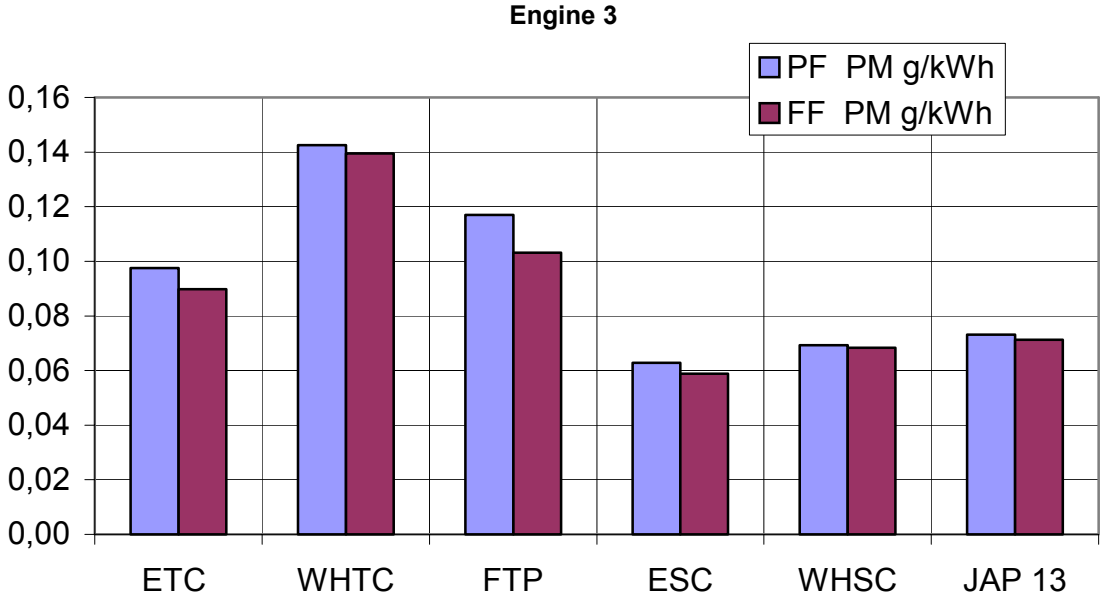

Fig. 2.3.2.3-1: PM results Engine 3

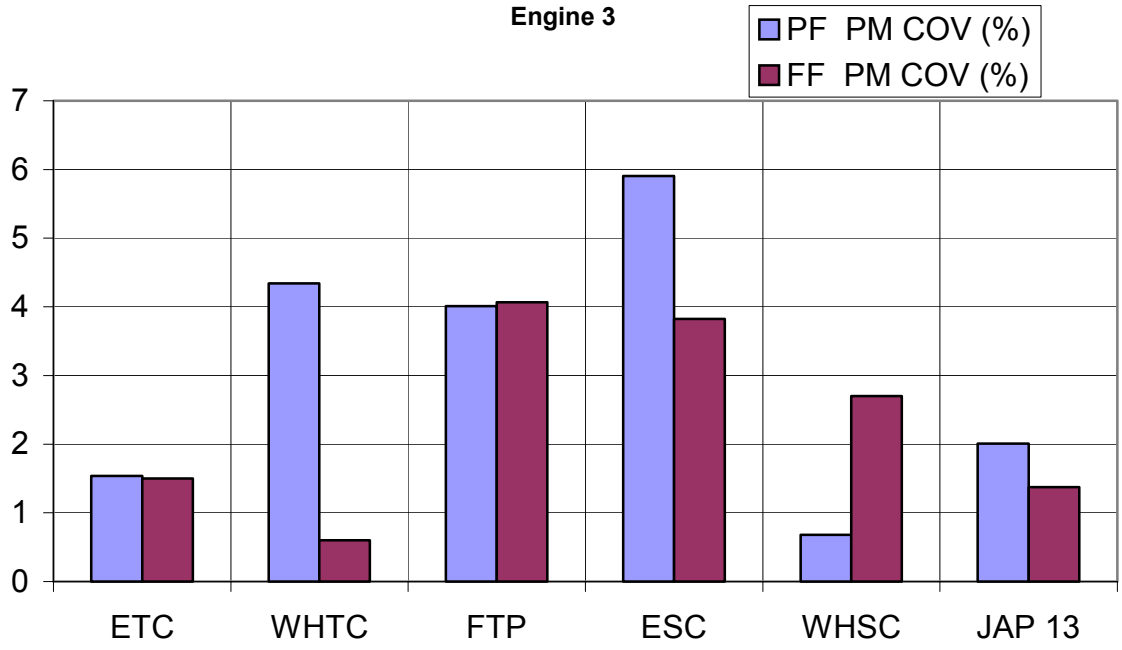

Fig. 2.3.2.3-2: PM-COV results Engine 3

PM results	ETC	WHTC	U.S.-FTP
PM FF mean value (g/kWh)	0.0898	0.139	0.103
PM PF mean value (g/kWh)	0.0975	0.142	0.117
FF stand. Deviation	0.0013	0.0008	0.0042
PF stand. Deviation	0.0015	0.0062	0.0047
FF COV	1.49	0.60	4.07
PF COV	1.54	4.34	4.01
percentage-deviation (FF basis)	-8.57	-2.15	-13.60

Table 2.3.2.3-1: Summary of Transient Cycle PM results / Engine 3

PM results	ESC	WHSC	JAP 13 mode
PM FF mean value (g/kWh)	0.0588	0.0683	0.0713
PM PF mean value (g/kWh)	0.0628	0.0693	0.0732
FF stand. Deviation	0.0023	0.0018	0.0010
PF stand. Deviation	0.0037	0.0005	0.0015
FF COV	3.82	2.69	1.37
PF COV	5.91	0.68	2.00
percentage-deviation (FF basis)	-6.80	-1.46	-2.66

Table 2.3.2.3-2: Summary of Steady-state Cycle PM results / Engine 3

2.3.2.4 Engine 4

The results of this engine (*engine 4*) correlate well with the results generated with the three other engines **(Fig. 2.3.2.4-1)**. The overall PM-emission values are higher than on *engine 3* and for that reason the variability is reduced again (**Fig. 2.3.2.4-2**). The highest deviation between the PM-measurement systems used again becomes evident for the U.S.-FTP (9.34%)

As for the *engines 1*, *2* and *3* the mean results are listed in the tables above (**Table 2.3.2.4-1** and **Table 2.3.2.4-2**). The percentage deviation between the full flow system and the partial flow system for the WHSC and WHTC is lowest on this engine (0,15% respectively 3%).

However this is also true for all other engines: The comparison of the partial flow and full flow system based on the percentage deviation shows the best values on all engines when operated in the WHSC / WHTC cycles.

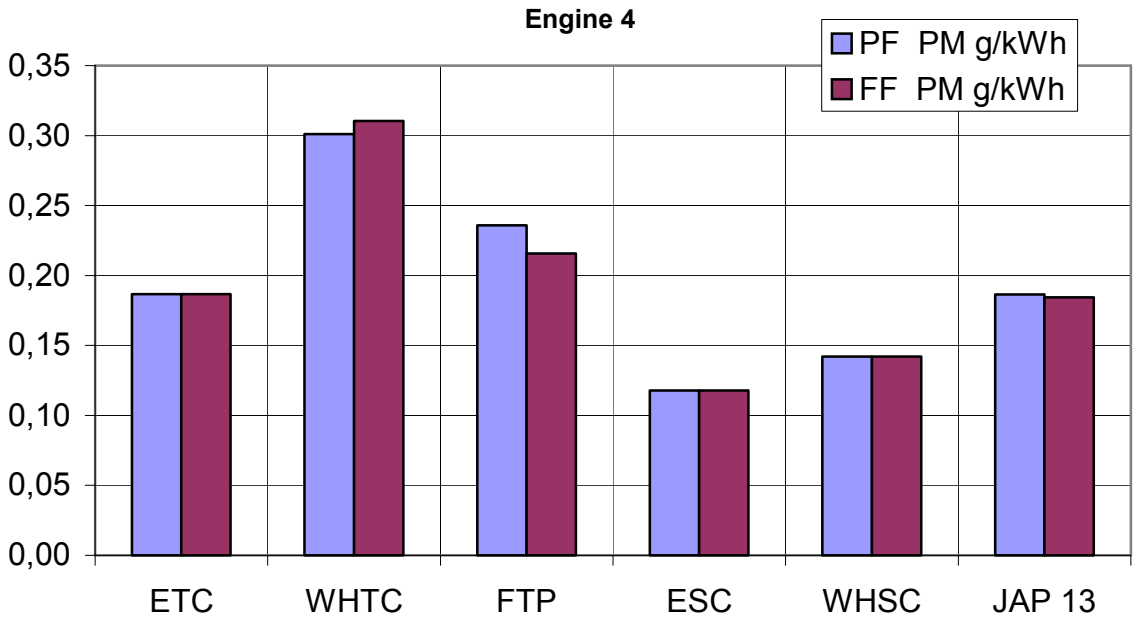

Fig. 2.3.2.4-1: PM results Engine 4

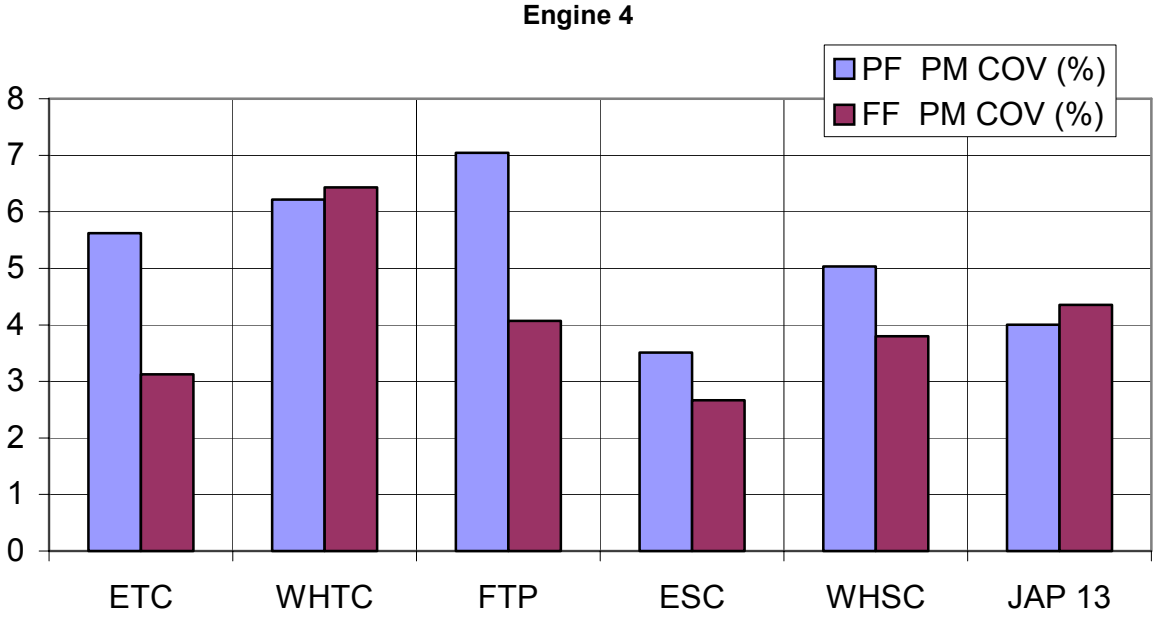

Fig. 2.3.2.4-2: PM-COV results Engine 4

PM results	ETC	WHTC	U.S.-FTP
PM FF mean value (g/kWh)	0.1867	0.3104	0.2156
PM PF mean value (g/kWh)	0.1868	0.3011	0.2358
FF stand. Deviation	0.0058	0.0262	0.0088
PF stand. Deviation	0.0105	0.0338	0.0166
FF COV	3.12	8.43	4.07
PF COV	5.62	9.22	7.05
Percentage deviation (FF basis)	0	2.99%	-9.34

Table 2.3.2.4-1: Summary of Transient Cycle PM results / Engine 4

PM results	ESC	WHSC	JAP 13 mode
PM FF mean value (g/kWh)	0.118	0.1422	0.184
PM PF mean value (g/kWh)	0.118	0.1420	0.186
FF stand. Deviation	0.0031	0.0054	0.0080
PF stand. Deviation	0.0041	0.0071	0.0075
FF COV	2.67	3.79	4.35
PF COV	3.51	5.03	4.00
Percentage deviation (FF basis)	0	0.15%	-1.08

Table 2.3.2.4-2: Summary of Steady-state Cycle PM results / Engine 4

2.3.3 Particulate analysis

In order to determine the soluble organic and insoluble (SOF / INSOF) fractions sampled on the PM measurement filters, a SOF- / INSOF-analysis was performed using chemical extraction methodologies. The SOF portion was determined by extraction of the filter with dichloro-methane and weighing afterwards. The loss of particle weight corresponds to SOF. The sulphate portion was then determined by extraction with a H_2O / isopropanol mixture (95% to 5%) and ICP-atomary spectroscopy. The soot fraction was then calculated by subtracting SOF and sulphate from the total particulate mass.

For the engines equipped with CRT systems the method described above was modified to overcome problems of the extraction method due to the very low filter loadings.

For that reason the INSOF fraction on the sampling filter was determined by using the black carbon black carbon method in parallel to the extraction methods. Details of this method are given in /8 to 10/.

For each cycle and each engine two full flow (FF) results and two partial flow (PF) results were analysed using this method. In the case of the two engines (*engine 1* and *engine 2*) equipped with CRT it has to be considered that the SOF-/ INSOF-values can only be used for showing a trend towards particulate matter composition, since the accuracy and sensitivity of the extraction method is poorer with the lower filter loadings..

Fig. 2.3.3-1 shows the results on *engine 1* with CRT. The SOF plus sulphate-values were calculated by using the mean values of the PM results and the percentage value of the SOF plus sulphate content in order to indicate the SOF plus sulphate or, rather, the non-soot / non-carbon portion in g/kWh. The WHDC cycles with the post-fix 1 shown in **Fig. 2.3.3-1** were generated using the penultimate cycle definition for comparison reasons (see chapter 2.2.1).

Nearly the total PM-emission consists of non-soot (SOF plus sulphate) on this engine due to the fact that the CRT-System is blocking the major part of the soot particles. The mean fraction of the SOF plus sulphate to the total gravimetric PM-value is at 93%. These values also show that there is no significant difference between the partial flow and full flow SOF plus sulphate portion at these very low values..

If the engine is operated without CRT-system the PM composition is changed. **Fig. 2.3.3-2** shows data of the final and version 1 WHDC cycles (see chapter 2.7.1) for *engine 1* without CRT-system. The SOF plus sulphate mean-value of all cycles is at approximately 40%, or 30% for the transient cycles only. The SOF plus sulphate level based on the mean values found on the partial flow systems sampling filter is very slightly higher than for the full flow system. The absolute SOF plus sulphate-level is more or less the same over all cycles. This shows that more soot is produced during transient operation of the engine.

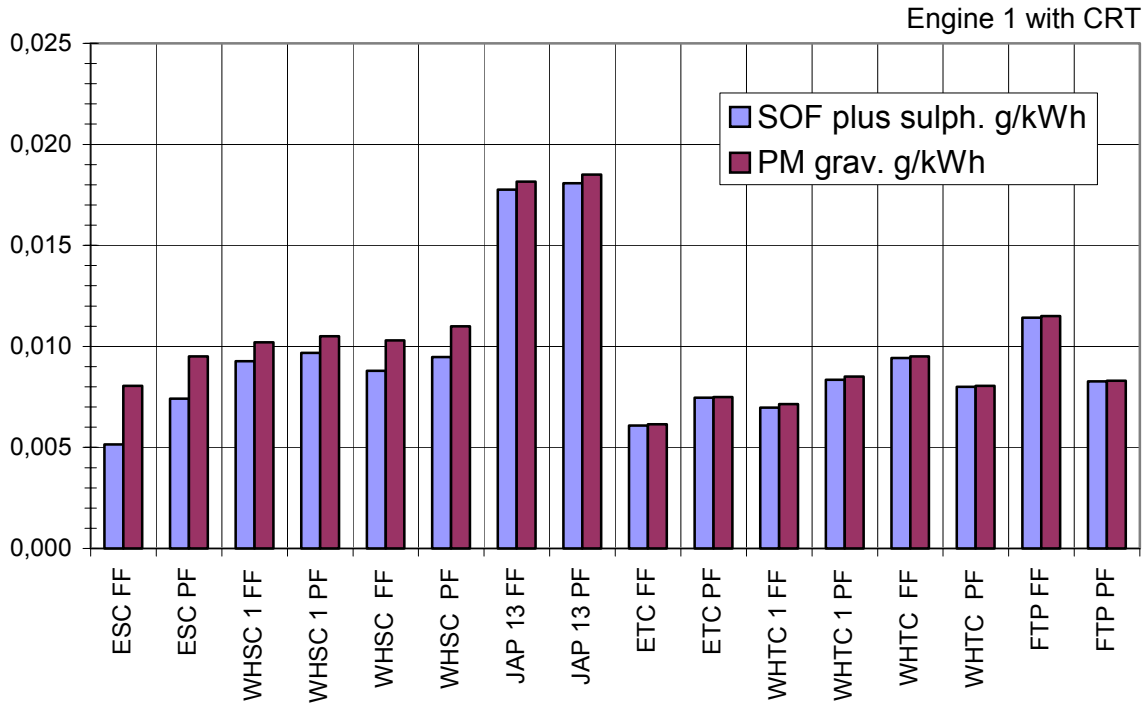

Fig. 2.3.3-1: SOF plus sulphate / PM, engine 1 with CRT

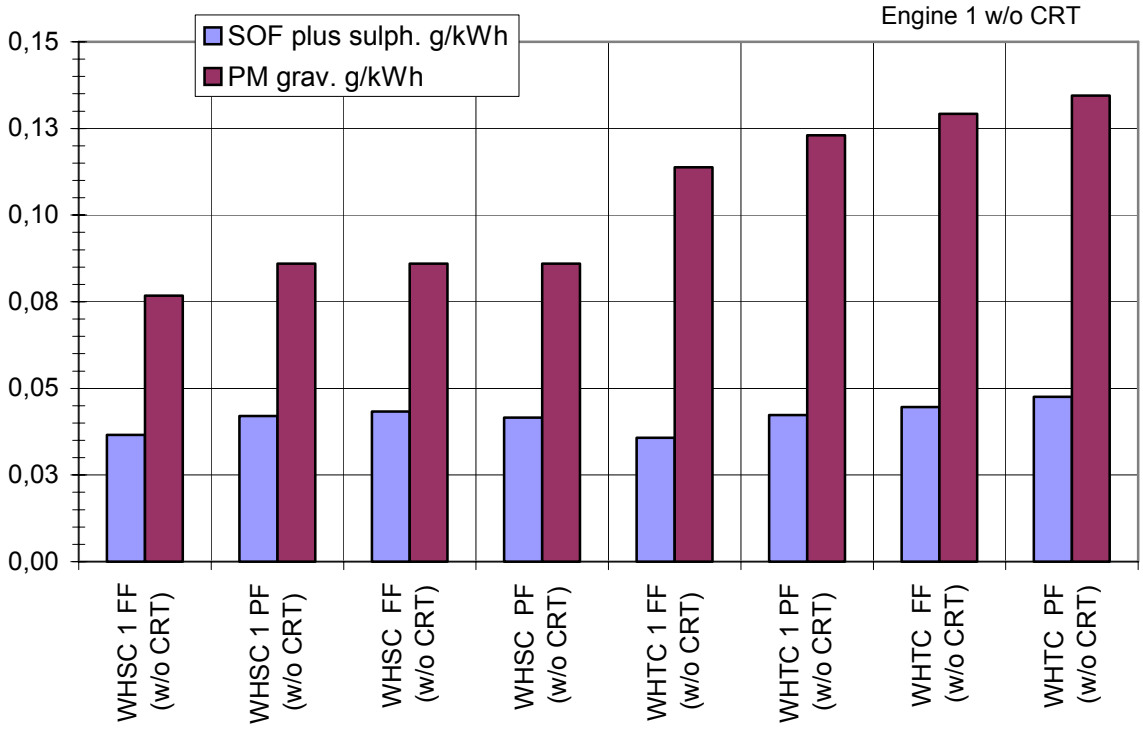

Fig. 2.3.3-2: SOF plus sulphate / PM, engine 1 without CRT

For *engine 2*, also equipped with CRT, the results look very much the same as for *engine 1*. Nearly the complete total gravimetric PM-emissions can be seen as non-soot (SOF plus sulphate) fraction (**Fig. 2.3.3-3**).

For *engine 3* (**Fig. 2.3.3-4**) the situation is similar to *engine 1* without CRT. The fraction of SOF plus sulphate to the total gravimetric PM-emission is at an average level of 21% for all cycles. Again it can be seen that in general the SOF plus sulphate level is relatively constant over all cycles. This was also found in other studies /7/. **Fig. 2.3.3-5** shows the SOF plus sulphate values for *engine 3* only.

The results for *engine 4* are shown in **Fig. 2.3.3.-6**. The overall SOF plus sulphate-portion of the total gravimetric PM-values is at an average of 45% over all cycles. In contrast to *engine 1* without CRT and *engine 3* the general SOF plus sulphate part shows some cycle dependency here, especially for the WHTC cycles on both systems (partial flow and full flow).

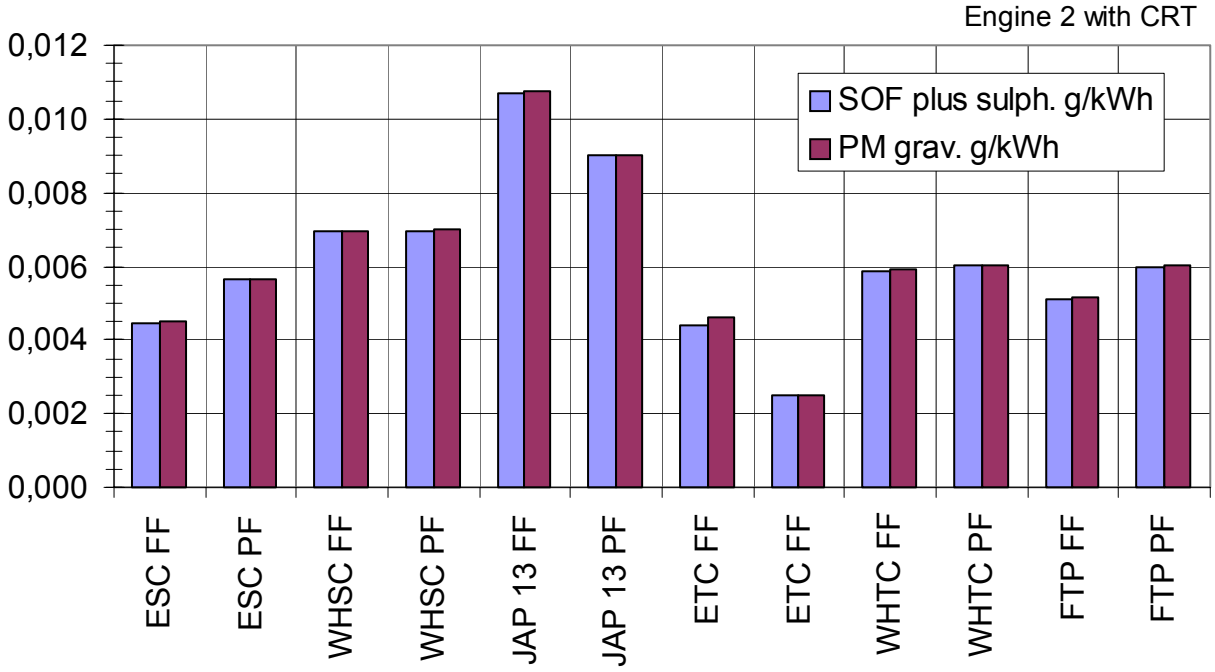

Fig. 2.3.3-3: SOF plus sulphate / PM, engine 2 with CRT

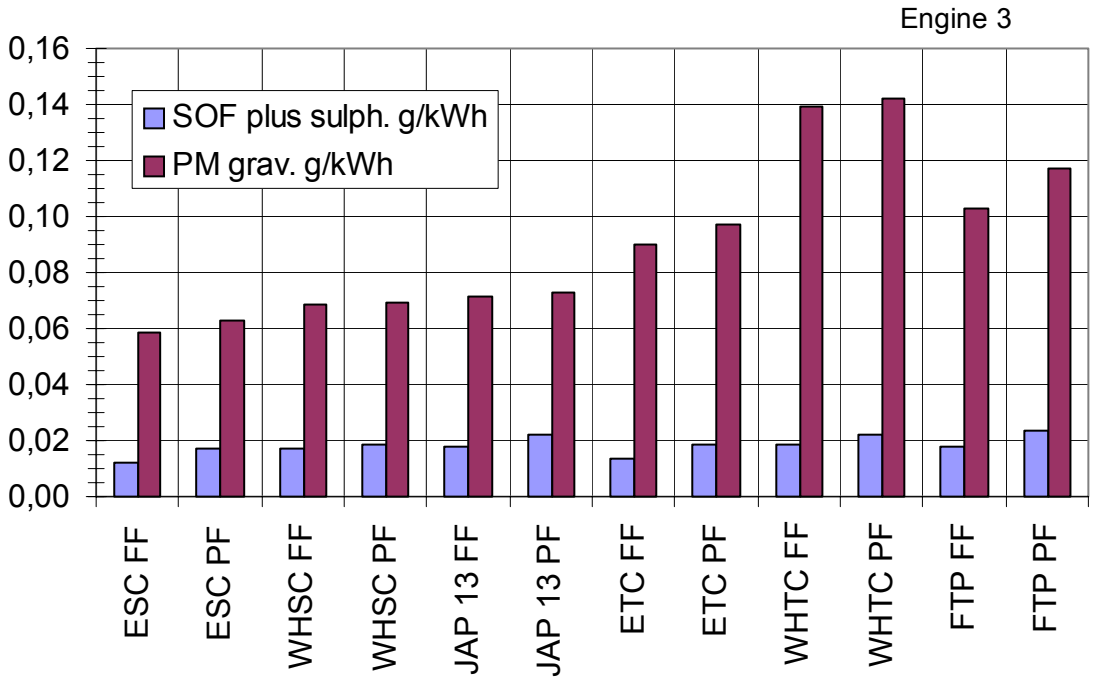

Fig. 2.3.3-4: SOF plus sulphate / PM, engine 3

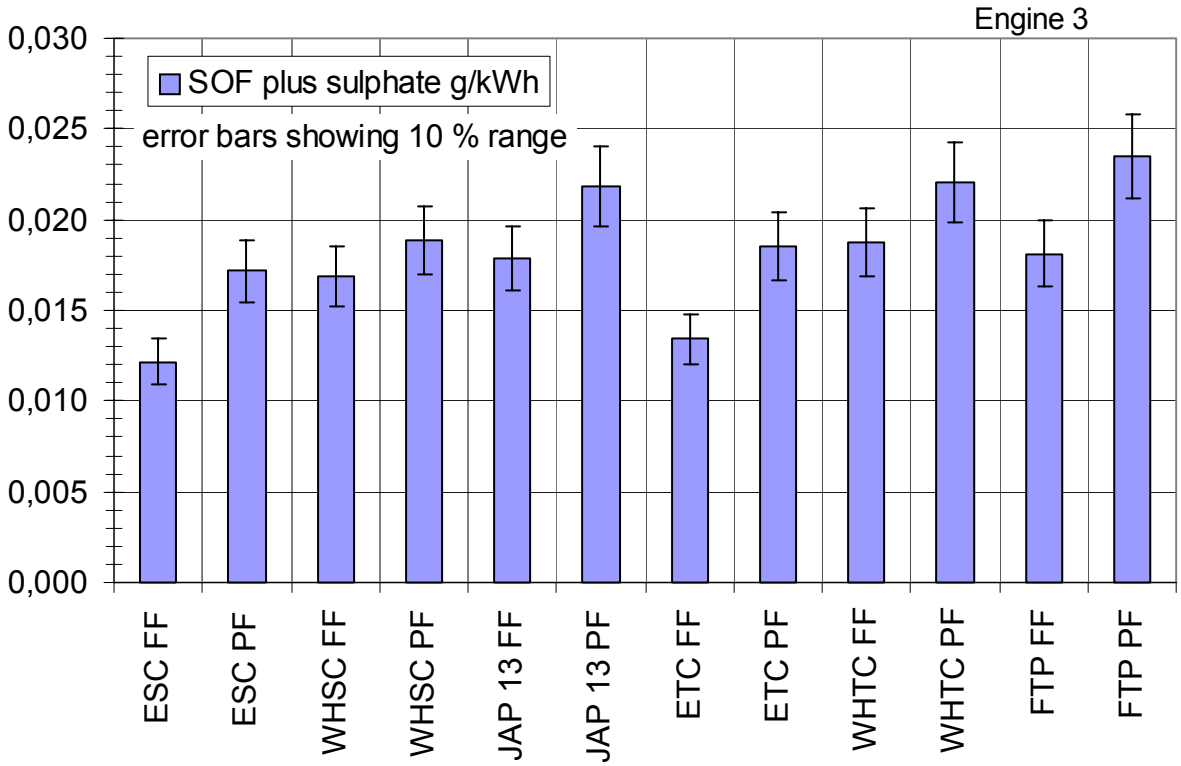

Fig. 2.3.3.-5. SOF plus sulphate, engine 3

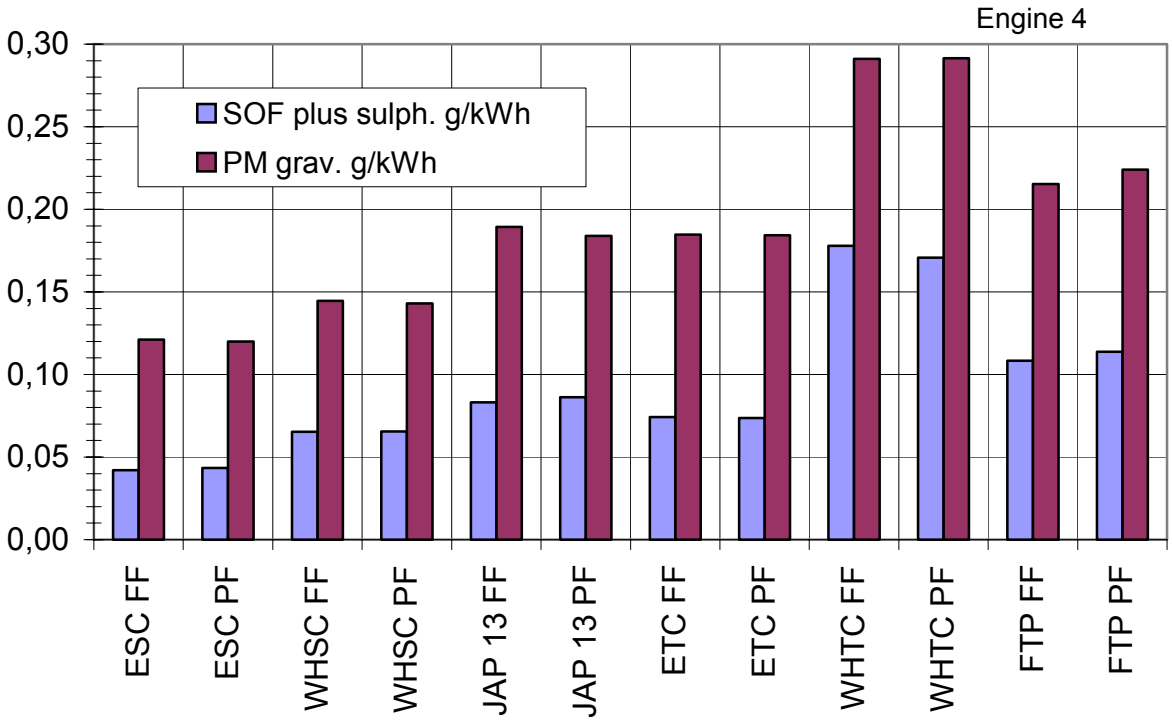

Fig. 2.3.3.-6. SOF plus sulphate / PM, engine 4

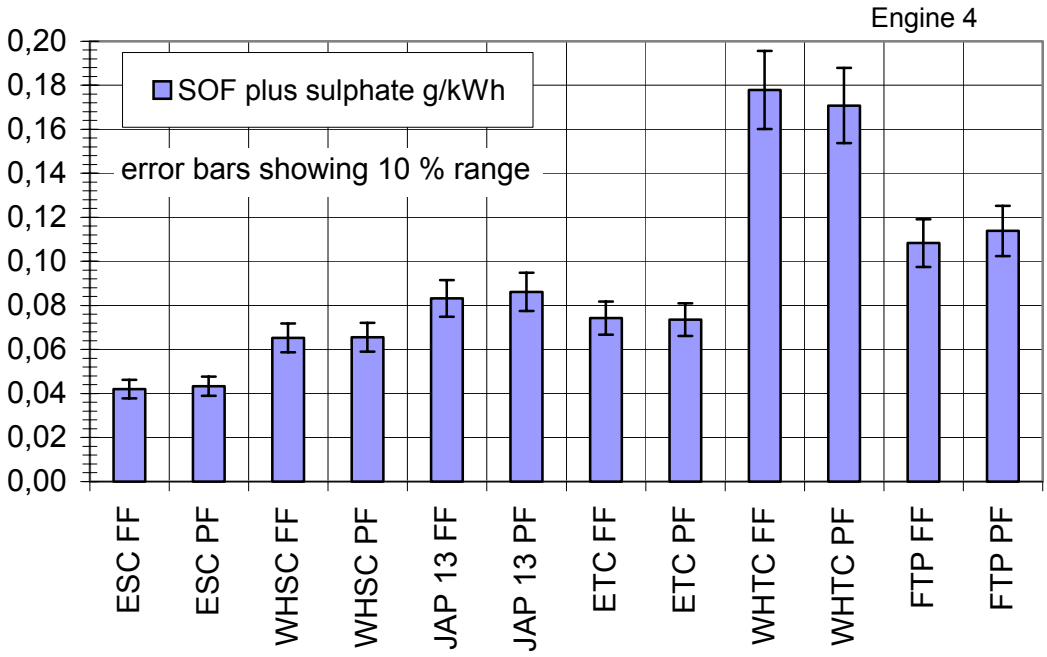

Fig. 2.3.3.-7. SOF plus sulphate, engine 4

In **Fig. 2.3.3-7** this higher SOF plus sulphate-portion for the WHTC can be seen. It is more than twice as high as for the WHSC-cycle. Nonetheless, there are again only minor differences between the partial flow and full flow SOF plus sulphur-portion. It can therefore be concluded that the two measurement principles are comparable.

2.4 Comparison of raw / diluted measured gaseous components

2.4.1 Measurement system description

The gaseous emissions were measured with two analyser racks (one in the raw, one in the diluted exhaust gas) operated in parallel during the test programme. Both systems were adjusted to operate with a maximum difference of ± 2% using a reference gas. Both racks met the requirements of the corresponding regulation; Directive 1999/96/EC amended by 2001/27/EC for the diluted line and ISO 16183 for the raw measurement line. The system used for the raw measurements was adjusted and operated in accordance to ISO 16183 including all necessary "sub"-measurement devices (e.g. determination of exhaust gas mass flow etc.). Both exhaust gas analyser systems were connected to one host computer in order to meet the time alignment criteria of the corresponding regulation, respectively the ISO-Standard. The systems were operated without an automatic measuring range switching.

Diluted line:

Siemens SIGAS 500

-- CO (NDIR): Siemens ULTRAMAT 5E-2R
-- CO2 (NDIR): Siemens ULTRAMAT 5E
-- HC (FID): Testa 2000 MP
-- NOx (CLD): Pierburg PM-2000
-- O2 (paramagn.): Siemens OXIMAT

Raw line:

Horiba Mexa 9130

-- CO (NDIR): Horiba AIA 320
-- CO2 (NDIR): Horiba AIA 310
-- HC (FID): Horiba FIA 325
-- NOx (CLD): Horiba CLA 355
-- O2 (paramagn.): Horiba MPA 320

2.4.2 Results of gaseous component measurements

The following figures show the results of the regulated gaseous components measured in the raw and in the diluted exhaust gas. Each diagram shows the mean values of all cycles driven during the entire programme separated for each engine. .

2.4.2.1 Engine 1

Fig. 2.4.2.1-1 shows the results of the regulated gaseous components for *engine 1* equipped with CRT-System. Due to the catalytic converter used in the CRT-system the absolute concentrations for CO and HC are very low on *engine 1*, especially in the diluted exhaust gas. For that reason the CO- and HC-emission results show relatively high variations for *engine 1*. Further it has to be noted that the background correction for the diluted (CVS-based) measurements according to /5/ and /6/ could have an enormous influence on the results of the diluted measurement.

This influence gets stronger with very low absolute emission values of an engine. A slight fluctuation of the background concentration of HC and CO may lead to a much higher fluctuation of the corrected emission value

Fig. 2.4.2.1-2 shows the NOx-emission variation range in percentage of the calculated average (mean)-value. The mean value was set to 0% (base line) and the maximum and minimum measured values are indicated as error bars. The variability range is very well within ± 2%. This indicates that the raw gas measurement can be applied to transient cycles although the minimum- / maximum-range is slightly wider than for the diluted measurement.

In **Fig. 2.4.2.1-3** the variation range for the CO-emission on *engine 1* with CRT is shown. Due to the very low absolute emission values the variation range is very wide even for the raw gas measurement.

Nonetheless, it could be seen that for this engine the range of the raw gas measurements (max. approx. ±30%) is smaller than that for the diluted sampling (max. approx. +60% / -50%). In principle, this is the same for the HC-emission with some differences in the absolute number of the minimum-/maximum-range (**Fig. 2.4.2.1-4**).

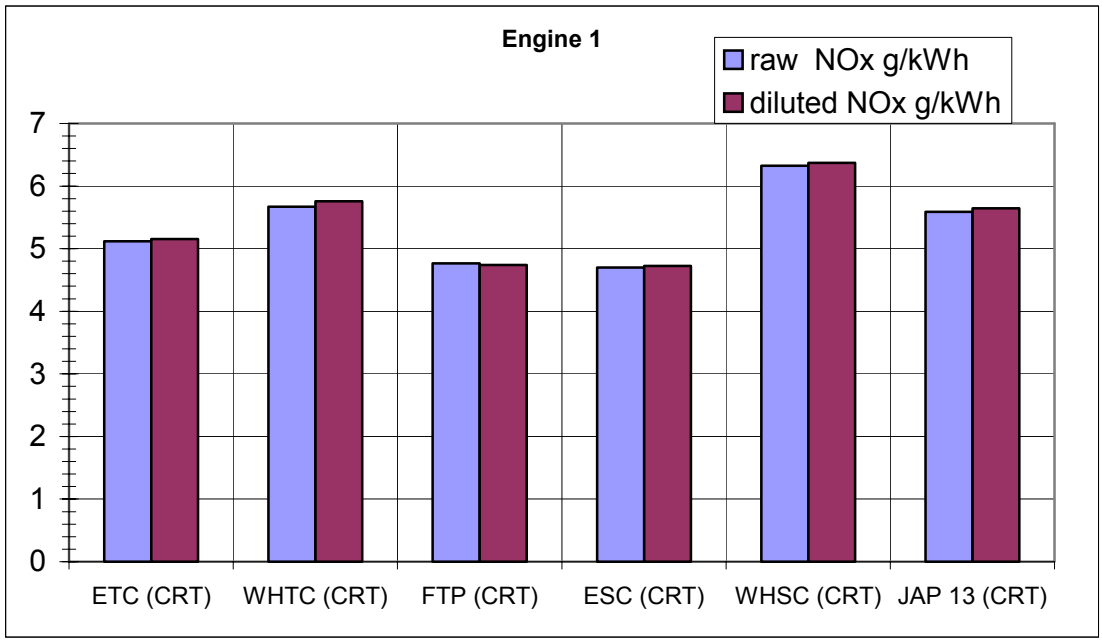

Fig. 2.4.2.1-1a: Gaseous Components engine 1 with CRT

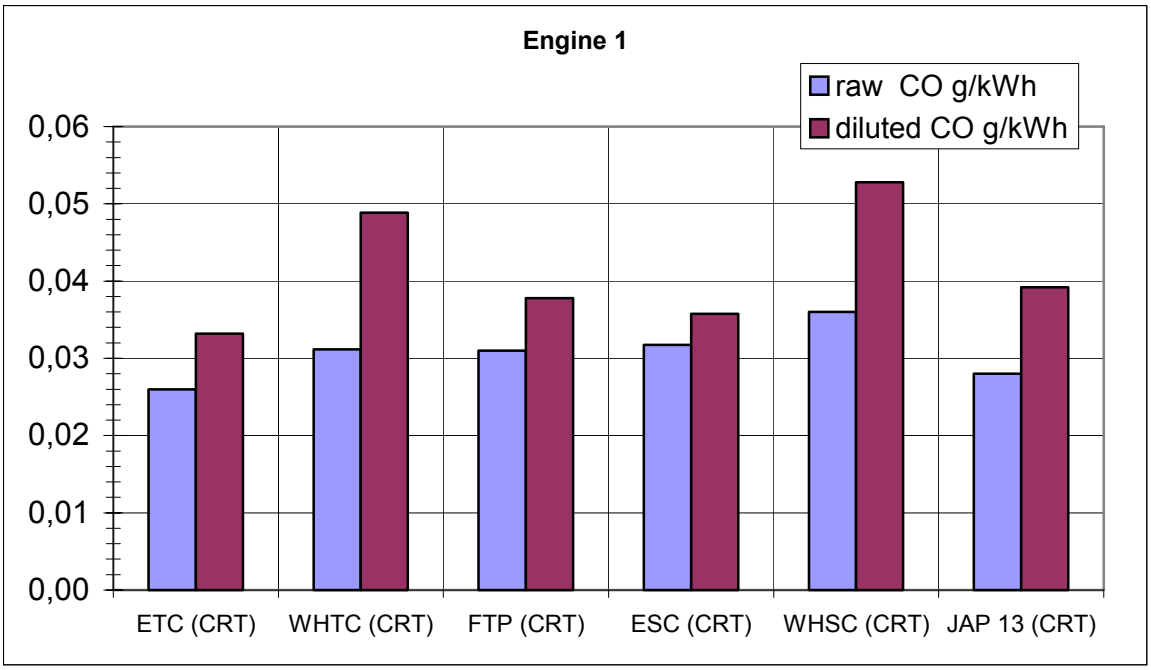

Fig. 2.4.2.1-1b: Gaseous Components Engine 1 with CRT

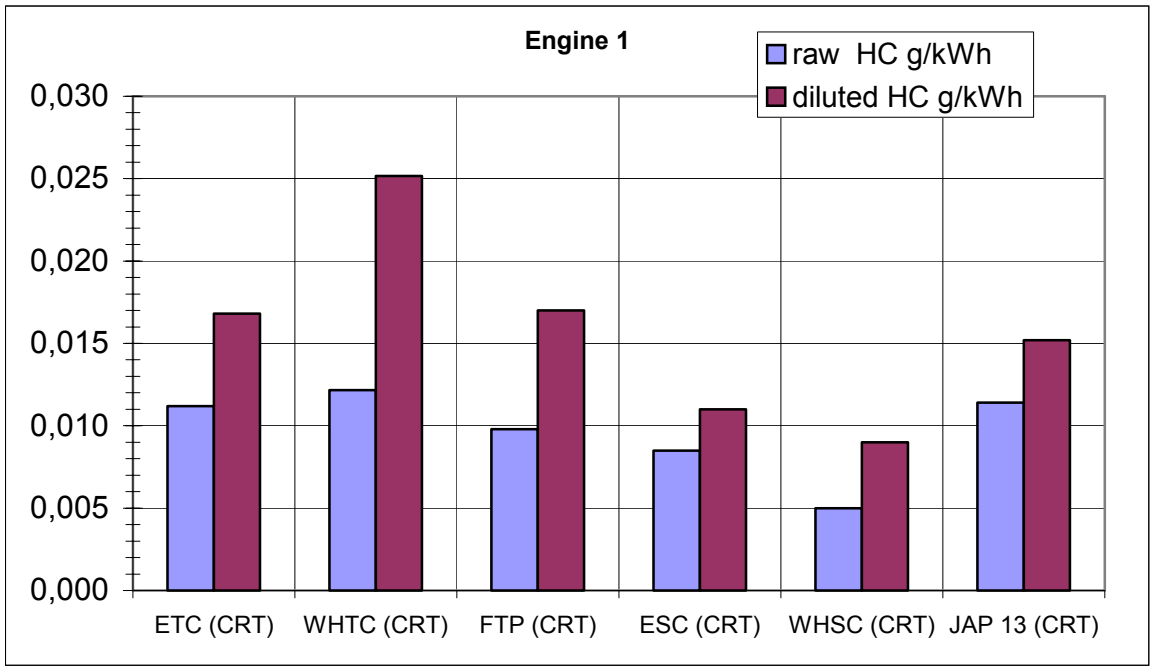

Fig. 2.4.2.1-1c: Gaseous Components Engine 1 with CRT

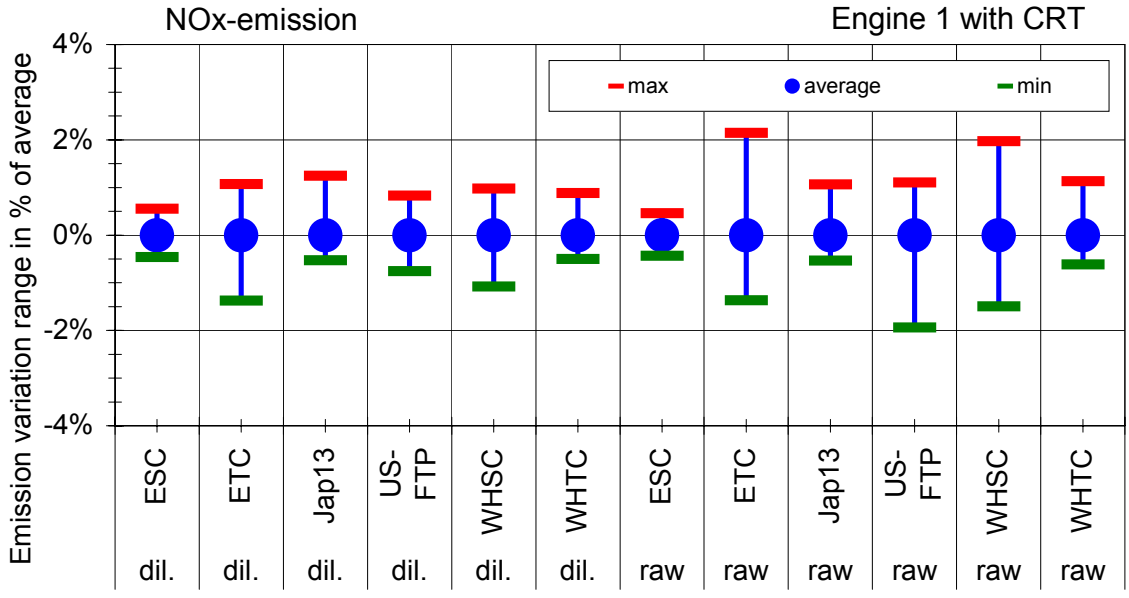

Fig. 2.4.2.1-2: NOx-emission variation range in percentage of average / Engine 1 with CRT

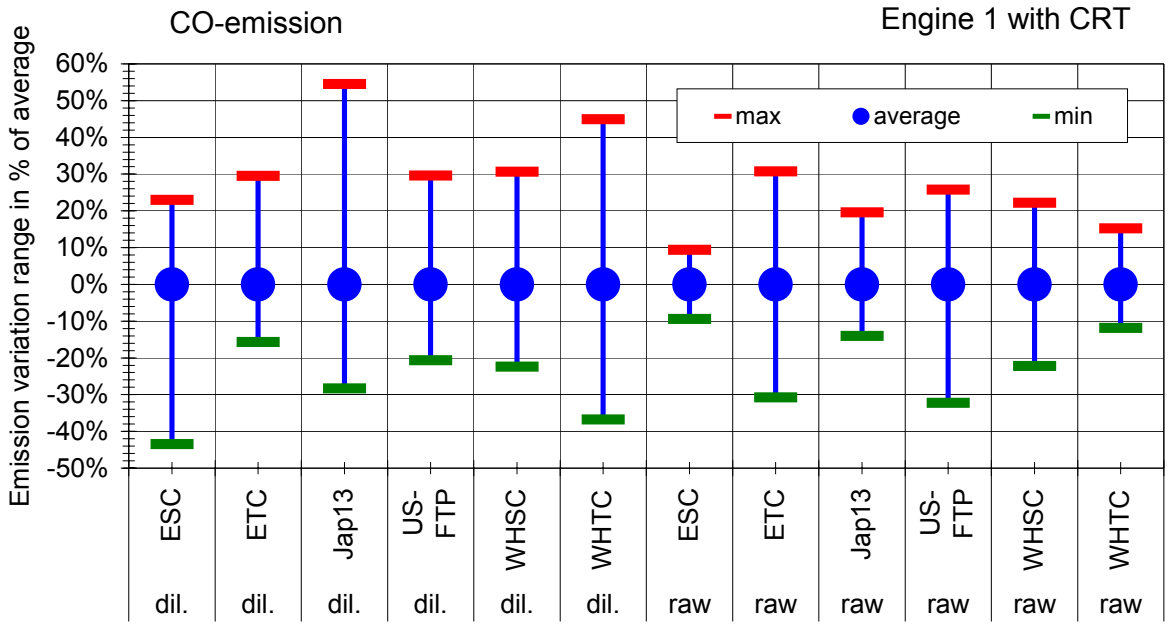

Fig. 2.4.2.1-3: CO-emission variation range in percentage of average / Engine 1 with CRT

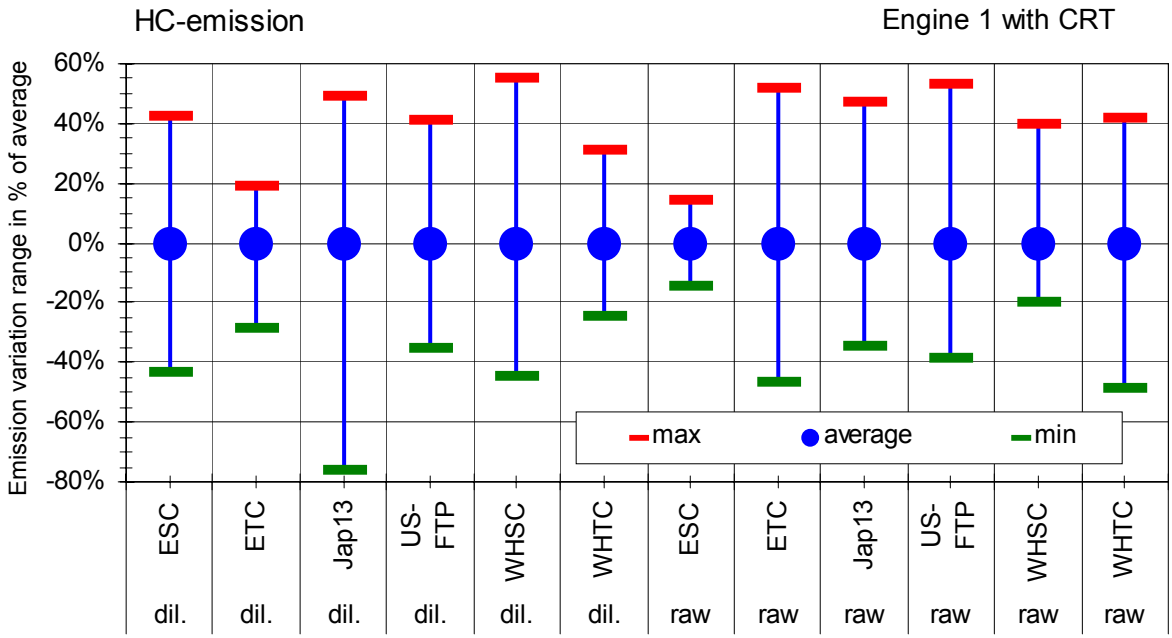

Fig. 2.4.2.1-4: HC-emission variation range in percentage of average / Engine 1 with CRT

2.4.2.2 Engine 2

Since *engine 2* was also equipped with a CRT-System the emission values of this engine are very similar to what could be seen on *engine 1* (**Fig. 2.4.2.2-1**) The comparison of the raw and diluted NOx-measurement again shows very good alignment. As for *engine 1*, the highest NOx-values were measured for the WHTC and WHSC cycles.

For the CO and HC measurement the same statement as already given for *engine 1* is applicable. Due to the oxidation process in the catalytic converter of the CRT-System the absolute values of these two components are very low. For that reason highly scattered results for both the raw and diluted measurements could be observed. This scattering becomes more obvious when looking at every cycle. These results could not be traced back to the measurement principle (raw or diluted), but are dependent on the very low absolute emission level.

Despite the fact that the scattering determined here is caused by approaching the limit of detection of the analysers it could be seen in the emission variation range in percentage of the average value that the raw measurement gives some advantage here. Nonetheless it has to be stated that measurement accuracy and sensitivity in the case of gaseous HC and CO emissions is compromised for CRT-Systems including highly active oxidation catalyst.

Fig. 2.4.2.2-2 shows the NOx-emission variation range in percent of average for *engine 2* (with CRT). The deviation around the mean value lies in a range of ± 6%. In **Figures 2.4.2.2-3** and **2.4.2.2-4** the variation range for the CO- and HC-results on *engine 2* are shown.

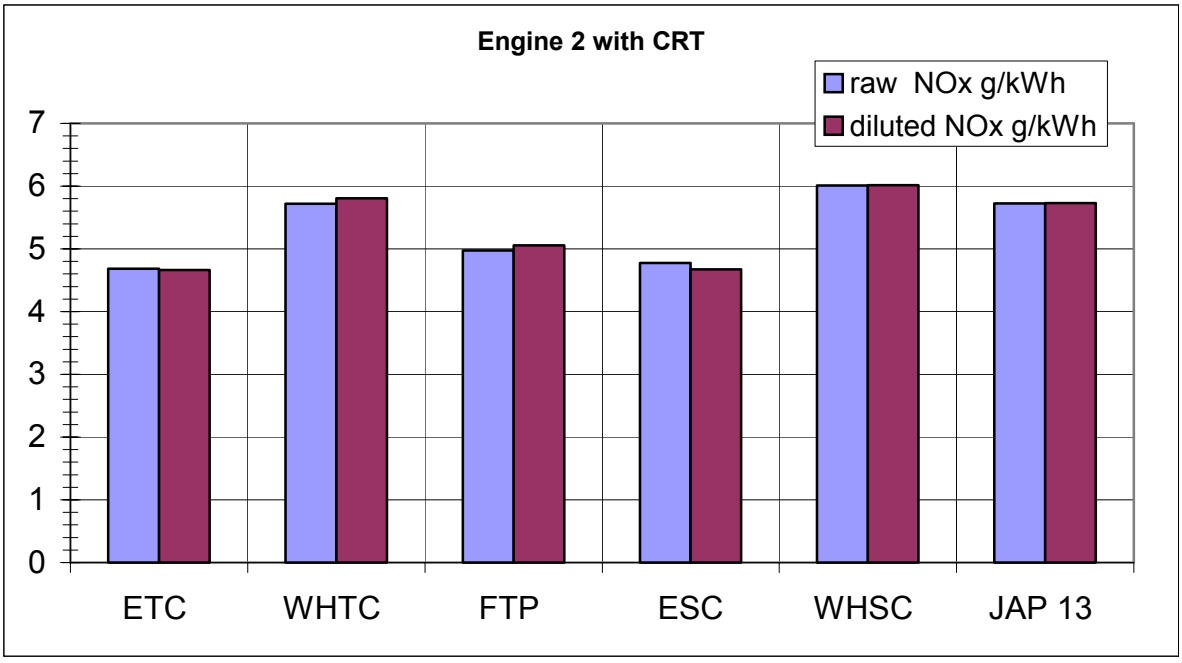

Fig. 2.4.2.2-1a: Gaseous Components Engine 2 with CRT

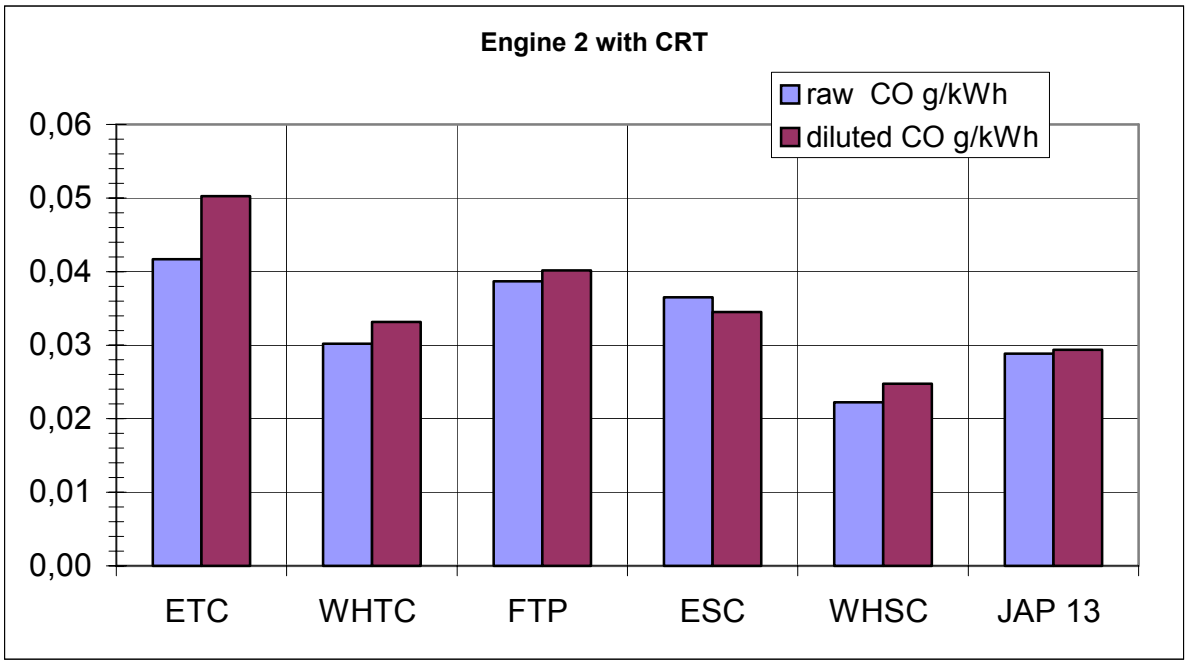

Fig. 2.4.2.2-1b: Gaseous Components Engine 2 with CRT

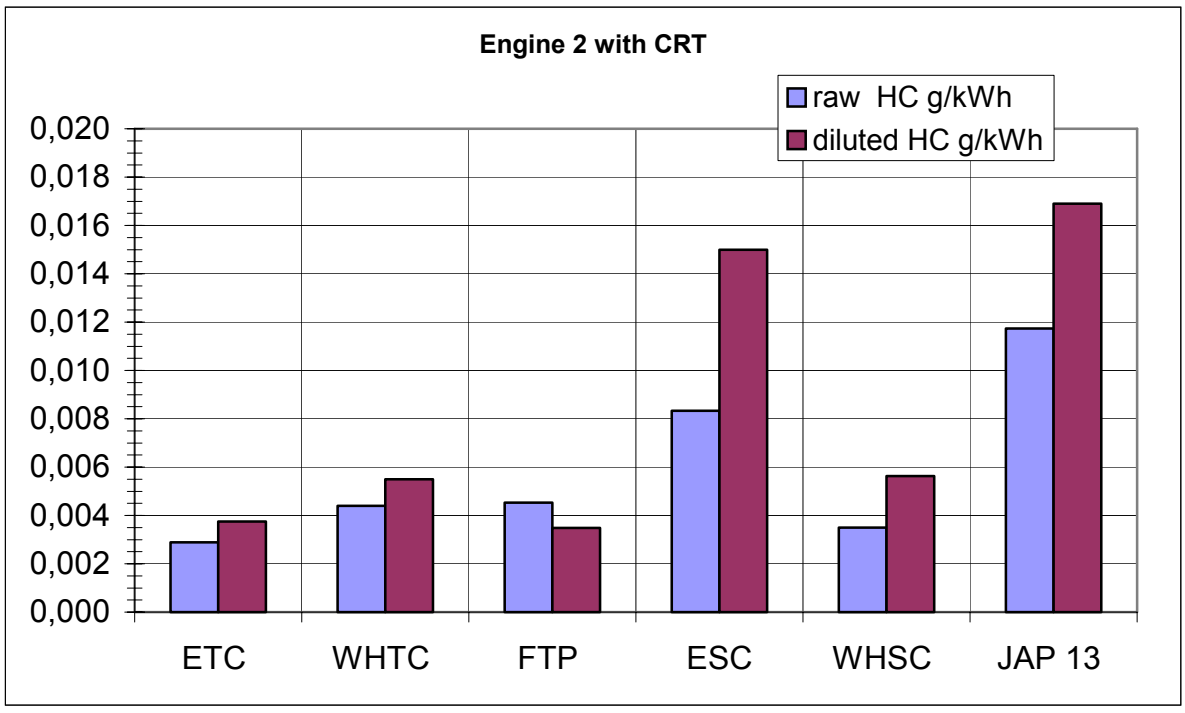

Fig. 2.4.2.2-1c: Gaseous Components Engine 2 with CRT

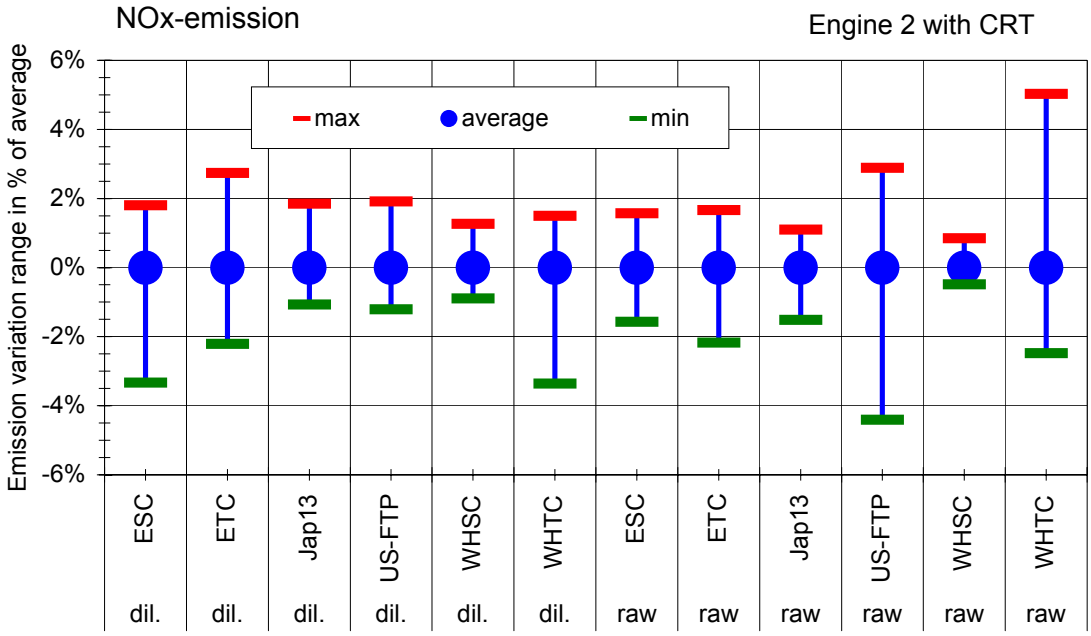

Fig. 2.4.2.2-2: NOx-emission variation range in percentage of average / Engine 2 with CRT

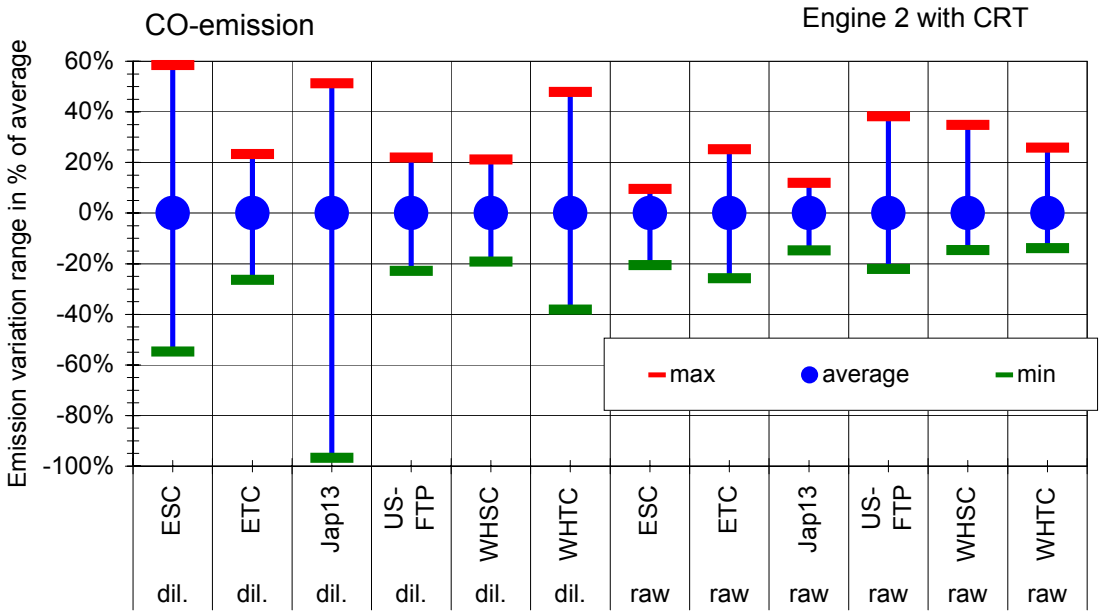

Fig. 2.4.2.2-3: CO-emission variation range in percentage of average / Engine 2 with CRT

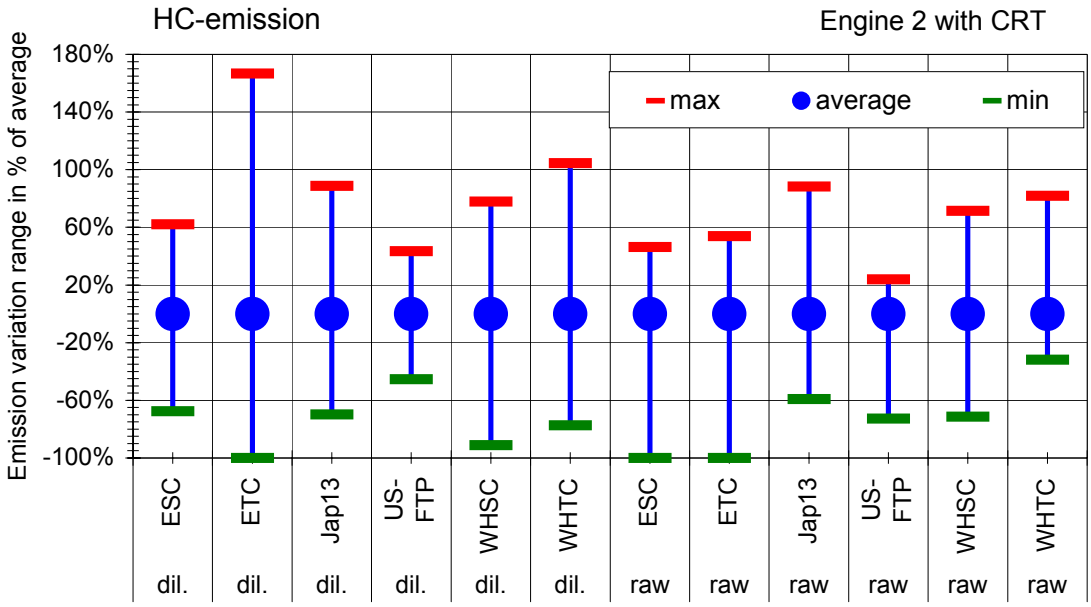

Fig. 2.4.2.2-4: HC-emission variation range in percentage of average / Engine 2 with CRT

2.4.2.3 Engine 3

The following figure shows the gaseous emission results of *engine 3* (**Fig. 2.4.2.3-1**). The absolute numbers for the NOx-measurements are very close together and in good correlation to the results of *engine 1* and *2*. The values measured with the diluted exhaust gas are slightly higher with the exception of the ESC-cycle and the Japanese 13-mode-cycle where both systems (raw and diluted) have measured at approximately the same level.

Since no advanced after-treatment system was employed on this engine, the values of CO and HC are higher and show much better agreement between raw and diluted measurement. Both measurement principles indicate the same emission behaviour of the engine trend between the cycles.

The variation range of the NOx-emissions on *engine 3* lies between approx. –2% and +3%, which shows again the good applicability of the raw measurement procedure (**Fig. 2.4.2.3-2**). For the CO-emission (**Fig. 2.4.2.3-3**) the variation range is somehow wider with a maximum of +12% for the raw measurement during WHTC operation. Compared to the diluted measurement, the raw measurement variations are lower. **Fig. 2.4.2.3-3** indicates clearly that the variations were monitored with both systems (raw and diluted) so that they are very likely to be caused by the engine itself. The fact that both system layouts were capable of measuring these engine variations, although at slightly different levels , is again a good indicator of the similarity of results generated with raw exhaust gas measurement compared to diluted exhaust gas measurement.

For the HC-measurement on *engine 3* both system (raw and diluted) showed very low variations from the mean value (**Fig. 2.4.2.3-4**). For the diluted measurement the maximum variation is ±6%, for the raw measurement ±3%, which shows the improvement possible with raw exhaust gas sampling.

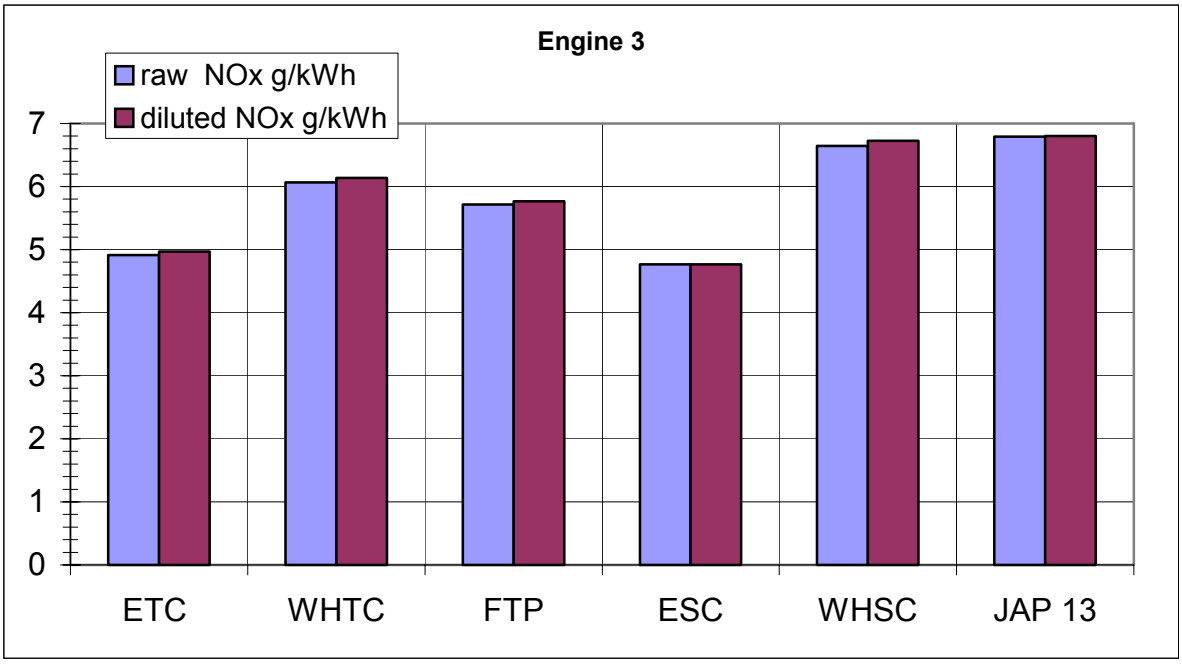

Fig. 2.4.2.3-1a: Gaseous Components Engine 3

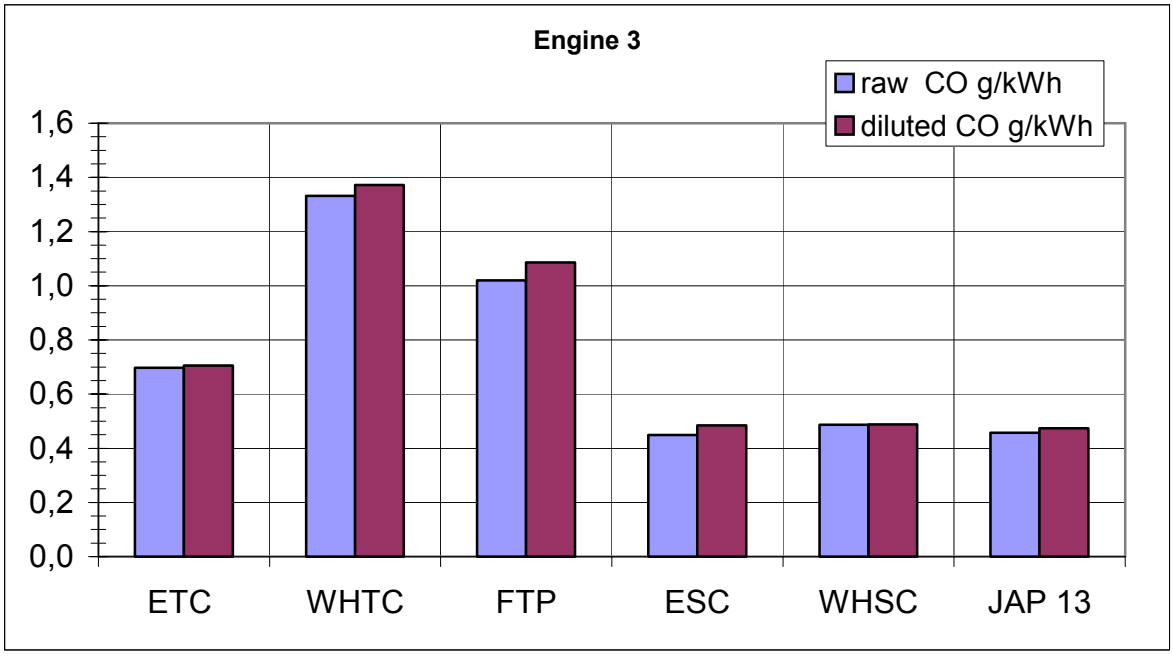

Fig. 2.4.2.3-1b: Gaseous Components Engine 3

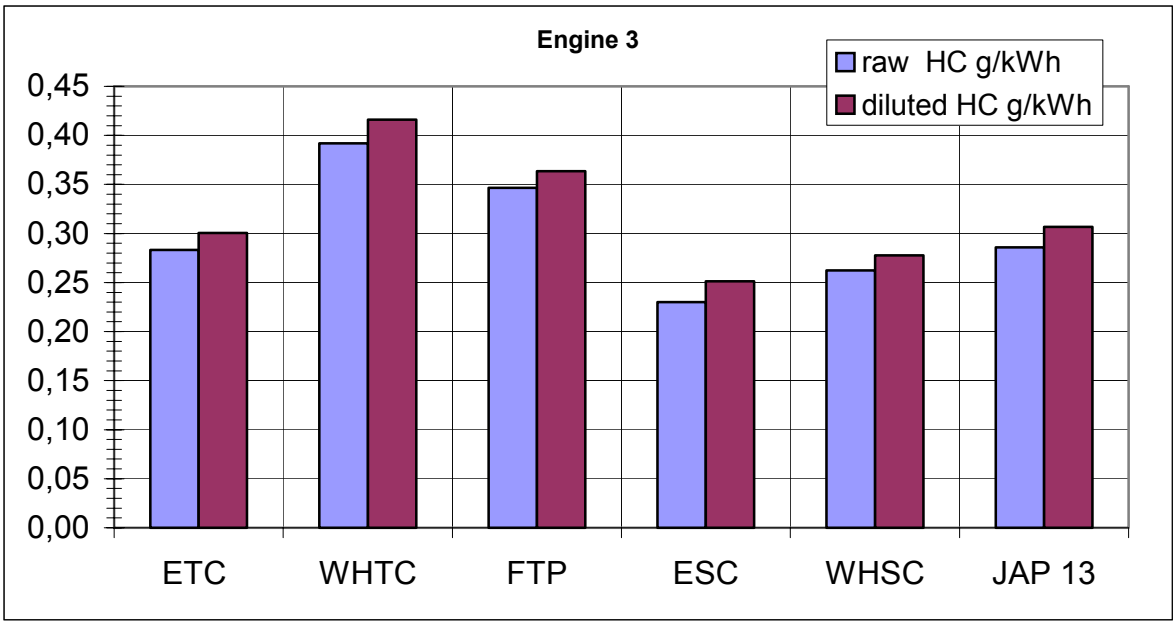

Fig. 2.4.2.3-1c: Gaseous Components Engine 3

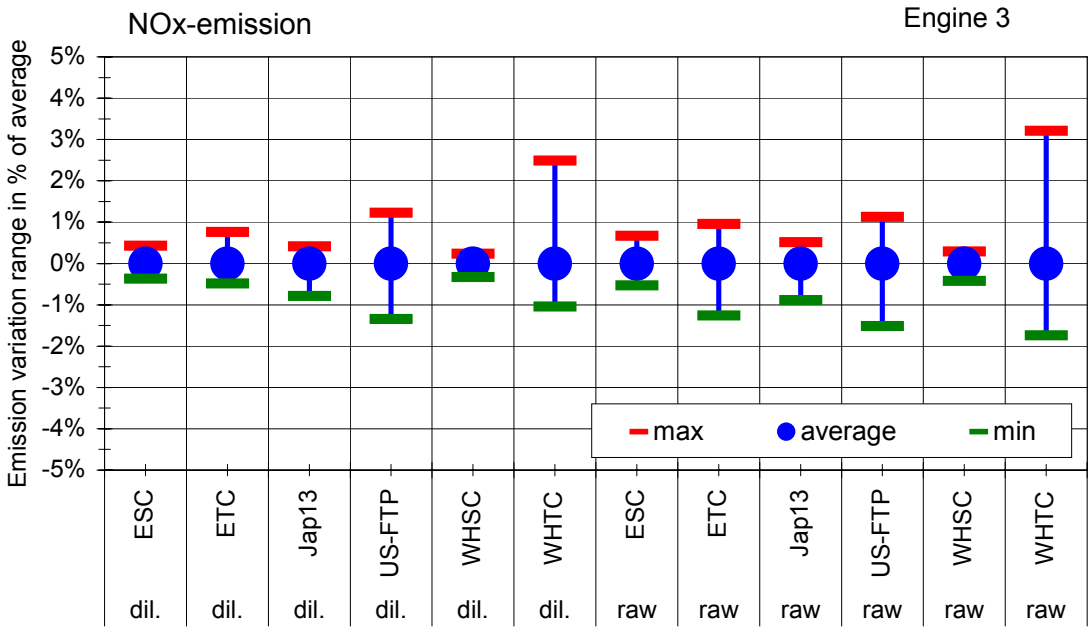

Fig. 2.4.2.3-2: NOx-emission variation range in percentage of average / Engine 3

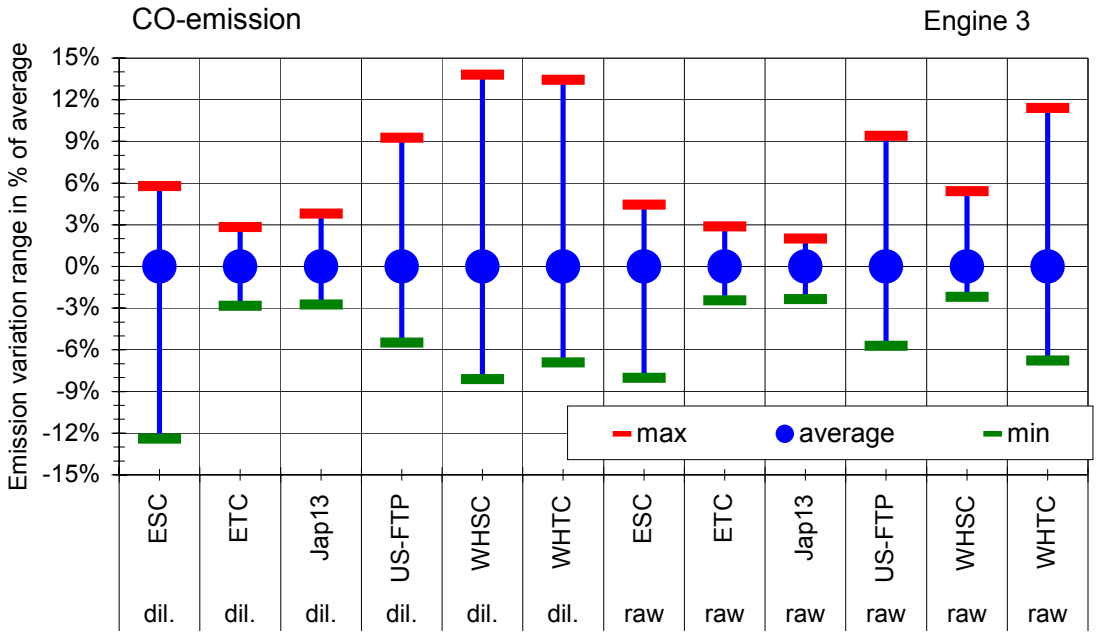

Fig. 2.4.2.3-3: CO-emission variation range in percentage of average / Engine 3

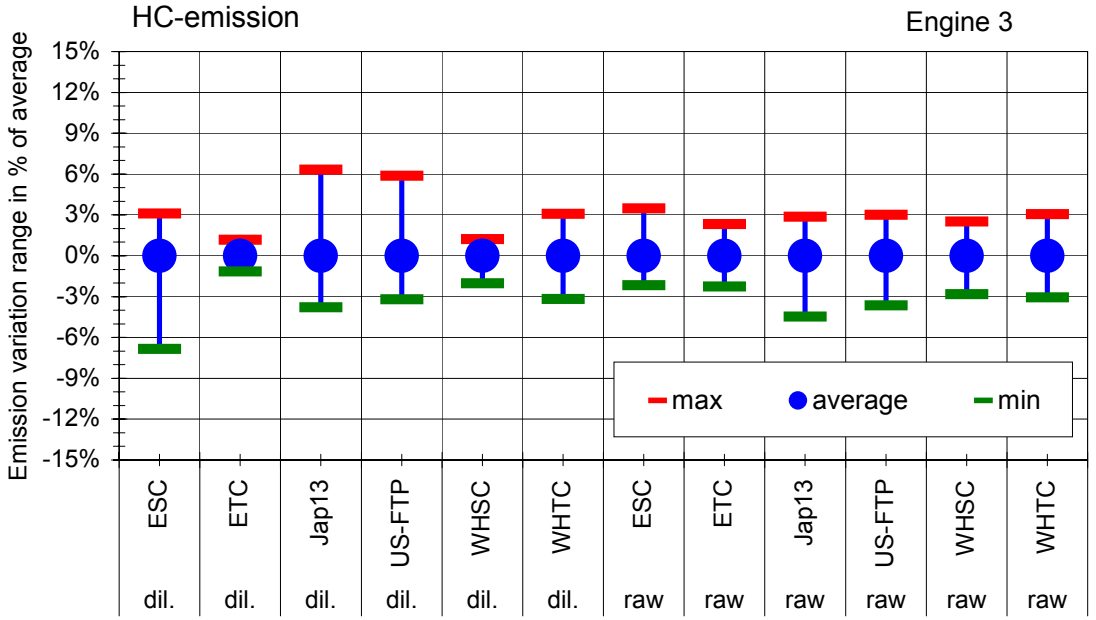

Fig. 2.4.2.3-4: HC-emission variation range in percentage of average / Engine 3

2.4.2.4 Engine 4

For *engine 4* (**Fig. 2.4.2.4-1**) the comparison of the gaseous components indicates the same good to very good comparability as for *engine 3* and for the NOx-results on *engine 1* and *2*. Both systems are monitoring the same emission behaviour and the same trends for cycle comparisons.

With respect to the emission variation range of each regulated component (**Figures 2.4.2.4-2** to **2.4.2.4-4**) the percentage values for the NOx- and CO-results are acceptable with a maximum range of approximately ±3% for the NOx and approximately ±8% for the CO. The HC-results show some similarity to the CO-variations on *engine 3*.

Also here some higher variations could be observed in a range around an approximately maximum of ±15%. Both WHDC-cycles (WHTC and WHSC) show some lesser variations in a range of approximately ±10% for both, the raw and the diluted measurement.

Since average values and measurement variation are similar for both systems, there is no evidence for any discrepancies that might be caused by the measurement procedures.

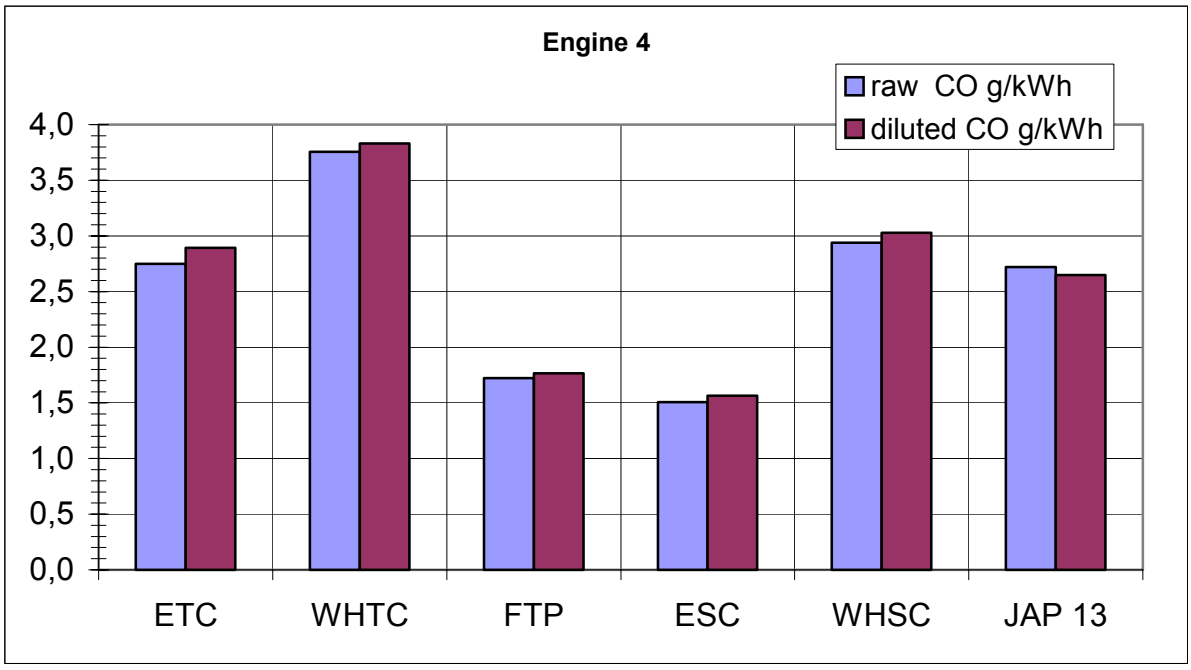

Fig. 2.4.2.4-1a: Gaseous Components Engine 4

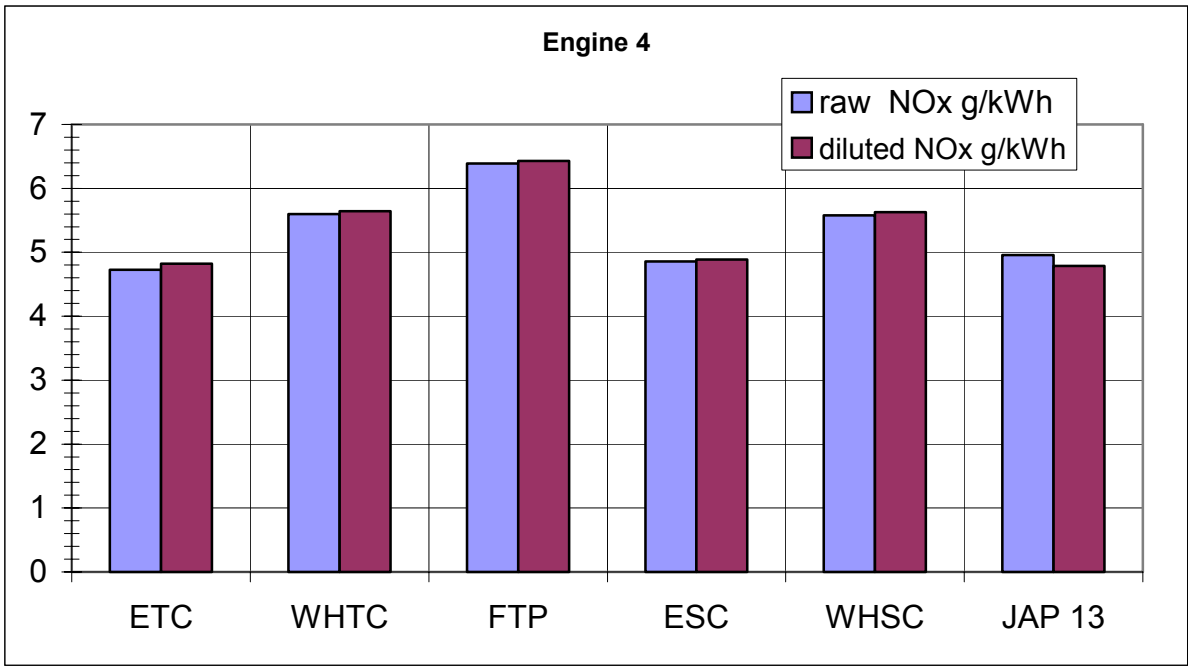

Fig. 2.4.2.4-1b: Gaseous Components Engine 4

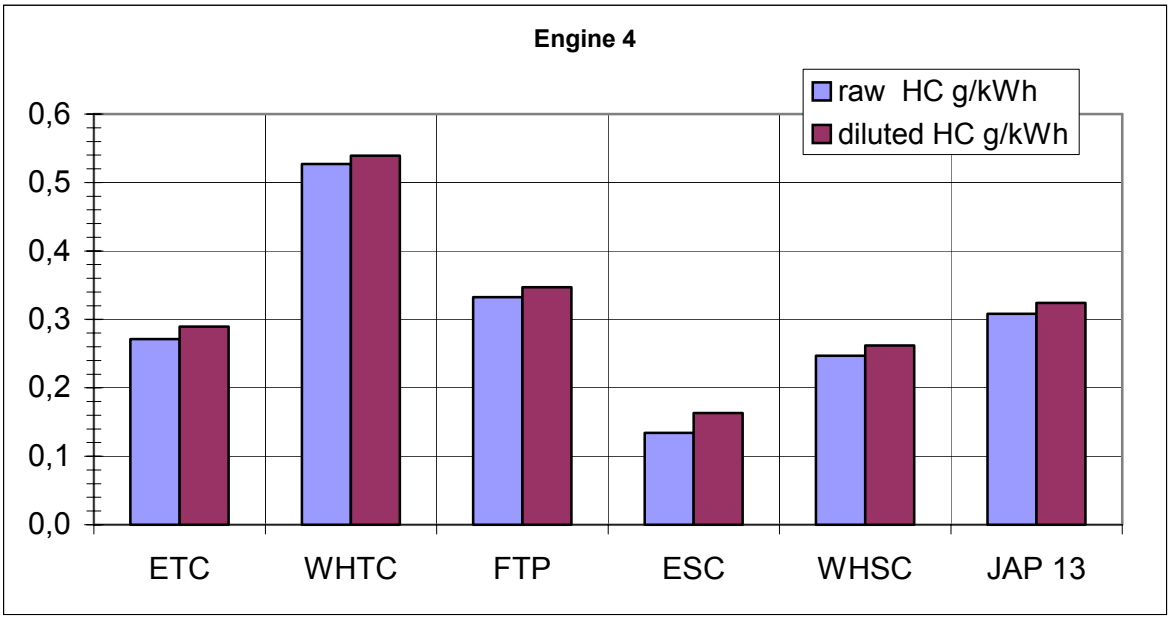

Fig. 2.4.2.4-1c: Gaseous Components Engine 4

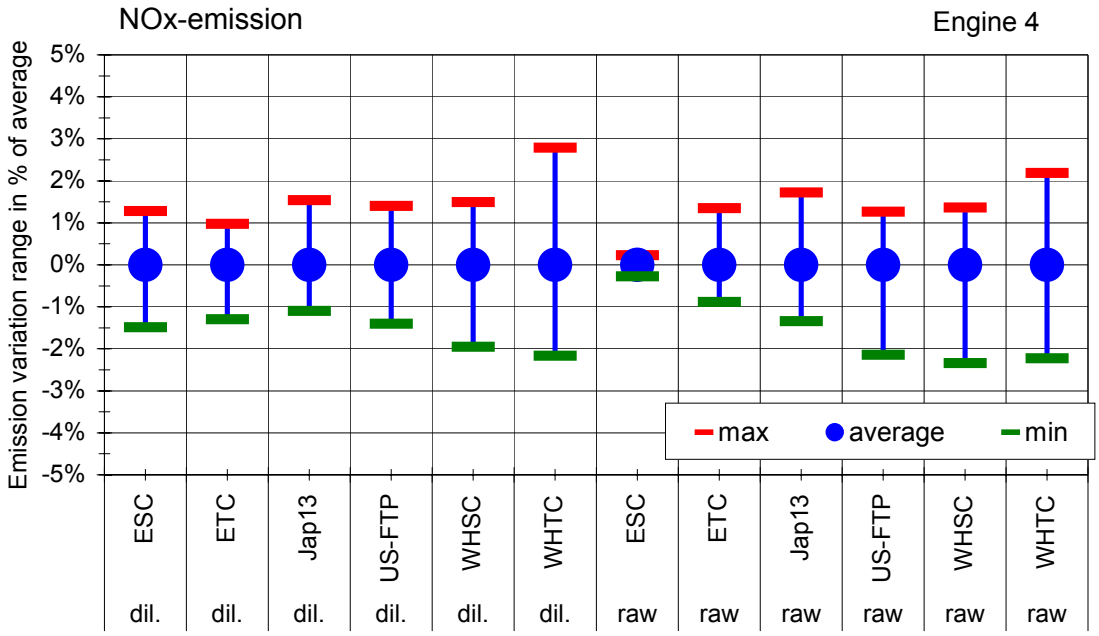

Fig. 2.4.2.4-2: NOx-emission variation range in percentage of average / Engine 4

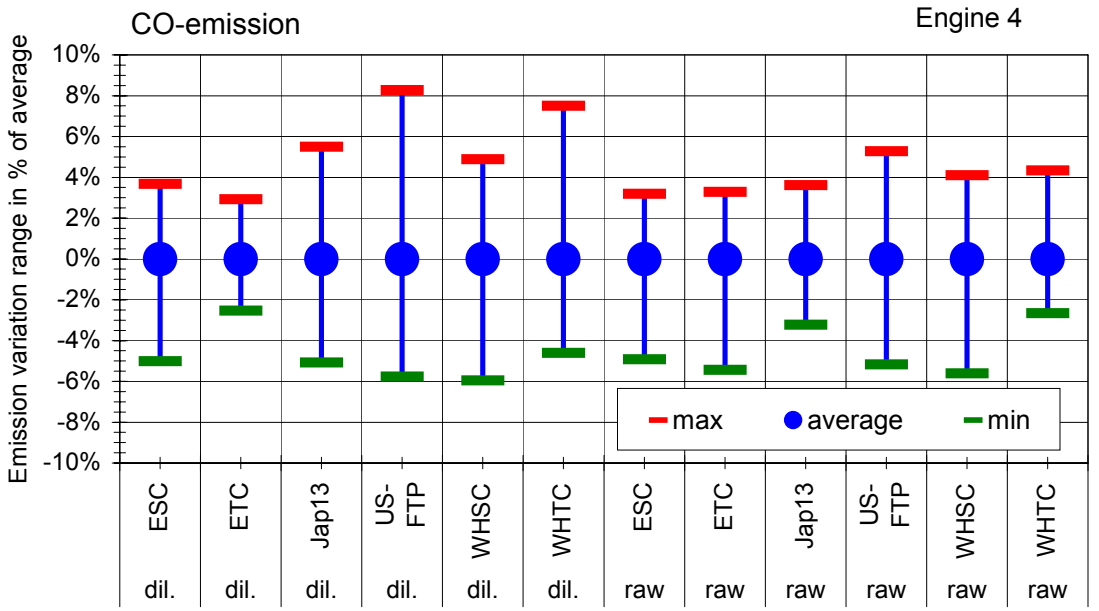

Fig. 2.4.2.4-3: CO-emission variation range in percentage of average / Engine 4

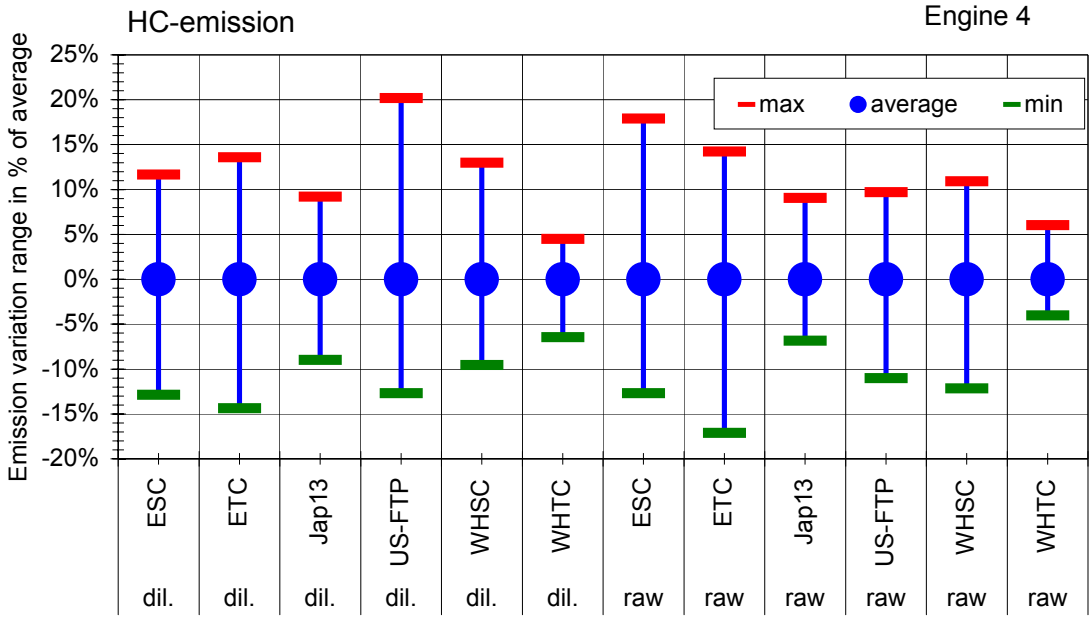

Fig. 2.4.2.4-4: HC-emission variation range in percentage of average / Engine 4

2.4.3 General comparability and deviations

For investigations on the comparability of the raw exhaust gas measurement results according to ISO 16183, the mean values of the raw gaseous components were compared on a percentage deviation basis to the CVS- (diluted measured) results. This means the CVS-results were used as a basis for reference. For non-transient, steady-state cycles the raw exhaust gas as well as the diluted measurement has been used for type approval purposes for many years. For this reason a comparison also for steady-state cycles is of some interest.

Fig. 2.4.3-1 shows the deviations between the raw and diluted exhaust gas components of *engine 1*.

The percentage bars show the absolute percentage deviation of the diluted (CVS-) measurement. For the NOx-results very small absolute deviations are apparent. The CVS-measurement shows a maximum of +1,5% compared to the raw sample in the WHTC and a minimum of approximately 0,5% less in the U.S.-FTP.

For the reasons discussed in chapter 2.4.2, the CO and HC values could not be used for systems evaluation, but are shown in the diagram for comparison.

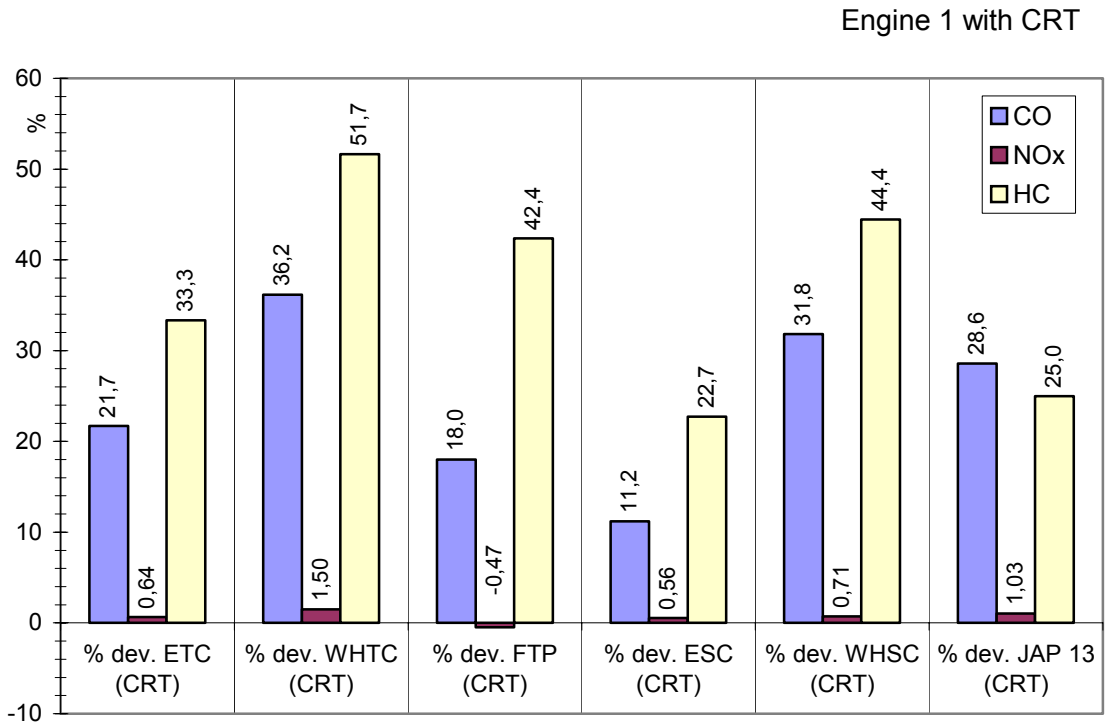

Fig. 2.4.3-1: Engine 1 (CRT), percentage-deviation raw exhaust gas vs. diluted exhaust gas

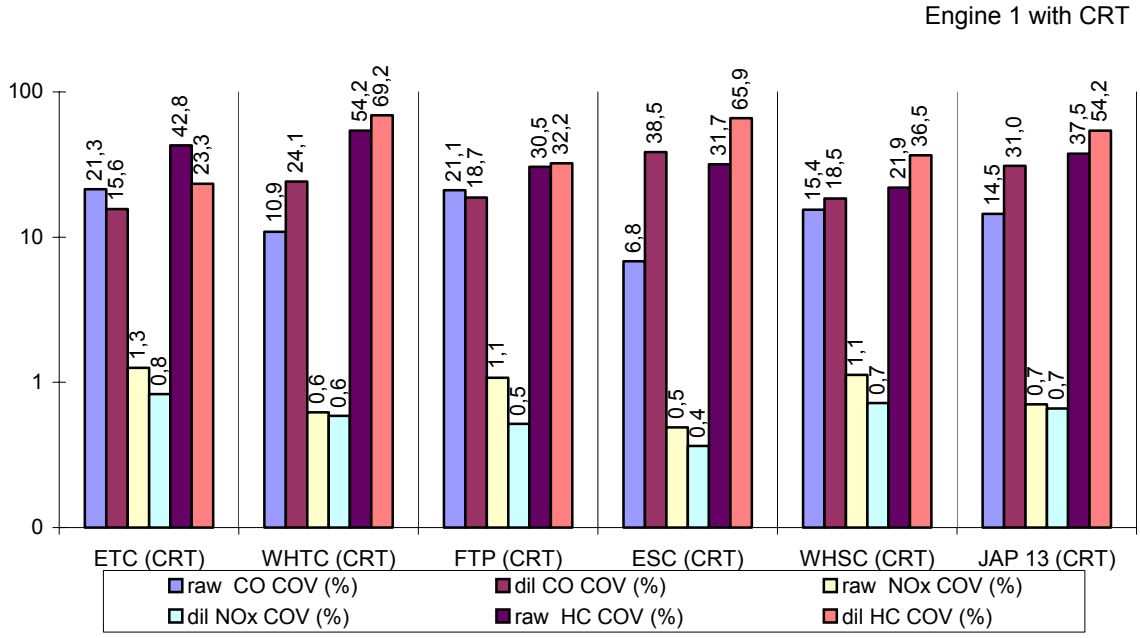

Fig. 2.4.3-2: Engine 1 (CRT), COV raw exhaust gas vs. diluted exhaust gas

Fig. 2.4.3-2 above gives an overview of the variability (coefficient of variation) of the raw and the diluted measurement results based on the mean values of all cycles driven. Both systems show very low variations for the NOx-emissions below ±2%. Again the HC- and CO-values could not be used for system assessment. Nonetheless it could be seen that the raw measurement has slight advantages here. For a clearer presentation the y-axis uses a logarithmic scale.

For *engine 2* the absolute percentage deviations are comparable to *engine 1* since this engine was also equipped with a CRT-System (**Fig. 2.4.3-3**). For NOx the comparison is slightly better and even the CO-deviations are in an acceptable range for engines using CRT-technology. The percentage HC differences are again very high and not suitable for system comparison. Since this engine showed similar emission behaviour in relation to *engine 1* also the COV's calculated with the *engine 2* results are similar. The NOx-COV's are well below 10%, all other COV's (HC, CO) are influenced by the very low absolute emission values provided through the CRT-system (**Fig. 2.4.3-4**).

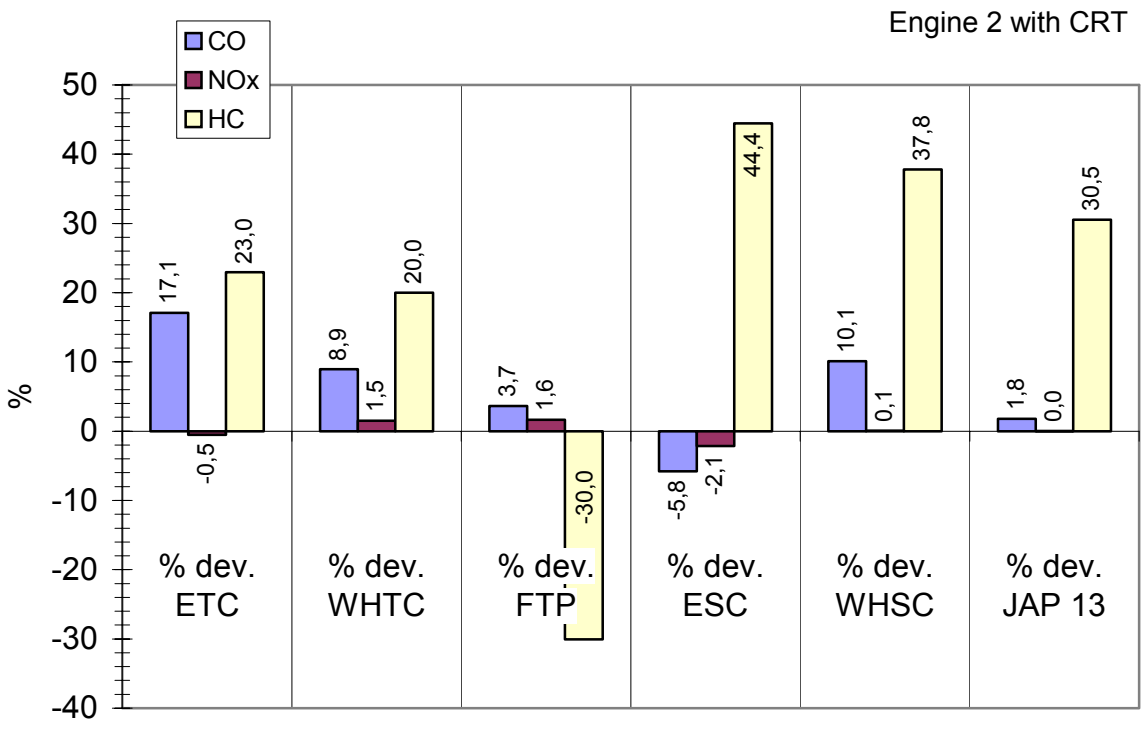

Fig. 2.4.3-3: Engine 2 (CRT), percentage-deviation raw exhaust gas vs. diluted exhaust gas

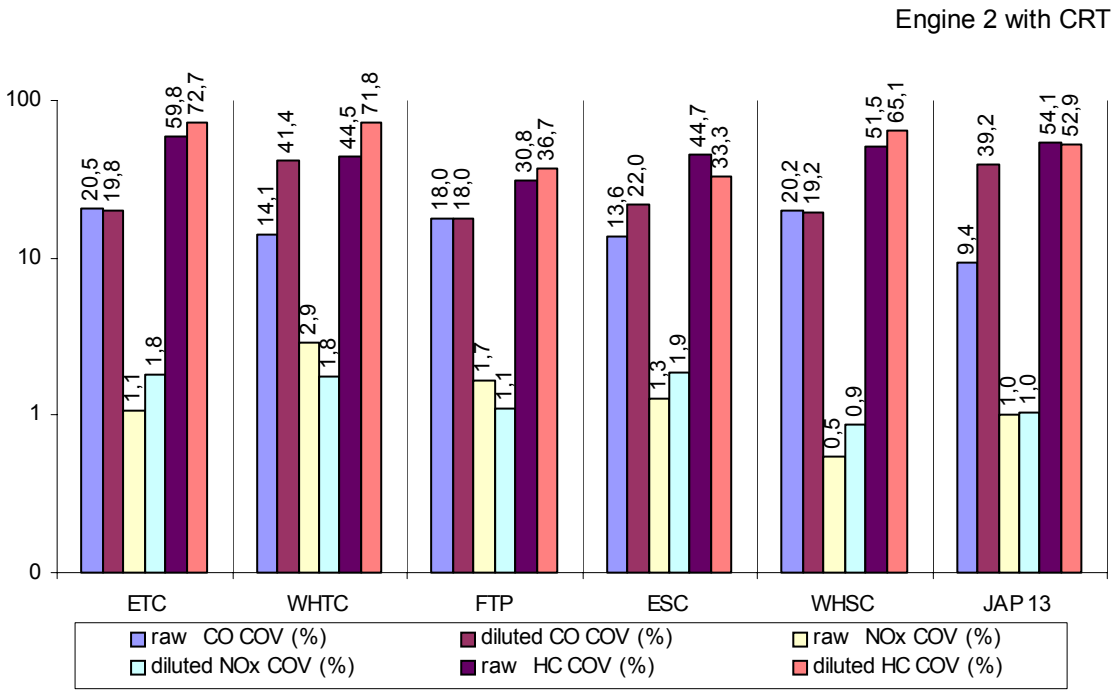

Fig. 2.4.3-4: Engine 2 (CRT), COV raw exhaust gas vs. diluted exhaust gas

For *engine 3* and *engine 4* (**Figures 2.4.3-5** and **2.4.3-6**) the deviations between the raw and diluted measurements show good to very good agreement between the systems. For all cycles and all gaseous components measured the deviations are < 10%. The best similarity could be achieved with the NOx-measurement. As with *engine 1* and *2* the raw measurement delivers results comparable to the diluted measurement within a very narrow range. The diluted measurement shows up to 2% (ETC) more NOx than the raw measurement with the exception of 3,5% less in the Japanese 13-mode. For HC and CO the diluted (CVS) system also provides continuously higher values with up to 8,4% more HC in the ESC for *engine 3* and 6,3% more HC in the ETC for *engine 4*. The highest CO deviation for *engine 3* can be seen in the ESC with 7,2% and for *engine 4* in the ETC with 5%.

This good agreement of the raw exhaust gas measurement according to ISO 16183 can also be seen in the examination of the variability from test to test (COV) (**Fig. 2.4.3-7** and **Fig. 2.4.3-8**).

Figures 2.4.3-7 and **2.4.3-8** clearly show that especially for HC and CO the COV of the raw measurement procedure is lower in most cases. For NOx, the raw measurement shows better COV on *engine 4* but slightly higher values on *engine 3* which are anyway excellent, being below 2%. The highest values near the acceptable 10% COV range are evident on both engines (*3* and *4*) for the diluted (CVS) HC and CO results.

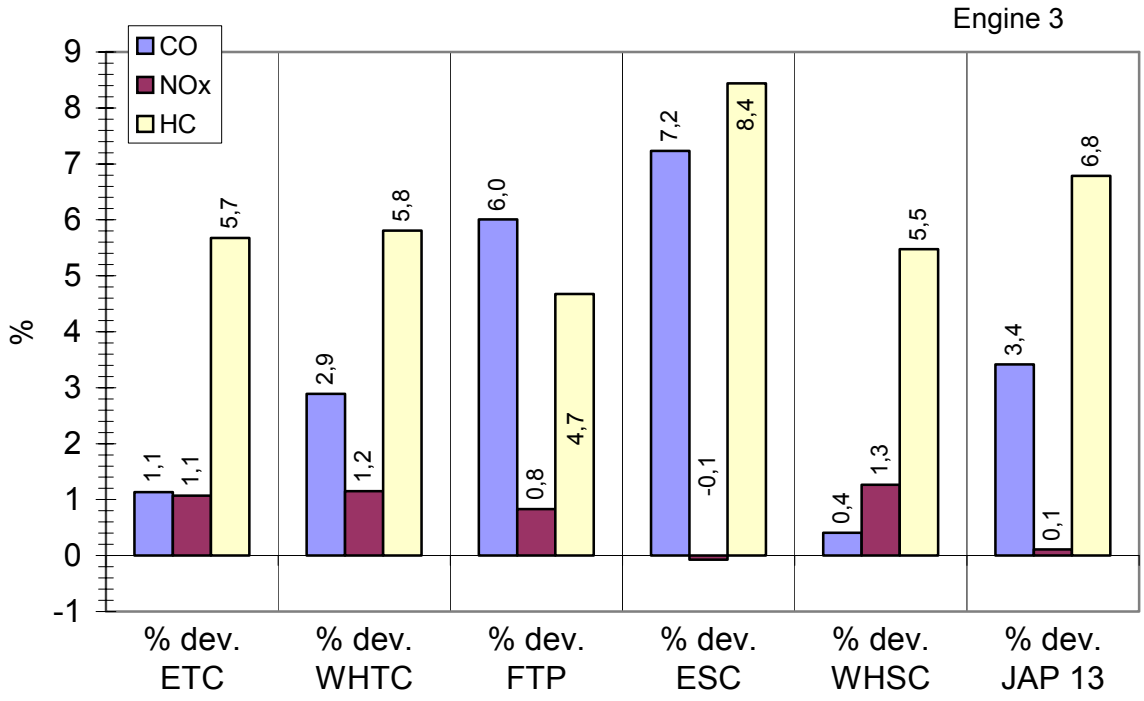

Fig. 2.4.3-5: Engine 3, percentage-deviation raw exhaust gas vs. diluted exhaust gas

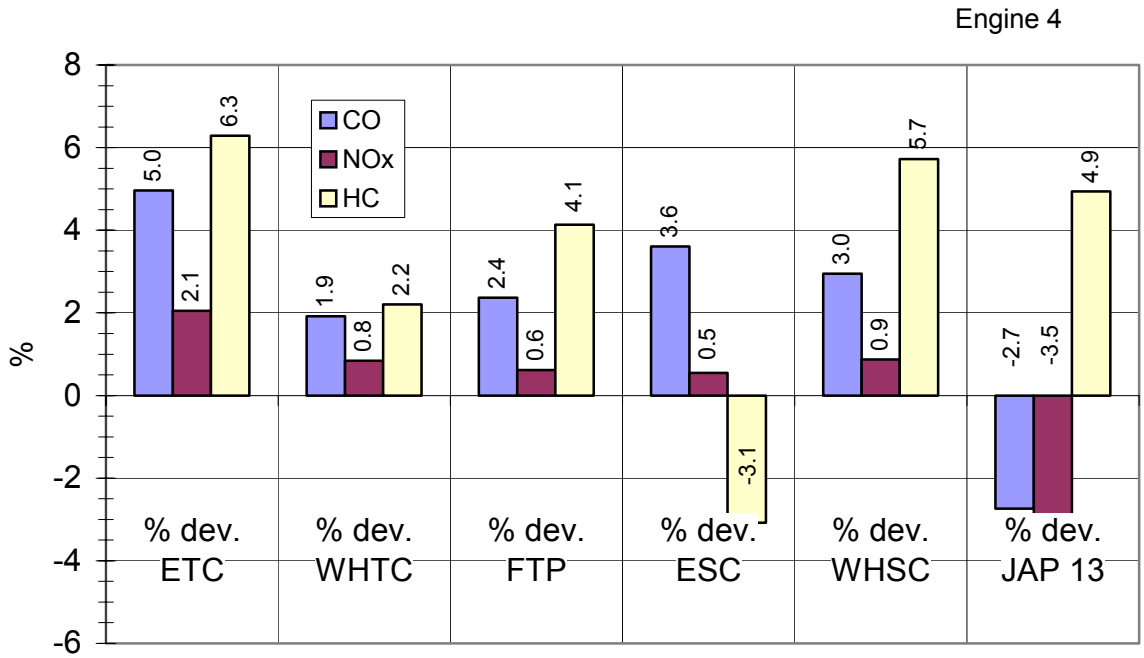

Fig. 2.4.3-6: Engine 4, percentage-deviation raw exhaust gas vs. diluted exhaust gas

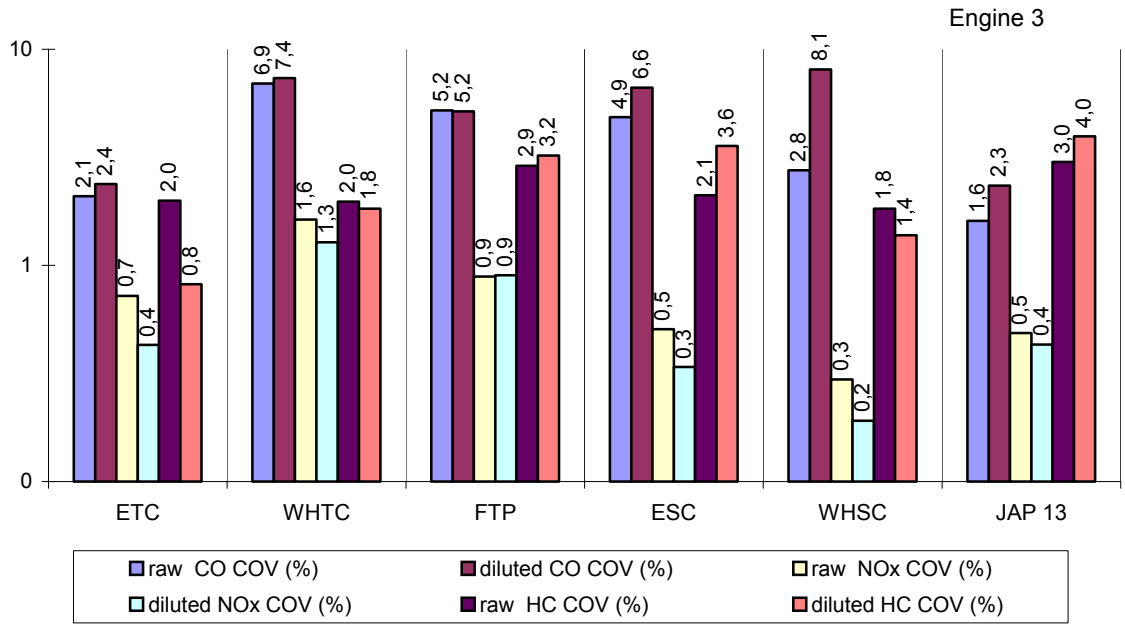

Fig. 2.4.3-7: Engine 3, COV raw exhaust gas vs. diluted exhaust gas

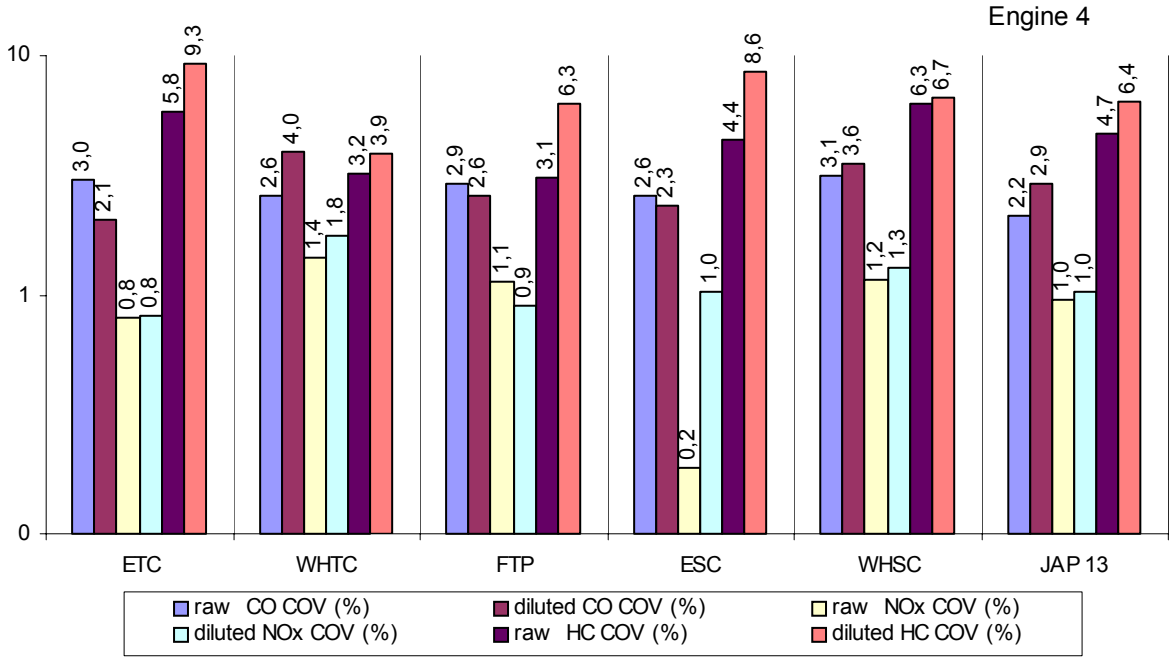

Fig. 2.4.3-8: Engine 4, COV raw exhaust gas vs. diluted exhaust gas

When analysing this data, it can be concluded that the raw measurement procedure is at least equivalent to the diluted CVS-procedure for the measurement of the gaseous regulated pollutants, and, for that reason, the procedures of ISO 16183 could be used for type approval purposes. Furthermore, raw sampling shows advantages regarding the variability of the single results. The main reason is the higher concentration measured by the analyser during raw gas sampling and the missing effects of dilution and background correction.

As soon as the absolute concentration in the exhaust gas is reduced to a level which is near to the detection limit of today's analysers (CO and HC for *engine 1* and *2*), either through dilution or CO and HC reducing after-treatment, the data thus measured could no longer be used for system assessment. High scatter on the measurement signals prevents this.

2.5 Engine operating areas defined by the test cycles

2.5.1 Summary of engine test speeds

Table 2.5.1 -1 lists the relevant speeds for all cycles run during the measurement programme.

Despite that fact that three heavy HD-engines (*engine 1*, *2* and *3*) had different shapes of their performance curves (line ***n rated, n torque max***.) the ESC / ETC relevant speeds ***n lo 50%*** and ***n hi 70%*** are close together in a range of max 160 1/min (compared maximum to minimum). Thus the test speeds for the ESC are also in a narrow range: 50 1/min for ***n A*** and ***n B***, 100 1/min for ***n C***. Also, high differences for **n ref** could not be observed. With those engines, n ref is lying in a range of 150 1/min.

The measured n low 55% could be observed in a 65 1/min range for all engines. These differences are also applicable to the steady-state speeds applicable to the WHSC: n A 25% to n E 75%. The only speeds showing more than 200 1/min difference were n pref. 51% (240 1/min range) and n high 95% (340 1/min range) to be used for the WHTC / WHSC. These differences together with the more complex denormalisation formula ensure that the most preferred speeds of the WHTC are more robust against power curve modifications than the FTP and ETC, which will be shown in the following sections.

For *engine 4* the range of applicable cycle speeds is much wider than for the other engines. Since this engine is designed for light HD-vehicle applications such as delivery vans, the wider range is fully in line with real life operation. This engine could be described as derivate of a passenger car diesel engine (please refer to chapter **2.1** for details). An indication is the significantly higher rated speed compared to the other three engines.

cycle relevance	*speed*		*engine 1*	*engine 2*	*engine 3*	*engine 4*
all	***n rated***	1/min	1800	2200	1900	3600
		normalised	100.0%	100.0%	100.0%	100.0%
	n torque max.	1/min	1080	1200	1100 - 1300	1800
		normalised	41.9%	33.3%	42.9%	35.7%
	n idle	1/min	560	700	500	800
		normalised	0.0%	0.0%	0.0%	0.0%
	n hi idle	1/min	2280	2465	2400	4200
		normalised	138.7%	117.7%	135.7%	121.4%
ESC / ETC	***n lo 50%***	1/min	1010	930	900	1500
		normalised	36.3%	15.3%	28.6%	25.0%
	n hi 70%	1/min	2200	2360	2300	4000
		normalised	132.3%	110.7%	128.6%	114.3%
ESC	***n A***	1/min	1300	1290	1250	2125
		normalised	59.7%	39.3%	53.6%	47.3%
	n B	1/min	1600	1650	1600	2750
		normalised	83.9%	63.3%	78.6%	69.6%
	n C	1/min	1900	2000	1950	3375
		normalised	108.1%	86.7%	103.6%	92.0%
ETC	***n ref***	1/min	2140	2290	2230	3875
		normalised	127.4%	106.0%	123.6%	109.8%
WHSC / WHTC	***n low 55%***	1/min	1015	980	950	1650
		normalised	36.7%	18.7%	32.1%	30.4%
	n hi 70%	1/min	2200	2360	2300	4000
		normalised	132.3%	110.7%	128.6%	114.3%
	n pref 51%	1/min	1300	1540	1335	2320
		normalised	59.7%	56.0%	59.6%	54.3%
	n high 95%	1/min	1935	2230	2275	3825
		normalised	110.9%	102.0%	126.8%	108.0%
WHSC	***n A 25%***	1/min	915	1040	885	1505
		normalised	28.6%	22.7%	27.5%	25.2%
	n B 35%	1/min	1060	1175	1040	1790
		normalised	40.3%	31.7%	38.6%	35.4%
	n C 45%	1/min	1200	1310	1195	2070
		normalised	51.6%	40.7%	49.6%	45.4%
	n D 55%	1/min	1345	1450	1350	2350
		normalised	63.3%	50.0%	60.7%	55.4%
	n E 75%	1/min	1630	1720	1655	2915
		normalised	86.3%	68.0%	82.5%	75.5%

Table 2.5.1-1: Cycle speed of the test engines

2.5.2 Comparison of engine maps

Figures 2.5.2-1 to **2.5.2-4** described below show the mapping curves of all four engines as measured during the dynamic mapping for the transient cycle generation. For this dynamic mapping the engine speed was increased at an average rate of 8 ± 1 min-1 per second from minimum to maximum mapping speed. Engine speed and torque points were recorded at a sample rate of ten points per second.

For the reason of the relatively high speed increase necessary for mapping a quasi-dynamic behaviour as well as for the high data sampling frequency of 10 Hz, the engine performance curves show small scatter around the ideal shape. Nonetheless, it can be seen that the shape of the performance curve of an engine can influence the speeds needed for the later cycle determination and generation.

With this in mind, it might be possible to design the shape of the performance curve in such a way that a large number of engine map points most used during a specific cycle could be situated in a selected area of engine operation. This is possible for steady-state cycles as well as for transient cycles. But the potential for such intentional curve shifting is much lower for the WHTC and WHSC than for the ETC and US-FTP.

Fig. 2.5.2-1 shows the performance curves of *engine 1* together with the map points of the different cycles. It can be seen that this engine has a significant “step” in its torque- respectively power-curve at around 1000 min^{-1}. This step ensures that the major parts of all transient cycle points are in the area above 1000 min^{-1}. One could argue that the step was designed in order to influence the location of the cycle measurement points although it is obvious that the area below 1000 rpm is rarely used during real life operation

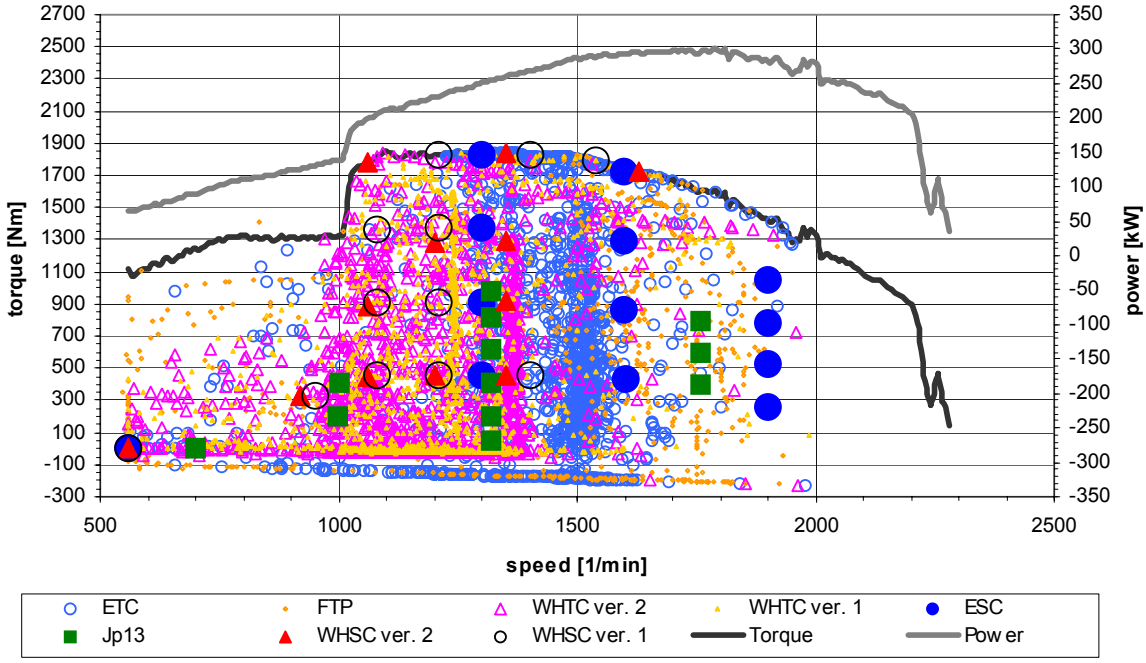

Fig 2.5.2-1: Engine mapping, cycle relevant speeds; Engine 1

By comparing the different speeds and engine maps for *engine 1* it can be seen that the ETC is focussed on 1500 min^{-1}. ESC and ETC do not match very well. The FTP profile is focussed on idling and speeds close to rated speed.

The final WHTC is covering a broader range of the engine map, focussed on an area between 1000 min^{-1} and 1500 min^{-1}. This speed range is of important significance for real driving pattern of this engine. The final WHSC is pretty much in line with the final WHTC. By comparing the steady-state Japanese 13-mode points with the ESC and the final WHSC it can be seen that for the mid-range test speed similar ranges of the engine map are covered.

Fig. 2.5.2-2 shows the engine mapping and the cycle relevant speeds of *engine 2*. The WHDC cycle maps indicated here and in **Fig. 2.5.2-3** and **Fig. 2.5.2-4** are only showing the final version 2 maps.

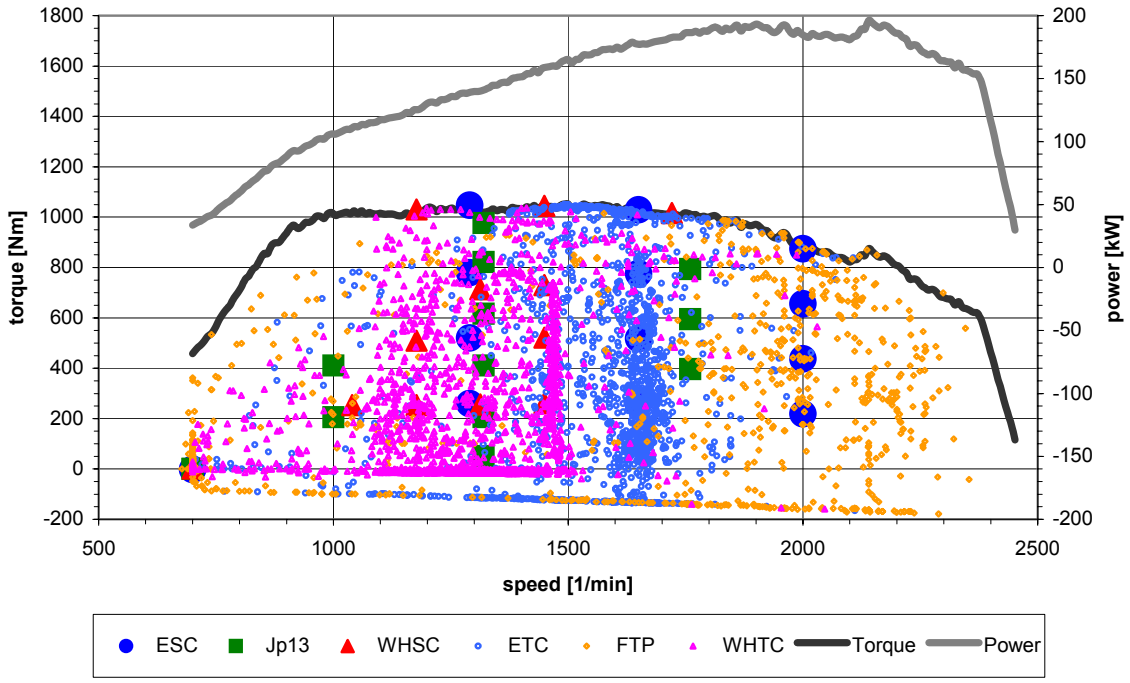

Fig 2.5.2-2: Engine mapping, cycle relevant speeds; Engine 2

On *engine 2* (**Fig 2.5.2-2)** similar ratios could be seen. The final WHTC driving pattern operates the engine in lower speed ranges than the ETC and FTP but covers a broader engine map area and is more in line with real world operation. Even here the FTP cycle considers a much more higher portion of high speed (1800 1/min – 2300 1/min) operation in direction of rated power than any other transient cycle. Due to the design of the performance map the ESC speed C as well as the most frequently used speed of the ETC are located relatively high. But it has to be mentioned that ETC and ESC are better in line than for *engine 1*.

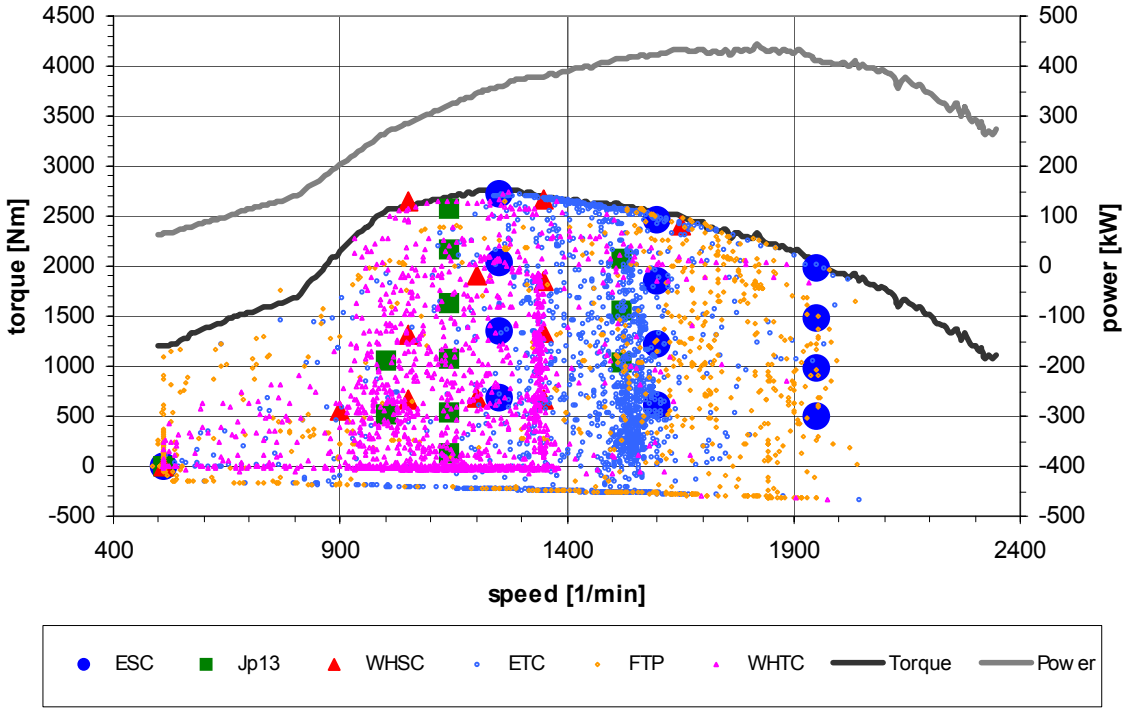

Fig 2.5.2-3: Engine mapping, cycle relevant speeds; Engine 3

For *engine 3* (**Fig. 2.5.2-3**) the cycle points for the different cycles again show a similar structure as for *engines 1* and *2*. A high portion of full load torque could be used from slightly more than 900 1/min so that the main operation area of the final WHTC is between 900 1/min and 1400 1/min. The figures showing the engine maps for *engines 1*, *2* and *3* (**Fig. 2.5.2-1, Fig. 2.5.2-2** and **Fig. 2.5.2-3**) are typical for heavy-duty applications and it could be seen that many cycle points are all located in more or less similar fields of the engine map.

For *engine 4* (**Fig. 2.5.2-4**) the range of applicable cycle speeds is much wider than for the other engines. Nevertheless the same differences between the cycles used are obvious here. The main parts of the WHTC driving pattern are in lower speed ranges than in an ETC cycle. The FTP is considering more idle parts as well as more operation in the range of rated power.

For test cell operation of such an engine on an engine dynamometer a much wider speed range must be covered. By comparing *engine 3* (**Fig. 2.5.2-3**) with *engine 4* (**Fig. 2.5.2-4**) it can be seen that the applicable speed range of the HD-*engine 3* lies within 1000 1/min. This can also be stated for *engine 1* and *engine 2*. For *engine 4* the most applicable speed range is situated between 1500 1/min and 3500 1/min, covering approximately 1000 1/min more than the heavy HD applications. The denormalisation of the cycles is very well reflecting real driving pattern since engines with small engine capacity have to be operated over a wider speed range than engines with higher capacities /7/.

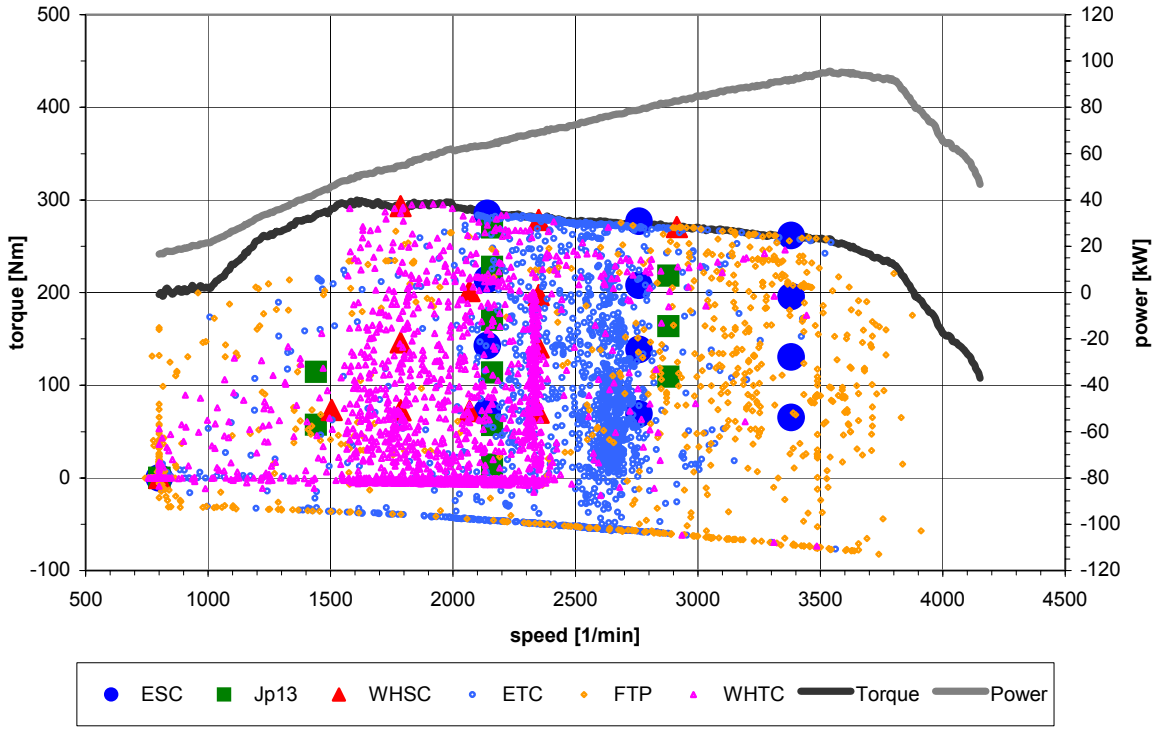

Fig 2.5.2-4: Engine mapping, cycle relevant speeds; Engine 4

By using other speeds than shown in the above figures**,** which could be made possible by designing a different mapping characteristic, the cycle map areas could be shifted to completely different areas of measurement in case of the FTP, ETC, ESC and Japanese 13-mode. Due to the more complex denormalisation the shifting potential is significantly reduced for the final WHSC and WHTC cycles. Anyway these cycles are covering more relevant mapping areas with respect to real world driving than the existing cycles.

2.6 Driveability of the final WHDC cycles

2.6.1 General cycle validation criteria

The driveability criteria for a transient test cycle are indicated in Directive 1999/96/EC amended by 2001/27/EC /5/. Those validation criteria are very similar to those used in the US. The validation algorithm employs a formula according to the least square method. This formula is shown below:

$$Y = b \cdot X + a \qquad \textbf{(14)}$$

where:

Y = *ordinate axis signal / actual value of torque, speed and power*

b = *slope of regression line*

X = *axis of abscissa signal /reference value of torque, speed and power*

a = *y intercept of regression line*

The verification of the regression between the actual and the reference values is performed via regression analysis. The coefficient of determination is calculated using the following formula:

$$R^2 = \frac{n(\sum XY) - (\sum X)(\sum Y)}{\sqrt{\left[n\sum X^2 - (\sum X)^2\right]\left[n\sum Y^2 - (\sum Y)^2\right]}} \qquad \textbf{(15)}$$

The following limit values (**Table 2.6.1-1**) must be met to pass a test (1999/96/EC amended by 2001/27/EC):

	speed	torque	power
Standard error of estimate (SE) of Y on X	max. 100min^{-1}	max. 13% of power map maximum engine torque	max. 8% of power map maximum engine power
Slope of regression line, b	0.95 to 1.03	0.83 - 1.03	0.89 - 1.03
Coefficient of determination, R²	min 0.9700	min 0.8800	min 0.9100
Y intercept of the regression line, a	±50min^{-1}	±20Nm or ±2% of max. torque whichever is greater	±4kW or ±2% of max. power whichever is greater
actual cycle work shall be between -15% and +5% of reference cycle work			

Table 2.6.1-1: Cycle validation criteria (1999/96/EC amended by 2001/27/EC)

Furthermore it is permitted to delete some certain cycle points under particular defined cycle conditions. These cycle conditions according to /5/ are shown in **Table 2.6.1-2** below. Further on it is also permitted to time align the reference and the feedback signal before performing the cycle validation.

cycle condition	**permitted point deletion**
full load and torque feedback ≠ torque reference	torque and/or power
no load, not an idle point, and torque feedback > torque reference	torque and/or power
no load/closed throttle, idle point and speed > reference idle speed	speed and/or power

Table 2.6.1-2: Permitted point deletions

2.6.2 Driveability of the final WHTC with engine 1

The first driveability tests (cycle validation statistics) were performed on *engine 1* without time shifting and point deletion.

By applying the formulas **(14)** and **(15)** to the final WHTC data of *engine 1* the coefficient of determination R^2 shows good to very good values for torque and speed meeting the limits shown in **Table 2.6.1-1**. **Fig. 2.6.1-1**, **Fig. 2.6.1-2** and **Fig. 2.6.1-3** show the function between reference and actual values for torque, speed and power without point deletions. The data shown here is based on a 1Hz measurement and a 10Hz control frequency.

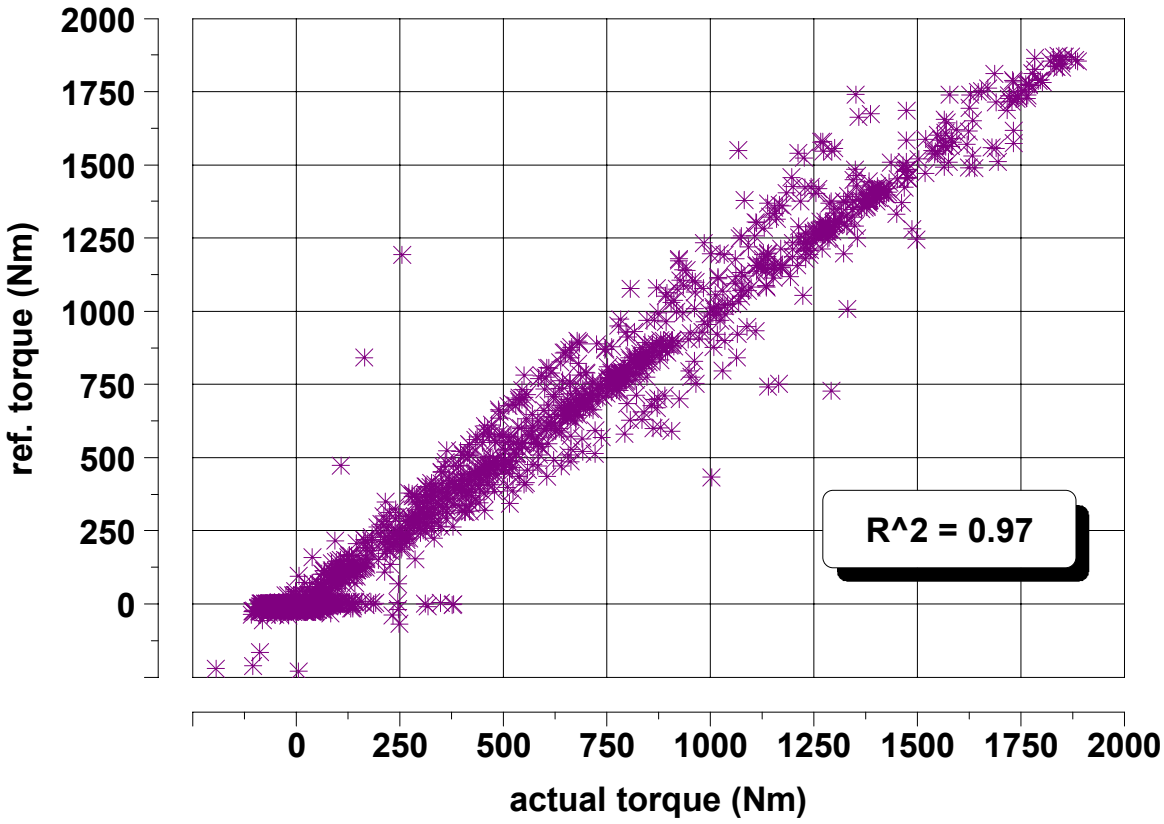

Fig. 2.6.1-1: Regression of reference and actual torque of engine 1 without time shifting and point deletion

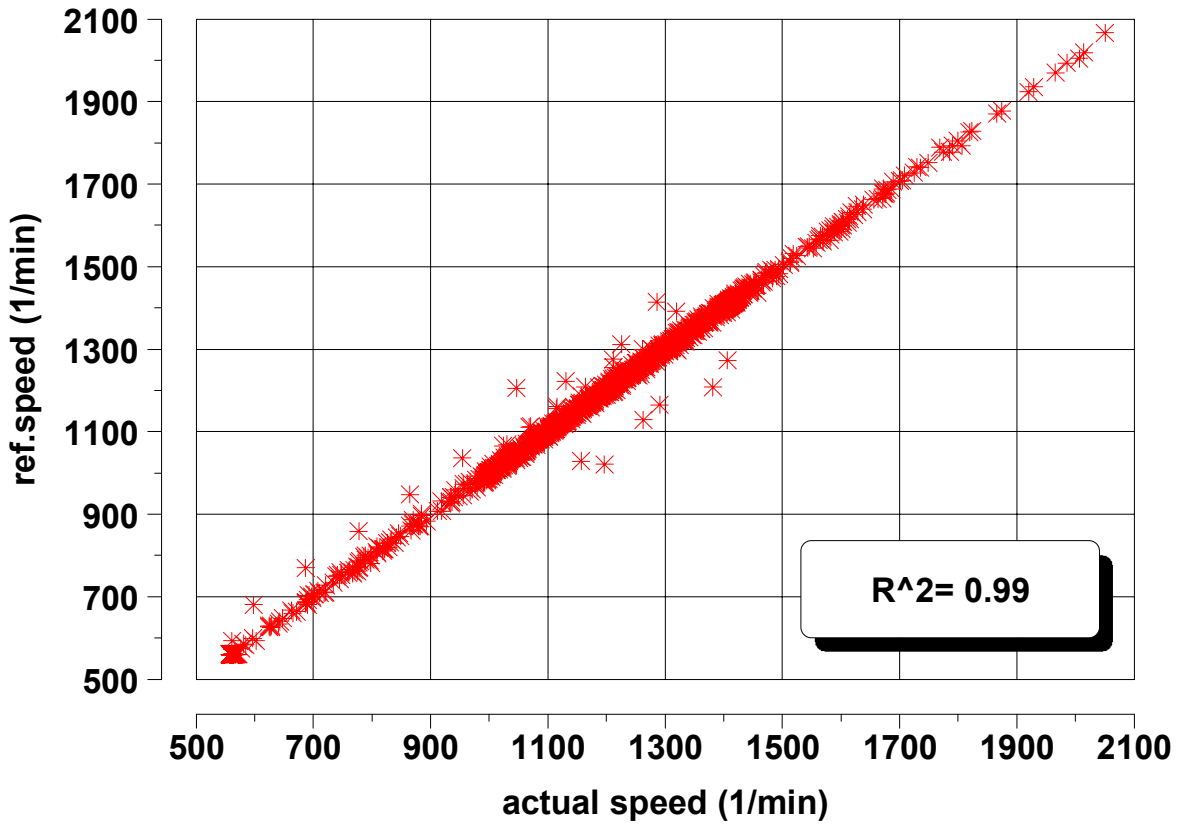

Fig. 2.6.1-2: Regression of reference and actual speed of engine 1 without time shifting and point deletion

It can be seen that the limit values of R^2 given in **Table 2.6.1-1** are already met without any point deletion. This depends strongly on the engine dynamometer control action and precision. The dynamometer used employs fully digital torque and speed governors and is for that reason capable of such good recovery curves. The feedback behaviour of the calculated power is a little bit poorer **(Fig. 2.6.1-3)**. This was to be expected due to the calculation of the power using torque and speed as well as through the engine idle points. The value achieved is still within the regression limits of **Table 2.6.1-1** (without point deletion).

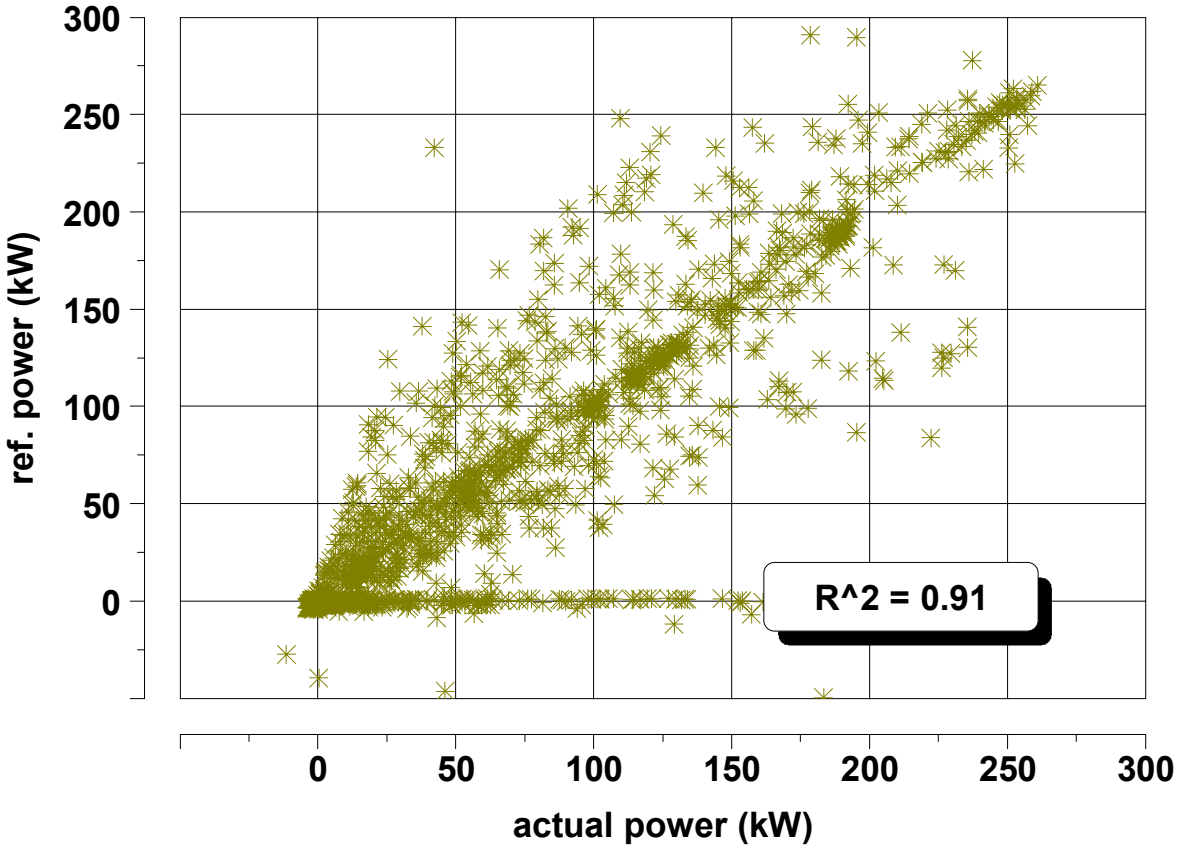

Fig. 2.6.1-3: Regression of reference and actual power of engine 1 without time shifting and point deletion

By using the permitted point deletions (**Table 2.6.1-2**) as well as the possibility to shift the reference torque and speed relative to the actual torque and speed in order to minimise the bias caused by data logging systems and the dynamometer control the validation data shown in **Table 2.6.1-3** could be achieved.

This data shows that the final WHTC has a good to very good capability to be driven with good engine response on the engine dynamometer.

	limit	actual	**limit**	actual	**limit**	actual
	speed	speed	**torque**	torque	**power**	power
std. error of estimate of y on x	max 100 1/min	32.98 1/min	241.8 Nm	80.52 Nm	23.6 kW	11.14 kW
slope of the regression line	0.95 to 1.03	1.01	0.83 - 1.03	0.97	0.89 - 1.03	0.99
coefficient of determination, R^2	min 0.9700	0.99	min 0.8800	0.99	min 0.9100	0.99
y intercept of regression	± 50 1/min	1.4 1/min	± 37 Nm	8.45 Nm	± 6 kW	0.91 kW

	min. limit	**max. limit**	cal. on ref.	cal. on actual
Cycle work	**24.3 kWh**	**30.1 kWh**	28.61 kWh	29.04 kWh

Table 2.6.1-3: Cycle validation statistics for final WHTC

2.6.3 Cycle validation with all engines

As already explained in **2.6.1** the transient cycle validation criteria must be met in order to judge a cycle valid for type approval purposes. The validation criteria based on a linear regression analysis (see **Table 2.6.1-1**) must be applied to the ETC and FTP test in accordance with current legislations.

In order to verify if any problems with these criteria might be occur for the final WHTC cycle this criteria was also applied to it. During the measurement programme all transient cycles (ETC, FTP and WHTC) were validated against the existing criteria of Table 2.6.1-2. . Since the driveability of the ETC and FTP is already proven this data are not shown here.

The dynamometer used during the entire programme was controlled by a digital closed loop control system, which can control the engine very close to the reference driving profile. For that reason, the validation criteria for all engines were very often met even without using the permitted point deletion as well as the time alignment of the response signals. It has to be clearly considered that engine test cells employing dynamometers with analogue control units may need all given possibilities to provide validation criteria matching engine running. Such systems may also need to be adjusted for each engine to be tested.

Fig 2.6.2-1 shows the raw signal validation data for *engine 1*. On the x-axis the reference driving profile is indicated, the y-axis shows the actual or better response signal of the engine.

It can be seen that the engine speed response is very good with a correlation coefficient (R^2) close to one. Also the torque response of this engine was good to very good. **Figures 2.6.2-2** to **Fig. 2.6.2-4** show the corresponding data for *engine 2*, *engine 3* and *engine 4*.

In principal the validation of the final WHTC on *engine 2* shows the same behaviour as on *engine 1*. By looking on the next diagram (**Fig 2.6.2-3**) for *engine 3* the uncorrected values show some poorer correlation, especially for the torque and power but still meeting the criteria for R^2. The reason for this is that *engine 3* was the largest engine during the programme representing the range of the most powerful engines for heavy-duty applications. Thus the dynamometer has to cover a wider torque range here, as well as more mass of inertia, which has to be moved.

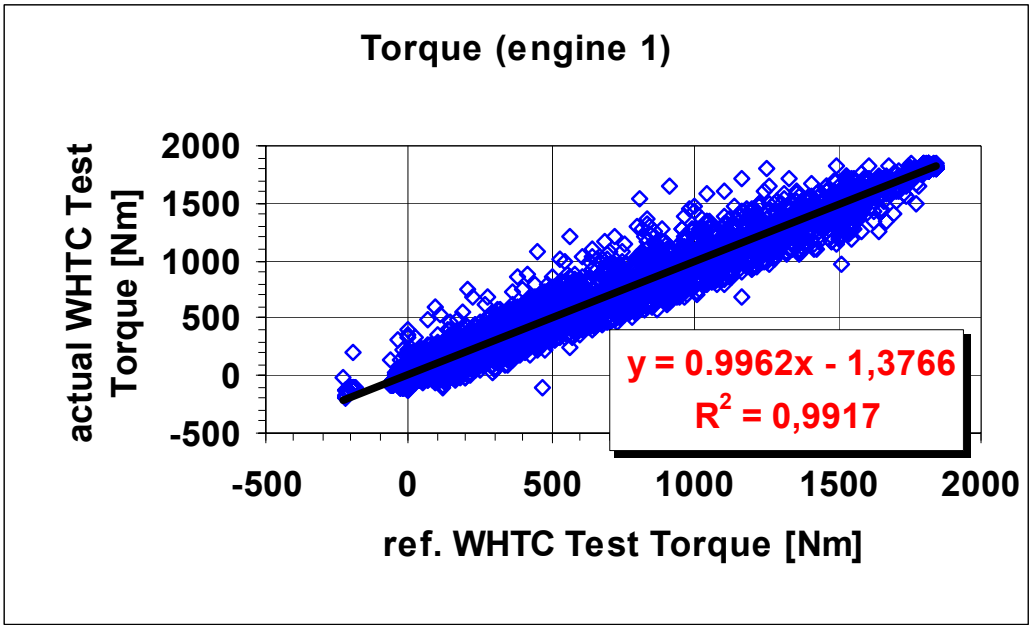

Fig 2.6.2-1a WHTC validation engine 1

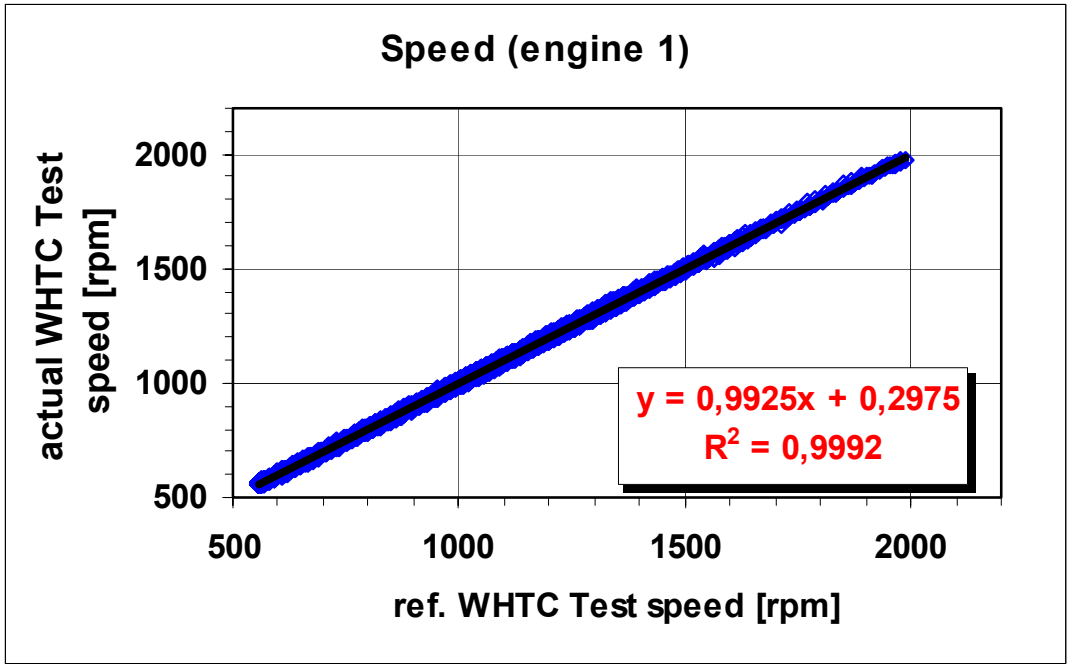

Fig 2.6.2-1b WHTC validation engine 1

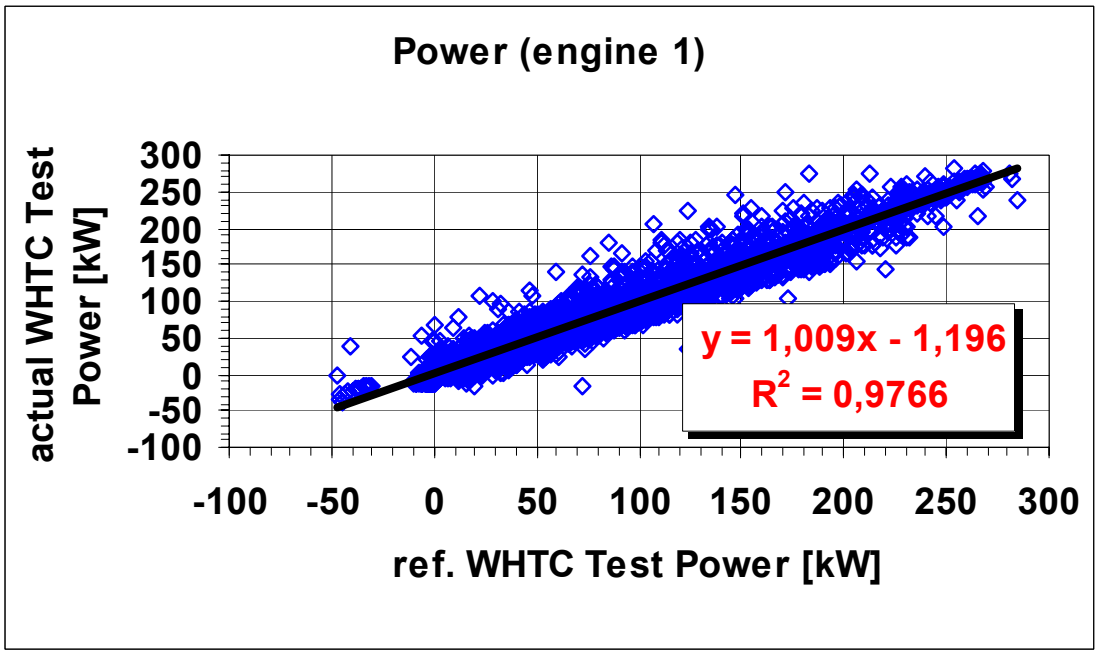

Fig 2.6.2-1c WHTC validation engine 1

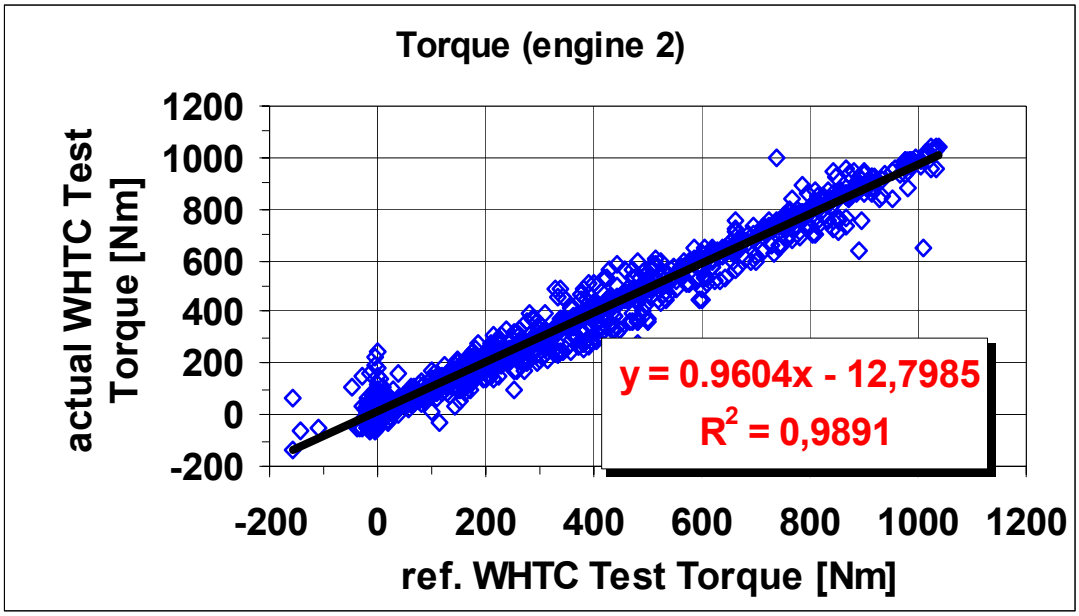

Fig 2.6.2-2a WHTC validation engine 2

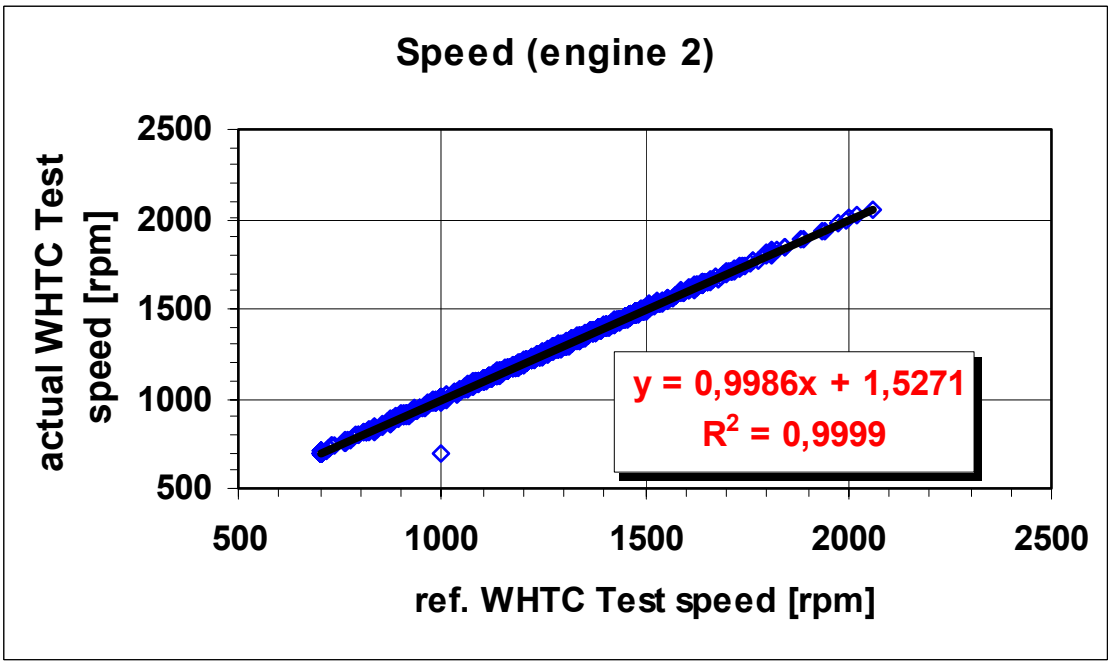

Fig 2.6.2-2b WHTC validation engine 2

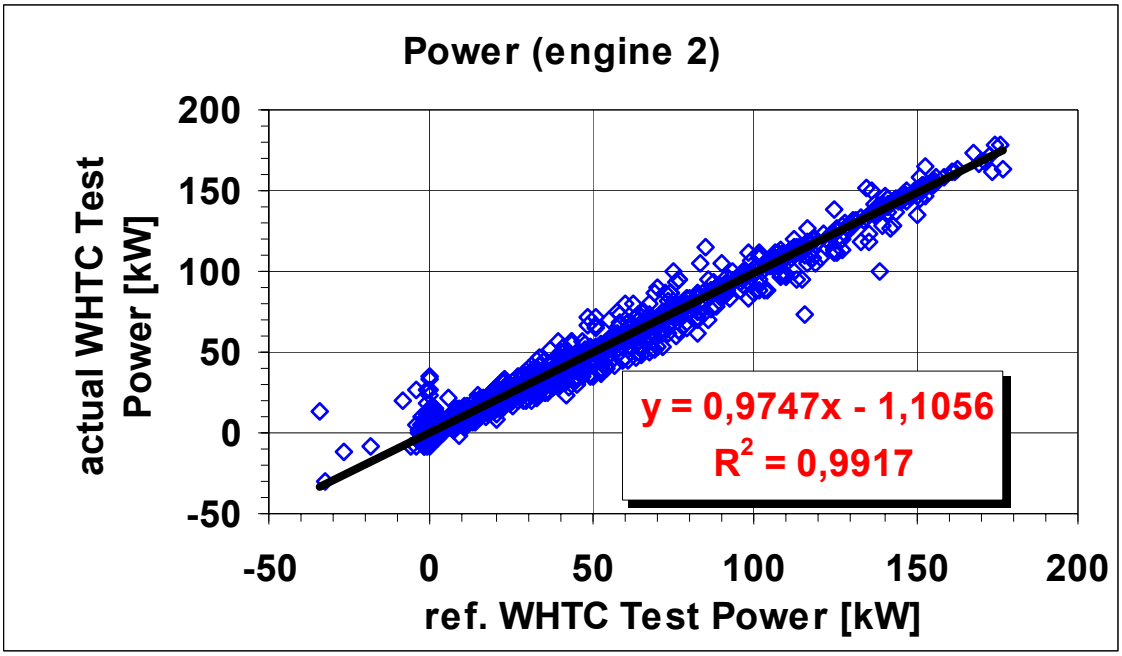

Fig 2.6.2-2c WHTC validation engine 2

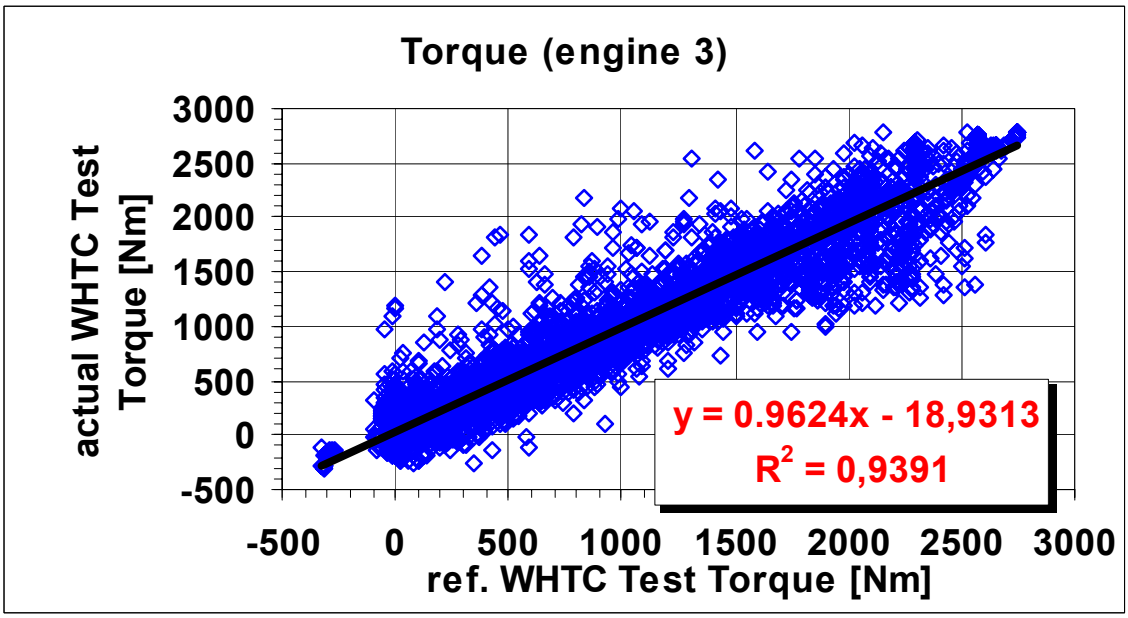

Fig 2.6.2-3a WHTC validation engine 3

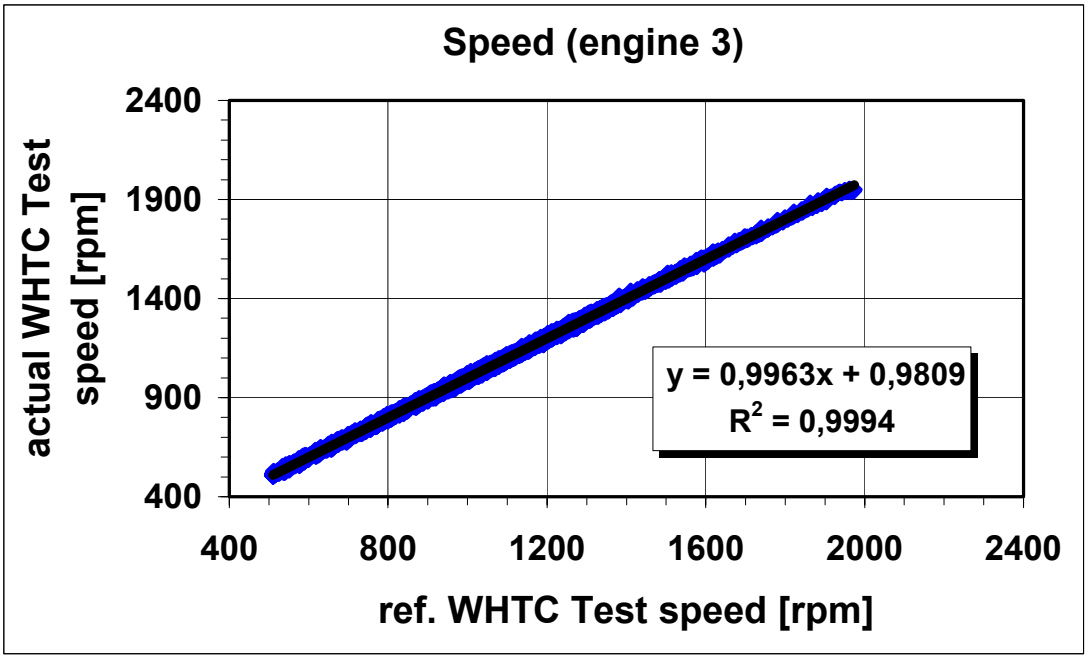

Fig 2.6.2-3b WHTC validation engine 3

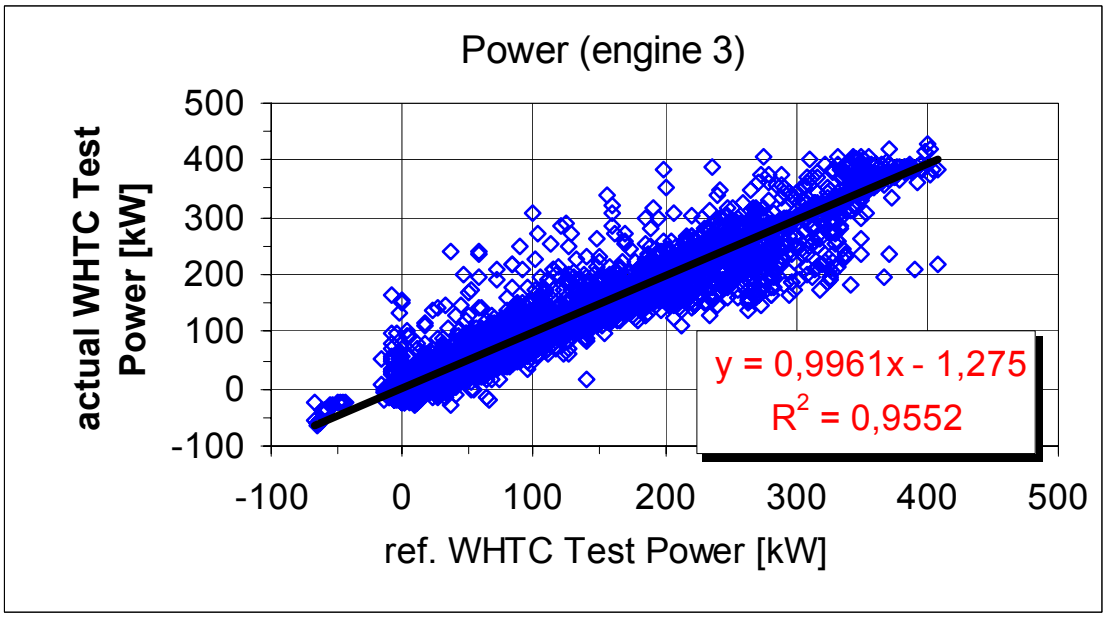

Fig 2.6.2-3c WHTC validation engine 3

For *engine 4* the situation is very different compared to *engine 3*. *Engine 4* was the smallest engine representing typical delivery truck applications. These engines have much less torque

and are operated over a much wider speed range. This speed range could be easily matched by a computer-controlled dynamometer. For that reason the correlation factors (R^2) are very good for in *engine 4* with respect to speed, torque and power as well.

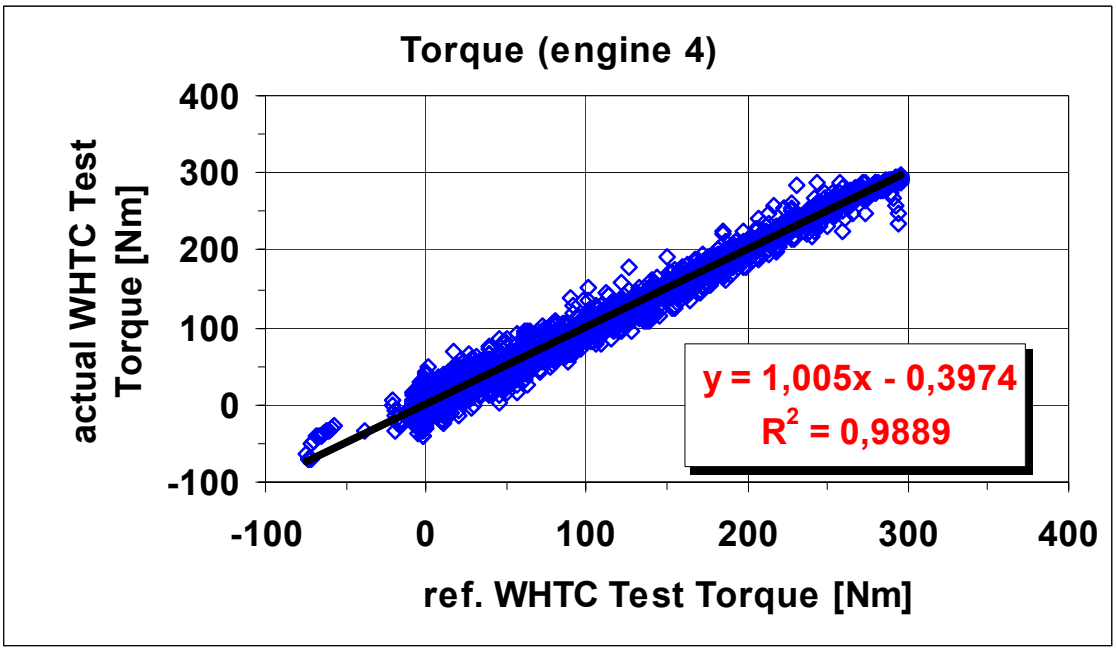

Fig. 2.6.2-4a WHTC validation engine 4

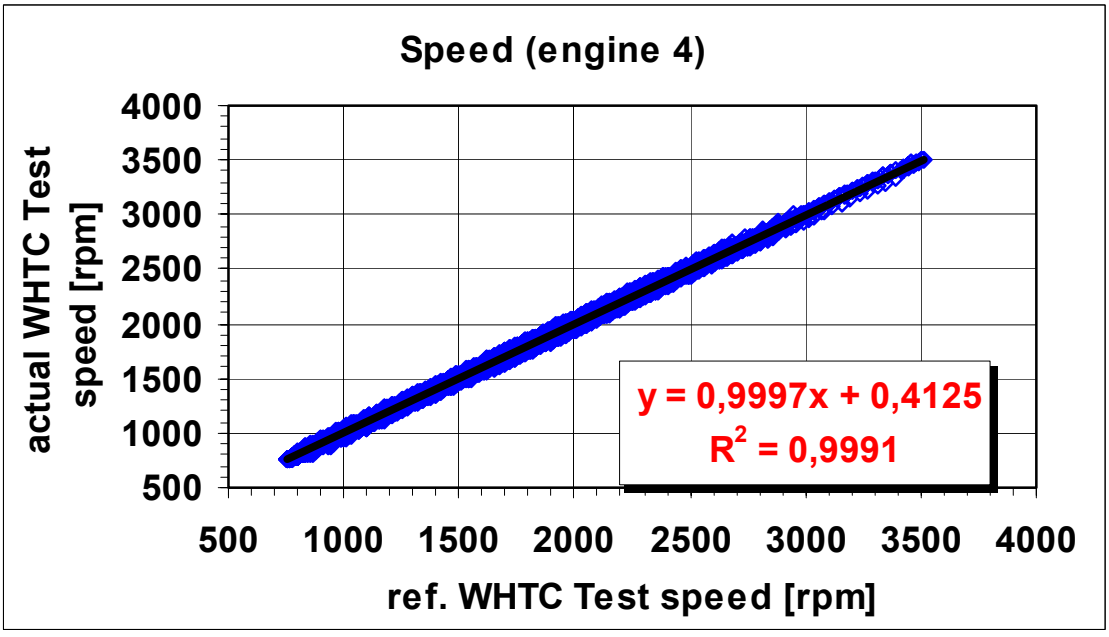

Fig. 2.6.2-4b WHTC validation engine

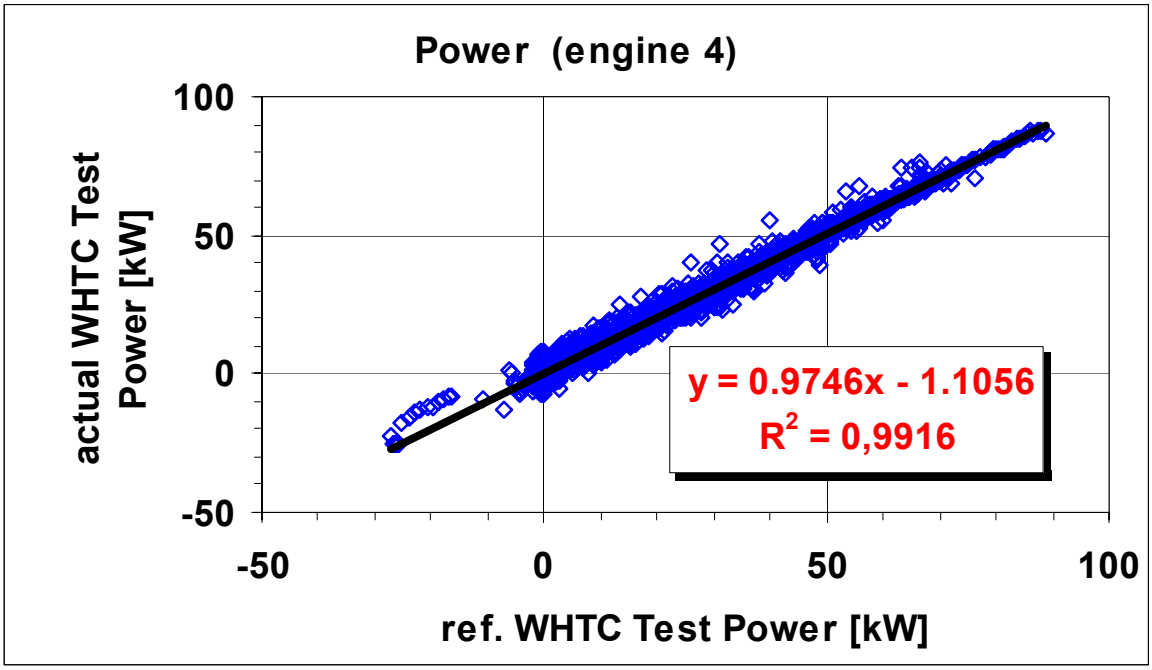

Fig. 2.6.2-4c WHTC validation engine 4

In order to compare the final WHTC validation criteria of all engines based on the possibilities of time alignment and point deletions the following tables show the mean data of all transient cycles performed for all four engines.

Table 2.6.2-1 shows this data for the engine speed. All validation criteria applicable for the speed could be matched well.

In **Table 2.6.2-2** the mean values of the torque criteria are summarised. The values of the standard error as well as for the y-axis intercept of the regression show the highest values for the ETC. This is a true indicator that the ETC has the highest torque demands on the engines in respect to acceleration and deceleration driving patterns. The FTP shows the lowest values, keeping in mind that approximately 30% of the FTP-cycle is at idle speed. The final WHTC shows values in between ETC and FTP. However all cycles could be performed in good to very good correlation to the reference cycle patterns. For each engine a cycle operation map was recorded for each cycle in order to have the dynamometer control adjusted for the particular test cycle. **Table 2.6.2-3** gives an overview of the calculated power validation statistic. As already mentioned the calculation procedure as well as the time alignment shows its influence here but nonetheless all validation criteria could be matched well. Again the ETC values show that this cycle has the greatest demand on an engine and dynamometer dynamic operation.

ETC		**speed**		**engine 1**	**engine 2**	**engine 3**	**engine 4**
Standard error of estimate of Y on X	SE	max 100min-1	[1/min]	27.48	16.37	25.91	37.37
Slope of regression line	b	0.95 to 1.03	[ ]	0.99	1.00	1.00	0.99
Coefficient of determination	R^2	min 0.9700	[ ]	0.99	1.00	1.00	0.99
Y intercept of regression line	a	±50min-1	[1/min]	6.11	0.61	-1.72	6.38
FTP		**speed**		**engine 1**	**engine 2**	**engine 3**	**engine 4**
Standard error of estimate of Y on X	SE	max 100min-1	[1/min]	7.67	8.89	14.15	20.57
Slope of regression line	b	0.95 to 1.03	[ ]	1.00	1.00	1.00	0.99
Coefficient of determination	R^2	min 0.9700	[ ]	1.00	1.00	1.00	1.00
Y intercept of regression line	a	±50min-1	[1/min]	0.15	0.91	-0.37	1.76
WHTC		**speed**		**engine 1**	**engine 2**	**engine 3**	**engine 4**
Standard error of estimate of Y on X	SE	max 100min-1	[1/min]	8.76	7.29	15.65	21.34
Slope of regression line	b	0.95 to 1.03	[ ]	0.99	0.99	0.99	0.98
Coefficient of determination	R^2	min 0.9700	[ ]	1.00	1.00	1.00	1.00
Y intercept of regression line	a	±50min-1	[1/min]	3.30	3.27	3.24	8.73

Table 2.6.2-1: Transient cycle validation statistic for engine speed

ETC	torque		engine 1	engine 2	engine 3	engine 4
Standard error of estimate of Y on X	max 13% of power map maximum engine torque	[Nm]	83.75	118.57	162.72	14.42
Slope of regression line	0.83 - 1.03	[ ]	0.98	0.95	0.97	1.00
Coefficient of determination	min 0.8800	[ ]	0.99	0.94	0.98	0.99
Y intercept of regression line	±20Nm or ±2% of max torque whichever is greater	[Nm]	10.67	15.38	18.67	-0.34
FTP	**torque**		**engine 1**	**engine 2**	**engine 3**	**engine 4**
Standard error of estimate of Y on X	max 13% of power map maximum engine torque	[Nm]	43.46	44.33	124.85	11.02
Slope of regression line	0.83 - 1.03	[ ]	0.99	0.96	0.96	1.00
Coefficient of determination	min 0.8800	[ ]	1.00	0.98	0.98	0.99
Y intercept of regression line	±20Nm or ±2% of max torque whichever is greater	[Nm]	0.02	10.91	10.12	-0.13
WHTC	**torque**		**engine 1**	**engine 2**	**engine 3**	**engine 4**
Standard error of estimate of Y on X	max 13% of power map maximum engine torque	[Nm]	46.98	34.84	134.96	8.85
Slope of regression line	0.83 - 1.03	[ ]	1.00	0.99	0.98	1.00
Coefficient of determination	min 0.8800	[ ]	0.99	0.99	0.97	0.99
Y intercept of regression line	±20Nm or ±2% of max torque whichever is greater	[Nm]	1.38	3.21	7.74	-0.33

Table 2.6.2-2: Transient cycle validation statistic for engine torque

ETC	power		engine 1	engine 2	engine 3	engine 4
Standard error of estimate of Y on X	max 8% of power map maximum engine power	[Nm]	13.8419	20.1427	23.3513	4.3249
Slope of regression line	0.89 - 1.03	[ ]	0.9928	0.9534	0.9890	1.0117
Coefficient of determination	min 0.9100	[ ]	0.9874	0.9430	0.9844	0.9851
Y intercept of regression line	±4kW or ±2% of max power whichever is greater	[Nm]	1.5472	1.2829	-1.2914	0.0447
FTP	**power**		**engine 1**	**engine 2**	**engine 3**	**engine 4**
Standard error of estimate of Y on X	max 8% of power map maximum engine power	[Nm]	3.2630	3.8586	10.5521	1.8464
Slope of regression line	0.89 - 1.03	[ ]	1.0075	0.9973	0.9953	1.0155
Coefficient of determination	min 0.9100	[ ]	0.9983	0.9942	0.9917	0.9948
Y intercept of regression line	±4kW or ±2% of max power whichever is greater	[Nm]	-0.4189	0.4953	-0.5836	-0.1934
WHTC	**power**		**engine 1**	**engine 2**	**engine 3**	**engine 4**
Standard error of estimate of Y on X	max 8% of power map maximum engine power	[Nm]	4.7098	4.1373	13.2613	1.5970
Slope of regression line	0.89 - 1.03	[ ]	1.0230	1.0038	0.9832	1.0137
Coefficient of determination	min 0.9100	[ ]	0.9921	0.9939	0.9686	0.9903
Y intercept of regression line	±4kW or ±2% of max power whichever is greater	[Nm]	-0.2857	0.3186	0.4499	-0.0069

Table 2.6.2-3: Transient cycle validation statistic for engine power

2.7 Comparison of WHTC and WHSC

2.7.1 WHDC cycles in version 1 and final version

Another task was to verify the steady-state / transient cycle equivalence of the final WHSC and WHTC. Both cycles (especially the WHSC) were modified /2/ as a result of validation step 1 /3/ shortly before the start of the measurement programme and therefore had to be validated with respect to driveability and cycle equivalence,

Figures 2.7.1-1 and **Fig. 2.7.1-2** show the differences between the final and version 1 reference WHDC.

Since the differences between the final WHTC and the version 1 WHTC are not as obvious as for the WHSC, the verification of the cycle equivalence was of high importance in this work. **Fig. 2.7.1-3** shows the reference speed schedule of the final WHTC and version 1., **Fig. 2.7.1-4** shows the reference torque schedule.

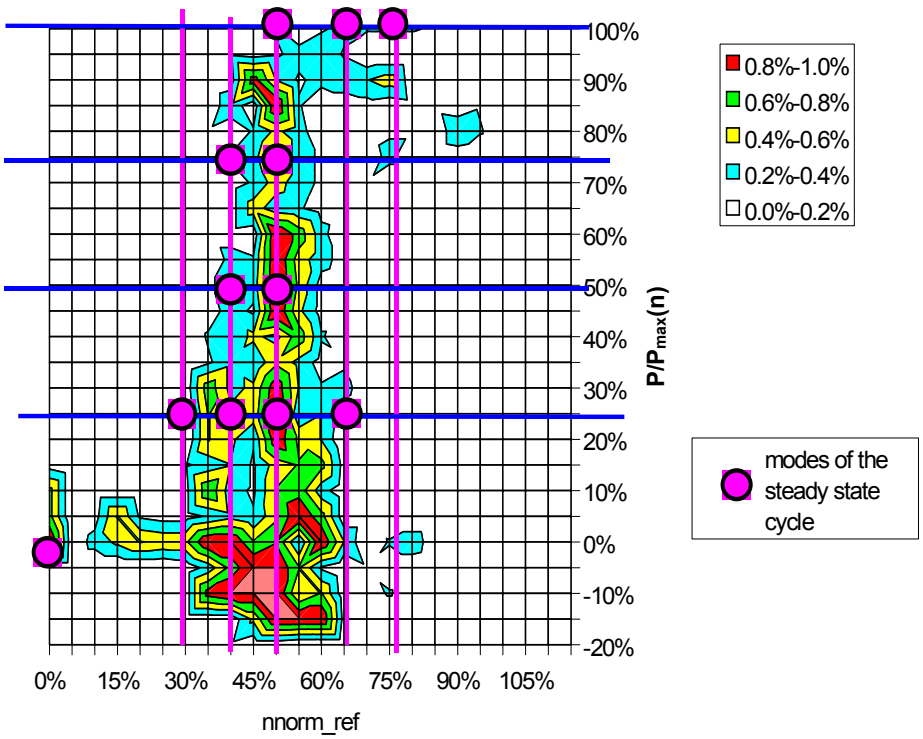

Fig. 2.7.1-1: WHSC Version 1

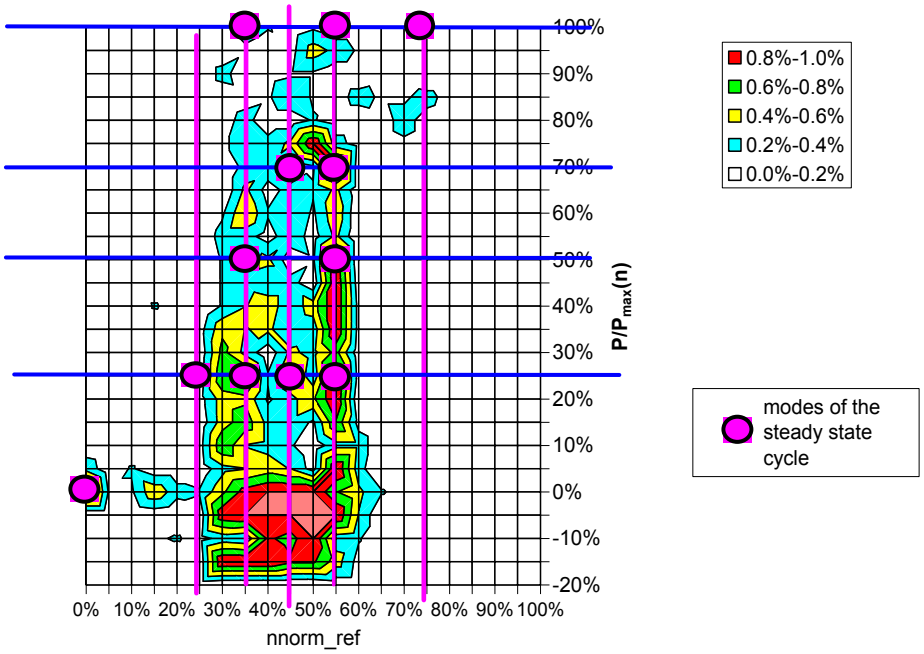

Fig. 2.7.1-2: Final WHSC

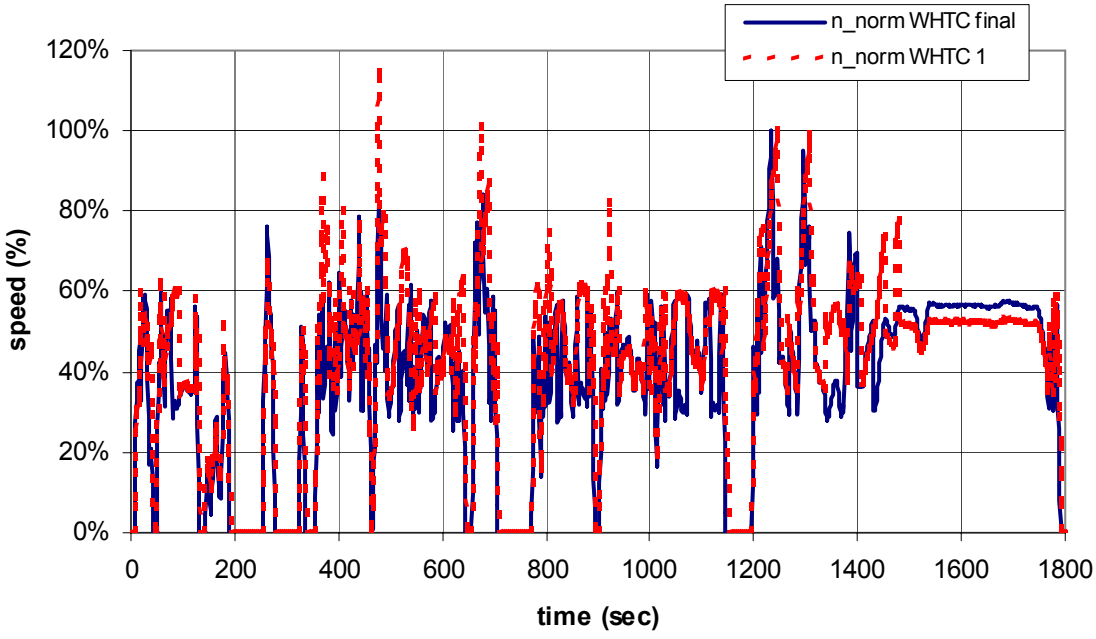

Fig. 2.7.1-3: Reference speed schedule of final and version 1 WHTC

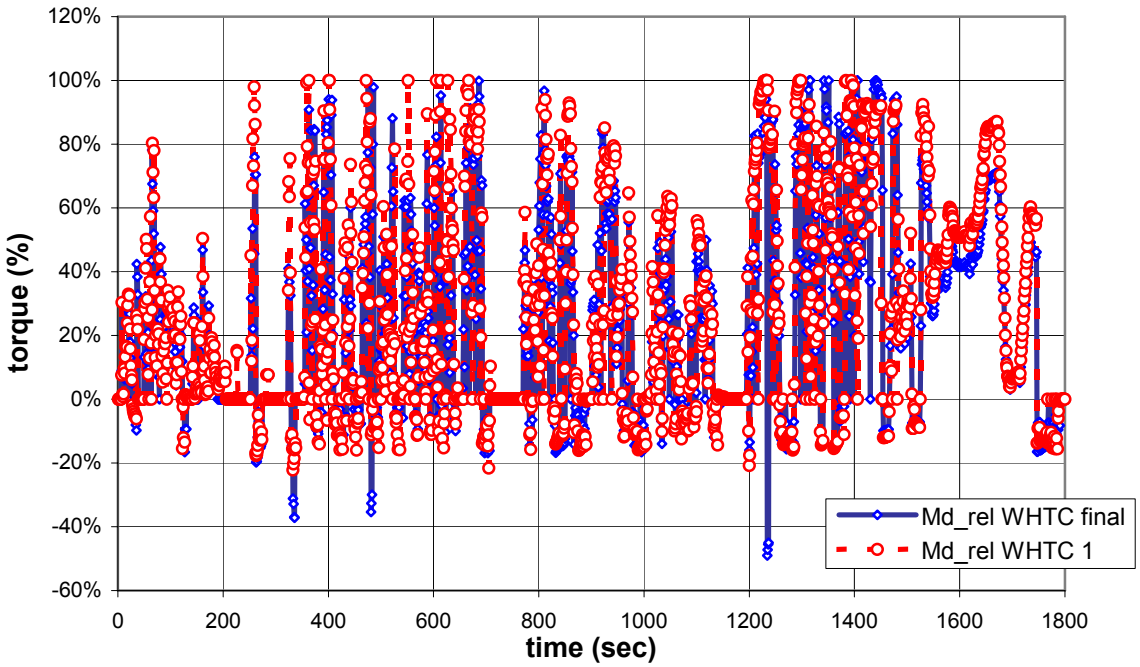

Fig. 2.7.1-4: Reference torque schedule of final and version 1 WHTC

For the equivalence study, the final and version 1 WHDC cycles were run and compared to one another with respect to cycle work (kWh) and NOx (g/kWh) on *engine 1* separate from the rest of the programme. Cycle work was chosen since the overall final emission results are depending on this value. NOx was chosen due to the fact that this is the emission component most influenced by the engine calibration. The regulated components CO and HC were not considered in this approach due to the measurement problems with those components caused by the CRT after-treatment system , as reported earlier. By comparing the measurement results (cycle work and NOx-emission) of the final WHSC and final WHTC steady-state / transient cycle equivalence is given for the NOx-values as well as for the cycle work by considering a 10% equivalence range. **Table 2.7.1-1** shows this data, **Fig. 2.7.1-5** compares cycle work.

	NOx (g/kWh)	**W (kWh)**
WHTC final mean	5.76	27.80
WHSC final mean	6.37	26.68
diff. SC to TC	0.61	-1.12
percentage SC to TC	9.57	-4.19

Table 2.7.1-1: Steady-state / transient cycle equivalence (engine 1 with CRT)

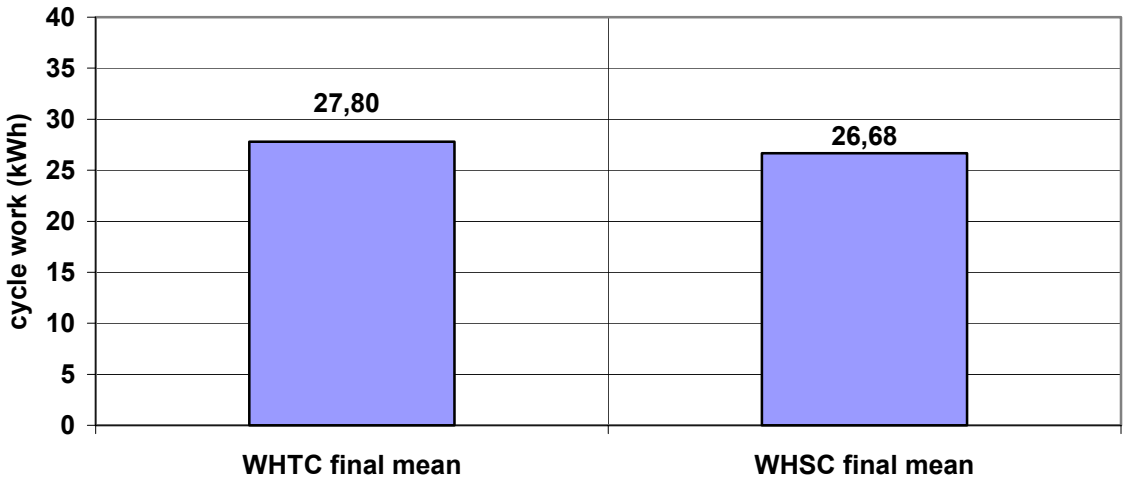

Fig. 2.7.1-5: Cycle work comparison final WHTC / final WHSC

2.7.2 Correlation between final WHTC and final WHSC

Fig. 2.7.2.1-1 shows the correlation between the WHTC and WHSC with respect to the particulate matter results of the four engines. Despite the fact that *engine 3* and *4*, that were not equipped with CRT gave some high readings here, the linear fit factor of 0.49 could also be well applied to the results of engine 1 and 2 (CRT).

In addition, the results of *engine 1* without CRT are also included. It can be seen that the transient (WHTC) results are significantly higher than the steady-state results (WHSC).

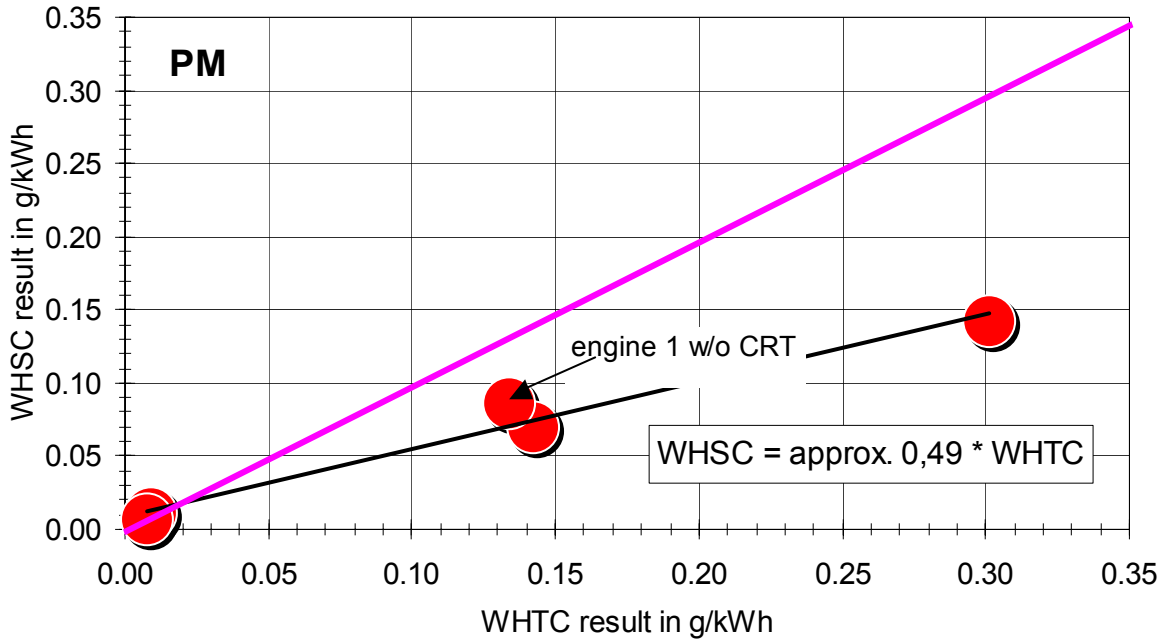

Fig. 2.7.2.1-1: WHTC / WHSC PM-correlation

This is contrasted by **Fig. 2.7.2.1-2** in which the NOx-correlation is shown. Here all engines show slightly higher mean values for steady-state WHSC operation.

Engine 1 without CRT is not considered here due to the fact that the CRT has no effect on the NOx-values.

No linear fit was possible for the CO-emissions of WHTC and WHSC due to the values produced by *engine 1* without CRT. The WHSC result is on the same level as for *engine 3* but the transient CO-value is considerably higher preventing the use of linear correlation (**Fig. 2.7.2.1-3**).

This is the same for the HC mean values. Here it is *engine 4* which does not allow do have a linear approach on the results. On this engine the steady-state HC value is relatively low compared to the transient value. The offset between *engine 1* without CRT and *engine 3* as seen on the CO is not evident for HC. As expected from engine combustion theory, both CO and HC values are higher under transient operation.

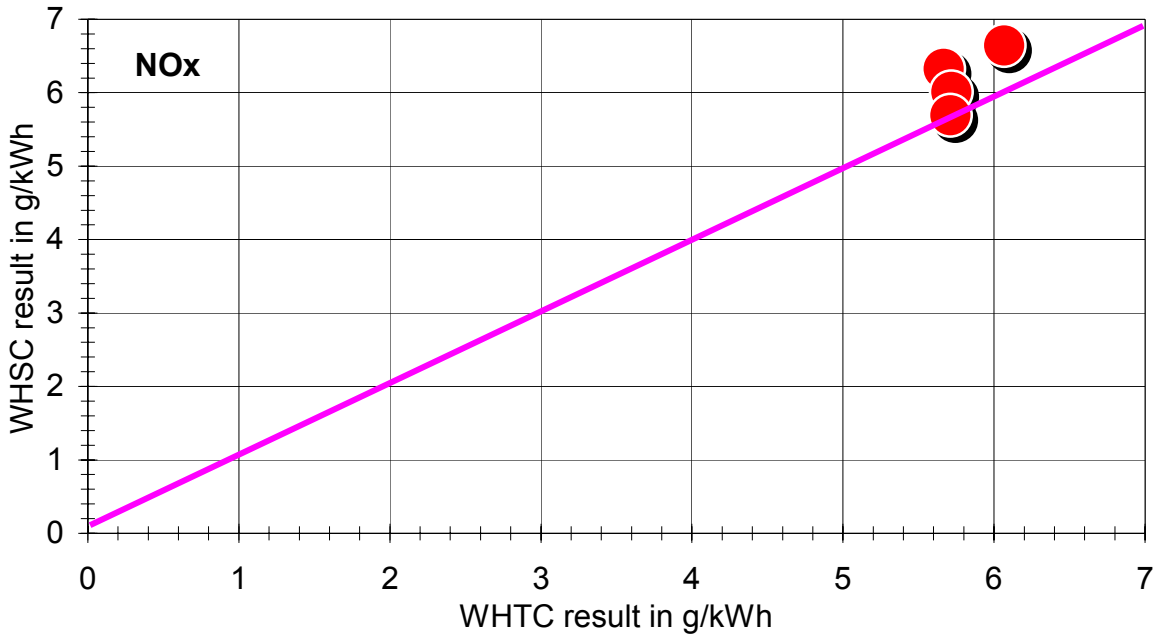

Fig. 2.7.2.1-2: WHTC / WHSC NOx-correlation

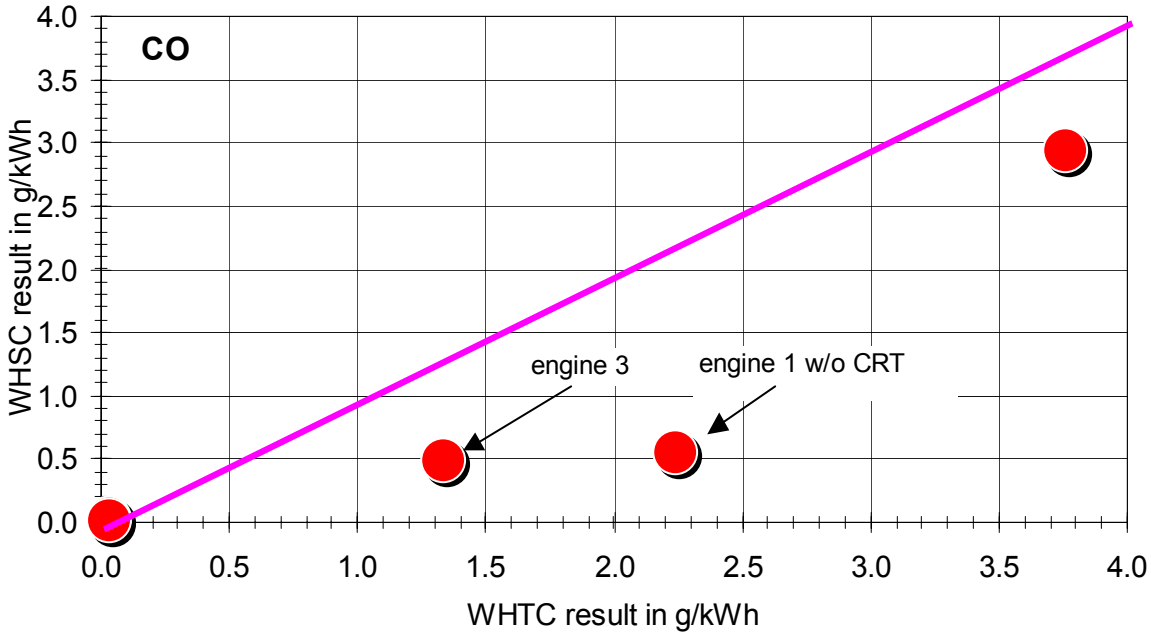

Fig. 2.7.2.1-3: WHTC / WHSC CO-correlation

For the cycle work and therefore also again for the steady-state and transient cycle equivalence a very clear linear coherence is existent (**Fig. 2.7.2.1-5**). For this reason it has to

be said again, that based on the cycle work the final WHSC- and WHTC-cycles show very good equivalence.

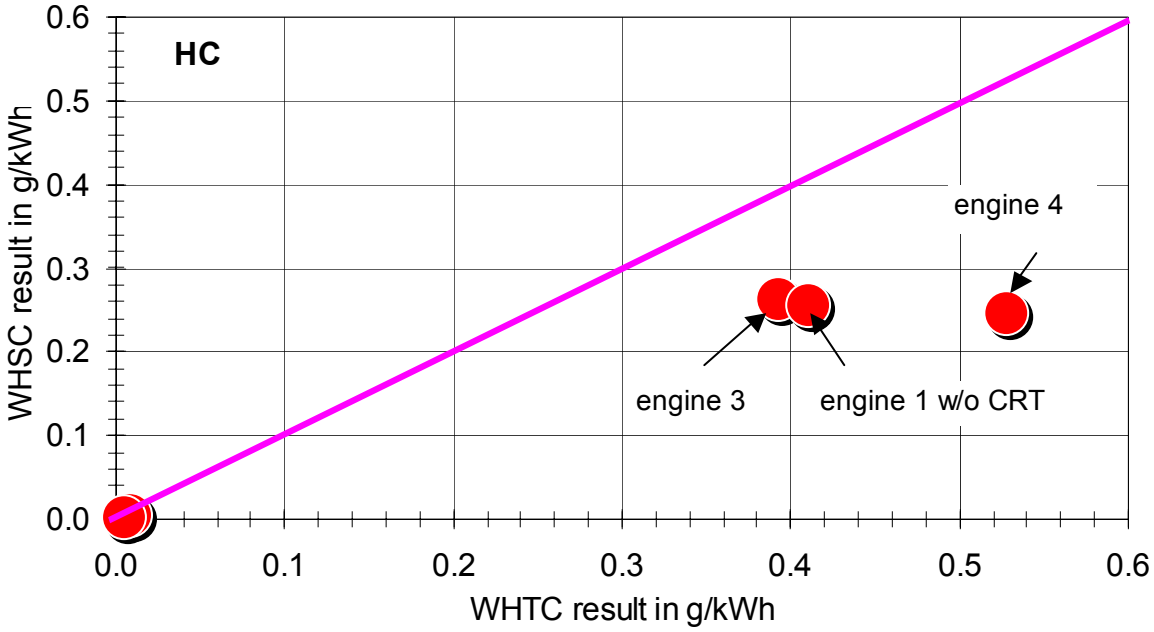

Fig. 2.7.2.1-4: WHTC / WHSC HC-correlation

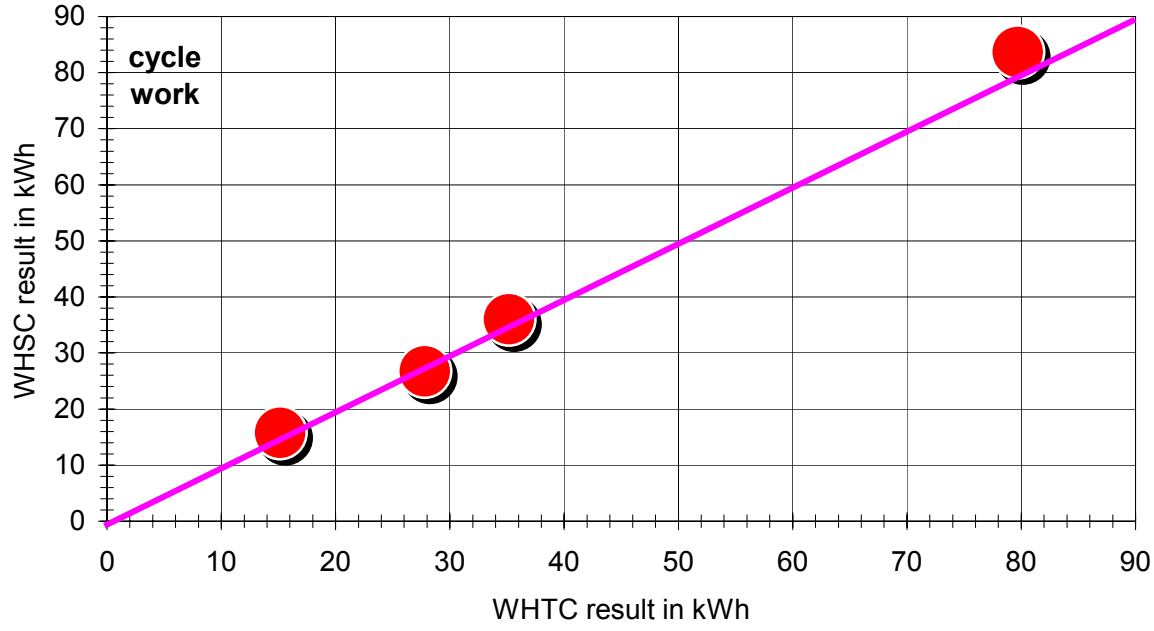

Fig. 2.7.2.1-5: WHTC / WHSC cycle work-correlation

2.8 Correlation of final WHDC cycles to existing test cycles

In order to gather some more knowledge about the relations between the final WHDC test cycles with the existing type approval cycles, the mean emission values as well as the cycle work were compared. Wherever possible a linear fit was applied to the results. For the analysis the WHDC-cycles were used as a reference, better reflecting real driving behaviour worldwide than the other cycles.

For the approach of the linear fit it has to be considered that the calibration of the engines may have a significant influence on the cycle results so that a general statement for correlation factors between the cycles could not be given.

The graphical displays are based on the mean values of the raw gaseous component measurements and the partial flow PM results in order to reflect this new measurement methodologies, especially for the transient cycles. Only the final WHDC cycle results were used for this study part. Where necessary, e.g. where no reasonable linear fit could be applied, the corresponding engine is indicated in the diagram.

2.8.1 Steady-state Cycles

For the steady-state cycle PM-emission the results of the ESC are lower and the results of the Japanese 13-mode are higher than for the WHSC (**Fig. 2.7.2.2-1**). Especially for *engine 4* the Japanese 13-mode result shows the highest difference to the others.

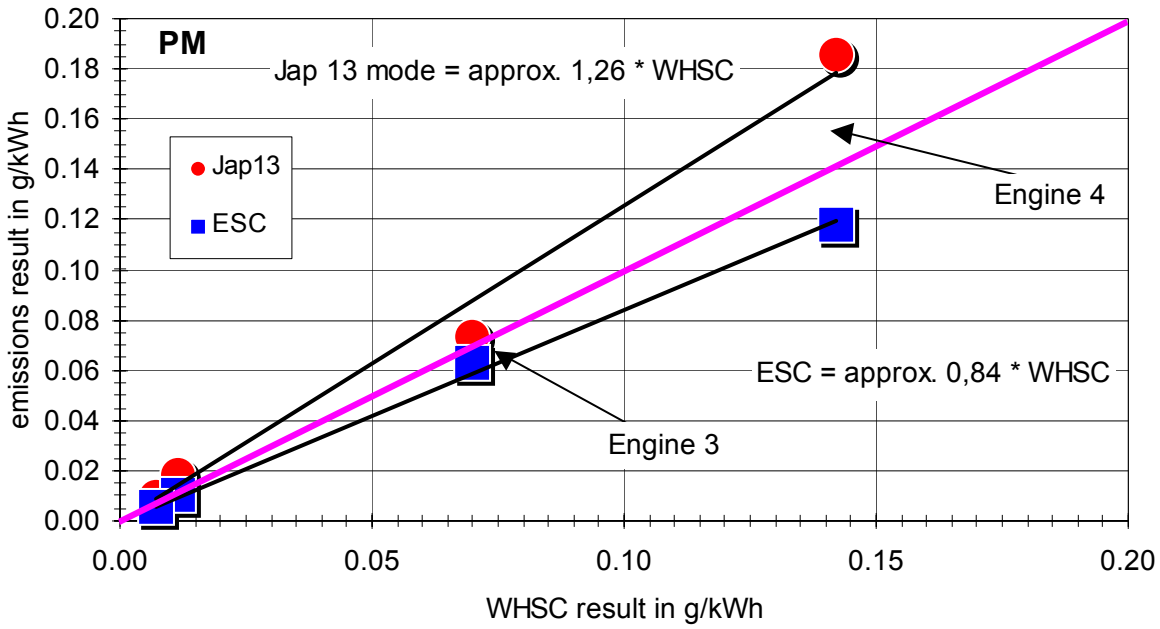

Fig. 2.7.2.2-1: Steady-state cycle PM-correlation

For steady-state NOx, some linear correlation can only be seen for WHSC and the Japanese 13-mode where the WHSC values are higher than for the 13-mode (**Fig. 2.7.2.2-2**).

A coherence between WHSC and the ESC is given in that all ESC-emissions of all four engines are more or less relatively close to the Euro 3 NOx-emission limit of 5 g/kWh. This was to be expected since all engines were meeting the standards and for that reason were calibrated for that. This was obviously not the case for the Japanese 13-mode and the WHSC-cycle except for *engine 4*.

This engine shows very similar results on the ESC and the Japanese 13-mode.

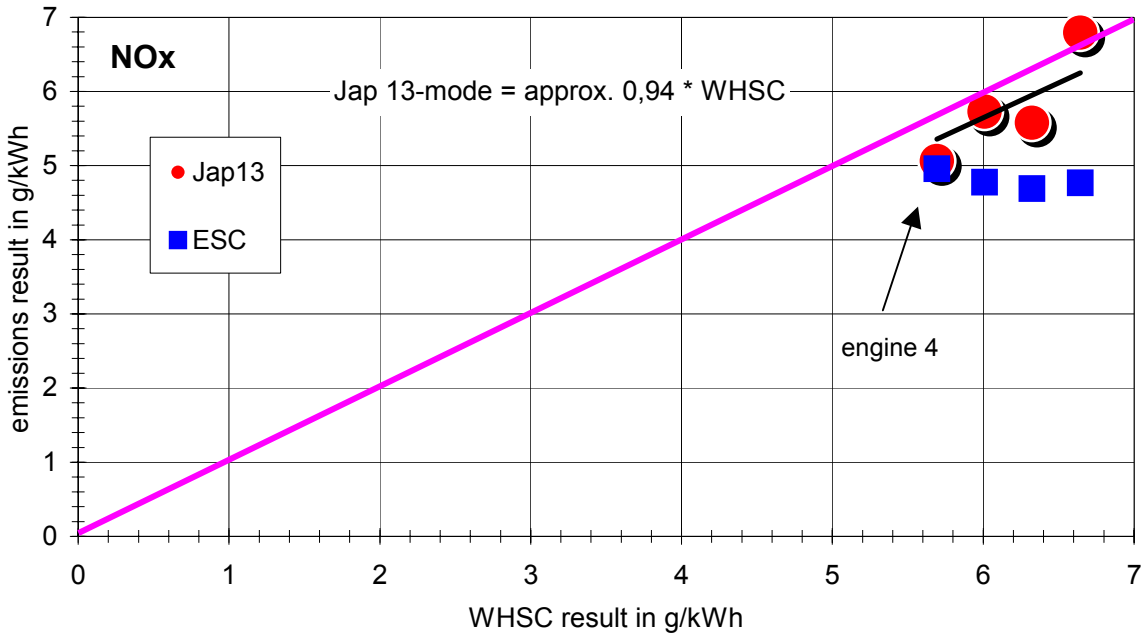

Fig. 2.7.2.2-2: Steady-state cycle NOx-correlation

The CO-relation reflects (**Fig. 2.7.2.2-3**) very well the PM-correlation shown in **Fig. 2.7.2.2-3**.

This was to be expected since there is coherence between these two exhaust components. For the reason of having two engines on a very low level and two engines on a relatively high level the linearity is clear but should not be overestimated, especially not for comparison reasons with the ESC.

For HC no linear fit was applied and the data are shown in **Fig 2.7.2.2-4**.

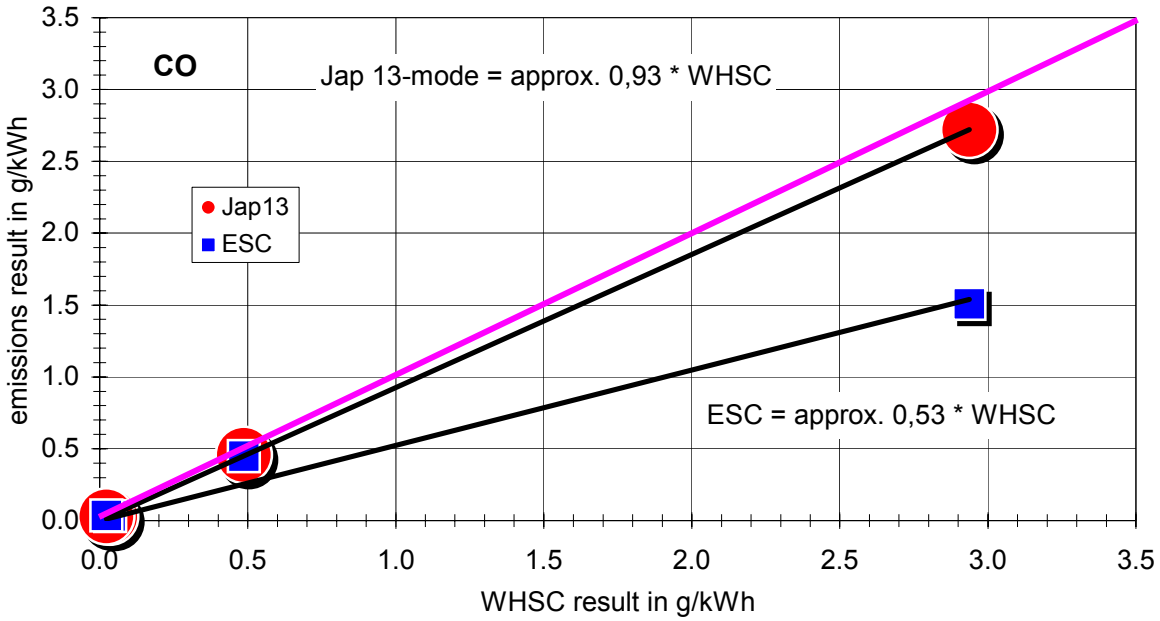

Fig. 2.7.2.2-3: Steady-state cycle CO-correlation

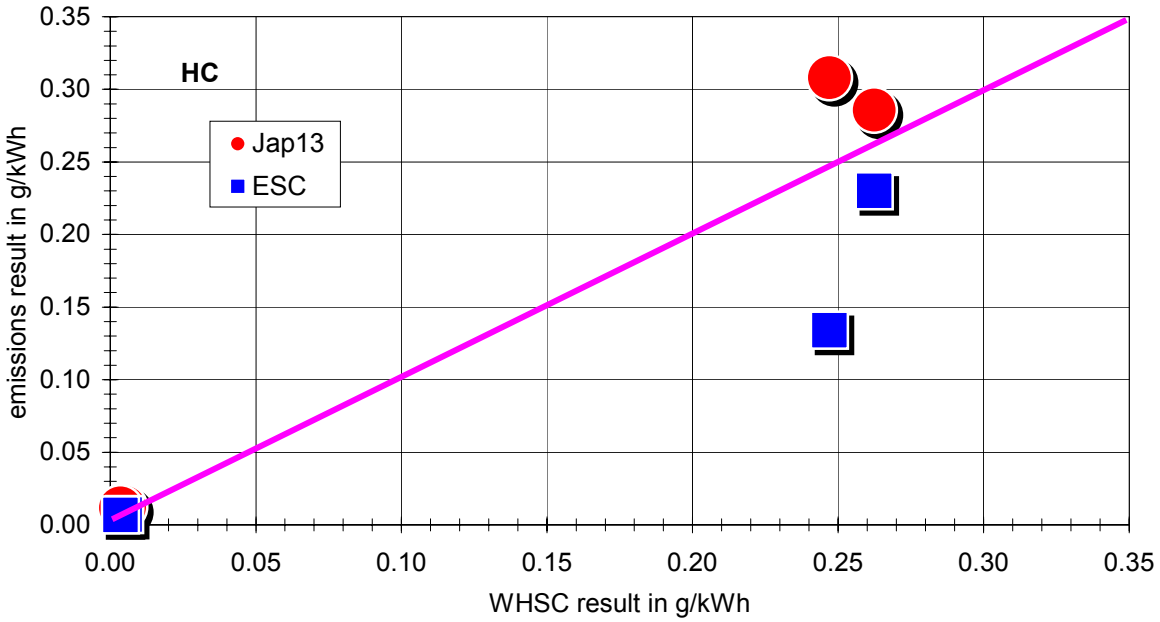

Fig. 2.7.2.2-4: Steady-state cycle HC-correlation

2.8.2 Transient cycles

For the transient cycles compared to the WHTC cycle the same coherence as already discussed for the steady-state cycles can be determined. In **Fig. 2.7.2.3-1** the PM-values of the transient cycles performed are presented.

On the engines tested a slight tendency can be seen to have higher PM-results on the WHTC than on the ETC and U.S.-FTP. The values generated here are generally higher than during steady-state testing.

This was to be expected due to the transient conditions. All engines met the current Euro 3 standards despite that fact that transient PM-testing is not mandatory for this emission stage without advanced after-treatment systems.

The transient NOx-results shown in **Fig. 2.7.2.3-2** are very similar to what could be seen for steady-state operation and scatter around the 1:1 correlation.

By comparing the ETC NOx-emissions with the ESC NOx-emissions (**Fig. 2.7.2.2-2**) a very distinctive ESC / ETC NOx-equivalence is evident. The U.S.-FTP values for *engine 1* and *2* are within the same range. *Engine 3* and *engine 4* show higher NOx for U.S.-FTP testing. A linear fit could not be applied to this NOx-data but to the CO-results again (**Fig. 2.7.2.3-3**).

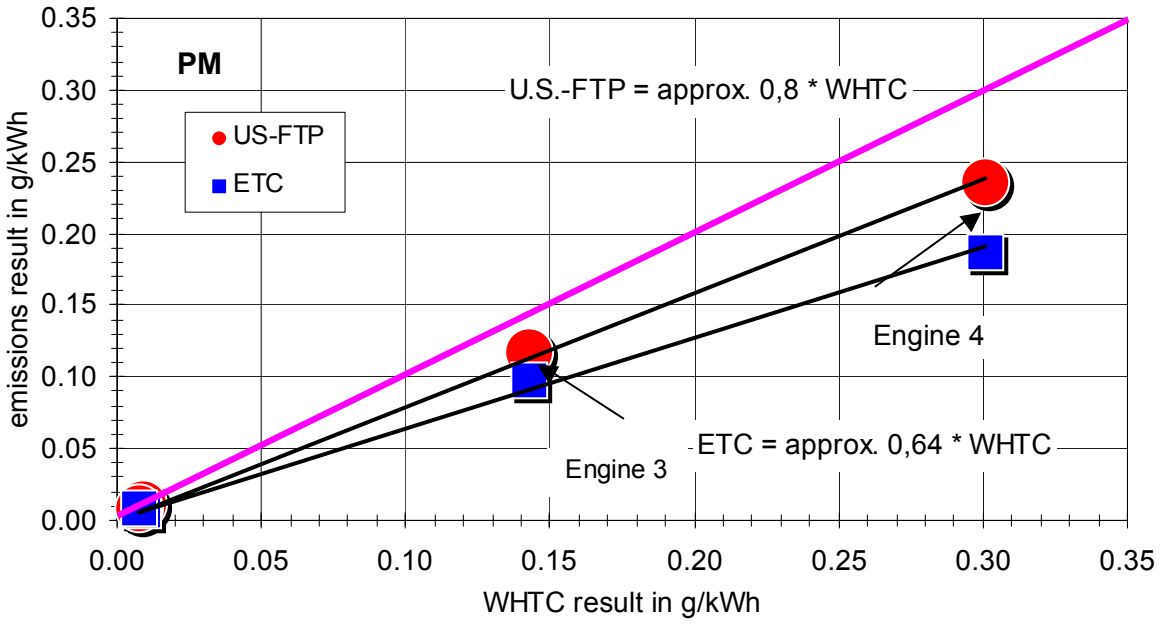

Fig. 2.7.2.3-1: Transient cycle PM-correlation

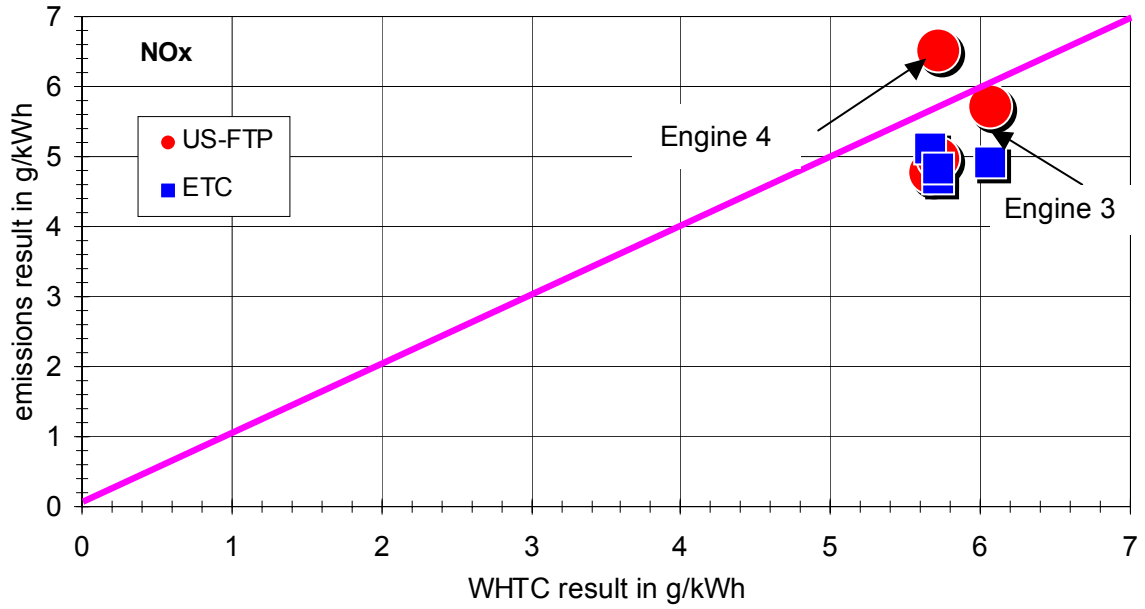

Fig. 2.7.2.3-2: Transient cycle NOx-correlation

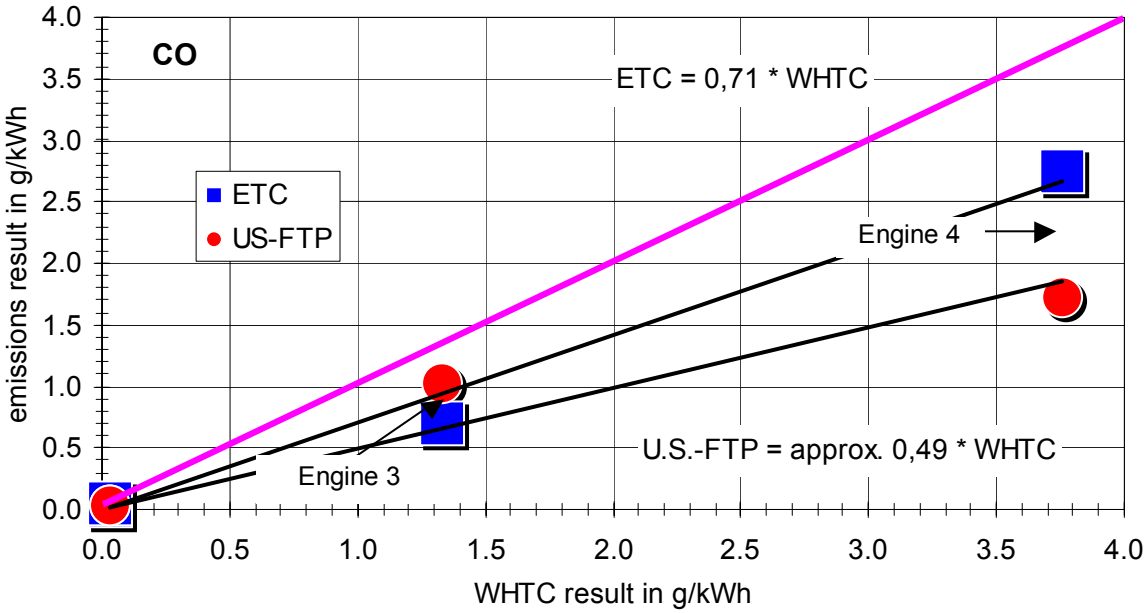

Fig. 2.7.2.3-3: Transient cycle CO-correlation

Since the relation between PM and CO is well known very similar coherence than for the PM are obvious for CO. The linearity factors are somehow different than for PM but indicate the same tendency. Compared to the steady-state ESC higher CO values are generated during transient operation (ETC).

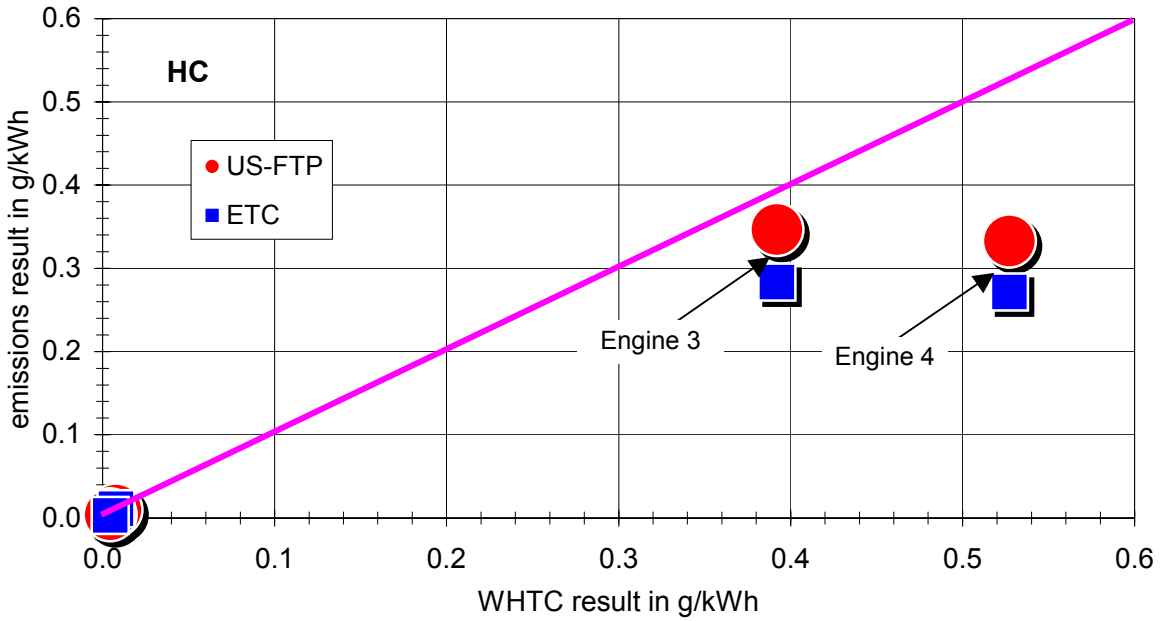

Fig. 2.7.2.3-4: Transient cycle HC-correlation

For the transient HC behaviour again no linearity function could be applied (**Fig. 2.7.2.3-4**). For *engine 1* and *engine 2* equipped with CRT the values are very low. The *engines 3* and *4* show similar values for the ETC and the U.S.-FTP but some reasonable difference for the WHTC.

3 Summary and Conclusions

3.1 WHDC cycle validation

The final WHDC-cycles showed very good steady-state / transient cycle equivalence in terms of cycle work and NOx-emissions. Both cycles cover a wide range of the engine map. Five speeds are used for the WHSC- (steady-state) cycle compared to three for the ESC-cycle currently applied in the EU. This ensures that a wider part of the engine map is tested. The WHTC- (transient cycle) was developed on the basis of an analysis of real-driving pattern with worldwide relevance so that this cycle has the closest link to real engine operation (**Chapter 2.5** ***ff***).

3.2 Driveability of the final WHDC test cycles

The driveability of the transient cycle in terms of the cycle validation criteria given in the EU and in the US is good to very good. Since more worldwide driving patterns are considered /2/, the final WHTC does not have as many dynamic parts as the ETC-cycle based only on European driving pattern. For that reason the validation criteria are a little easier to match than for an engine operated on the ETC. However, state of the art engine dynamometer technology is capable to meet the validation criteria even for more dynamic cycles than the ETC (**Chapter 2.6 and 2.7**).

3.3 Comparison of the new and existing measurement procedures

The capability of partial flow dilution systems operated according to ISO 16183 for particulate matter measurement under transient conditions was proven. The partial flow system showed good to very good comparability to the well-established full flow dilution-CVS-system. This was demonstrated by the absolute deviations between the systems as well as by some improved repeatability of the partial flow system with respect to particulate matter measurement (**Chapter 2.3** ***ff***).

The PM analysis by extraction showed no significant differences in the particulate matter composition sampled by a partial flow system.

For the raw measurement of the regulated gaseous components the same statement can be given. Also here the provisions given in ISO 16183 provide a reliable tool for the application of this measurement and sample methodology for transient operation of an engine (**Chapter 2.4** ***ff***).

The agreement of both procedures (full flow / CVS and raw gas / partial flow) was good over the entire measurement programme.

For both the particulate matter and the gaseous components, good measurement accuracy becomes more difficult to achieve as soon as very low general emission levels are reached due to the fact that the limit of detection of the measurement systems is being approached. The raw gas measurement has some advantage here since no concentration reduction through dilution is given. Due to the higher gas concentrations in the raw gas the ISO 16183 measurement procedure is more reliable.

Some of the results of the engines equipped with CRT-System (*engine 1* and *engine 2*) could not be used for comparison and correlation purposes due to the very low emission values reached by such technologies for PM, CO and HC. However, it was demonstrated that also in this case the new ISO 16183 procedures are fully applicable with even some advantage compared to the established CVS-procedure.

3.4 Adaptation of final WHDC cycles

Based on the results described within this report no proposals for further modifications on the final WHDC cycles are necessary. The applicability of the ISO 16183 measurement procedure is given. The results on *engine 4* (small capacity, high rated speed) show that even relatively small, more or less passenger car / light-duty vehicle engine derived, HD applications can be measured with the WHDC cycles and the ISO measurement procedure.

3.5 Outlook for Otto-cycle engines

All WHDC-validation and -measurement programmes carried out so far only covered diesel engines. For throttled engines (Otto-cycle LPG and CNG for heavy-duty purpose), the applicability of the ISO procedure is not proven yet. Additionally, the WHTC driveability for throttled engines has to be validated, since such engines do not have the direct response behaviour of a diesel engine. This will be evaluated in a further WHDC validation step.

4. References

/1/ ISO 16183, Heavy duty engines - Measurement of gaseous emissions from raw exhaust gas and of particulate emissions using partial flow dilution systems under transient test conditions, 2002

/2/ Worldwide Harmonized Heavy Duty Emissions Certification Procedure, Final Summary, 15th WHDC, Geneva, 21 May 2003

/3/ Worldwide Harmonized Heavy Duty Certification, Results of Validation Step 1 Final Report, 44th GRPE Session, 10-14 June 2002

/4/ L.-E. Schulte, G. Pohlmann, New health-effect related particle measurement methodology for diesel and gasoline engines. Final Report Umweltbundesamt (German Contribution to GRPE PMP Project Phase 2), 2003.

/5/ Directive 1999/96/EC relating to measures to be taken against the emission of gaseous and particulate pollutants from compression ignition engines for use in vehicles, and the emission of gaseous pollutants from positive ignition engines fuelled with natural gas or liquefied petroleum gas for use in vehicles and amending Council Directive 88/77/EEC, 13. December 1999

/6/ Code of Federal Regulations, 40 CFR §86.1310-2007, Subpart N, Emission Regulations for New Otto-Cycle and Diesel Heavy-Duty Engines, Gaseous and Particulate Exhaust test Procedures, 2001 Edition

/7/ Worldwide Heavy-Duty Certification, Results of Validation Step 1, Final Report, Dutch Ministry of the Environment (VROM), International Organization of Motor Vehicle Manufacturers (OICA), Dr. Cornelis Havenith, H. Juergen Stein, Thomas Schweizer, 2002

/8/ A Study of Composition and Size Distribution of Particulate Matter from DI Diesel Engine, Shigeyuki Tanaka and Toshio Shimizu, COSMO Research Institute; SAE Paper 1999-01-3487

/9/ Characterization of Soluble Organic Fraction in DPM: Optimization of the Extraction Method, Antonio de Lucas, Antonio Durán, Manuel Carmona and Magín Lapuerta, University of Castilla-La Mancha; SAE Paper 1999-01-3532

/10/ Characterization of Diesel Particulate Emissions of Two IDI Diesel Engines using Diesel and Kerosene Fuels; G. E. Andrews, S. M. Abdelhalim, and P. T. Williams, Leeds Univ.; SAE Paper 961231, 1996